Carbon, Oxygen And Strontium Isotopic Composition Of Diagenetic Calcite And Siderite From The Upper Cretaceous Cardium Formation Of Western Alberta

by

Steve Zymela, M.Sc.

A Thesis

Submitted to the School of Graduate Studies

in Partial Fulfilment of the Requirements

for the Degree

Doctor of Philosophy

McMaster University

August 1996

Carbon, Oxygen And Strontium Isotopic Composition Of Diagenetic Calcite And Siderite From The Upper Cretaceous Cardium Formation Of Western Alberta

Doctor of Philosophy (1996)
(Geology)

McMaster University
Hamilton, Ontario

TITLE: Carbon, Oxygen And Strontium Isotopic Composition Of Diagenetic Calcite And Siderite From The Upper Cretaceous Cardium Formation Of Western Alberta

AUTHOR: Steve Zymela, Hon. B.Sc. (Univ. of Western Ontario, 1979)
M.Sc. (McMaster University, 1986)

SUPERVISOR: Drs. H.P. Schwarcz and R.H. McNutt

NUMBER OF PAGES: xi, 133

Abstract

The Upper Cretaceous (Turonian) Cardium Formation of western Alberta consists of a sequence of interbedded mudstones, sandstones and some conglomerates. Siderite is a common mineral constituent in the Cardium Formation and occurs as an early pore-filling cementing phase in marine conglomerates (Carrot Creek) and as concretions in marine mudstones and brackish/continental (Kakwa) sediments. Diagenetically later calcite cements are also common in the conglomerate and sandstone units.

Petrographic investigation of the diagenetic mineral phases defines the sequence of mineral precipitation to be pyrite, siderite, calcite, quartz, kaolinite, fracture-filling calcite. The siderites precipitated below the sediment seawater interface under reducing conditions in porewaters depleted in sulphate via sulphate reduction and sulphide precipitation. The reduction of organic rich matter and Fe^{3+} by bacterial processes increased the DIC and Fe/Ca ratio of the porewaters so that siderite precipitated preferentially over calcite.

Sedimentary siderites have a high clay content and an analytical procedure was established to prevent contamination from the interlocked, highly radiogenic clays Sr.

Marine siderite concretions are distinguishable from their brackish/continental counterparts by their Sr and O isotopic composition. Brackish/continental siderites have lighter oxygen isotopic values and a more radiogenic strontium composition compared to the marine equivalents. Sr and O isotopic composition of the calcites reveals that they precipitated at a later stage, following meteoric water encroachment into the basin.

Acknowledgements

I wish to thank my supervisors Dr. Henry Schwarcz and Dr. Robert McNutt for suggesting and funding of this research project. I would like to thank Dr. R.G. Walker for his help in the Calgary core lab and Dr. Katherine Bergman for providing numerous core samples and thin sections. I would also like to thank Dr. Fred Longstaffe for use of his XRD facilities.

Table of Contents

List of Figures

List of Tables

CHAPTER 1

Introduction

1.1 General Geology of the Cardium Formation

The Upper Cretaceous (Turonian) Cardium Formation consists of a sequence of interbedded mudstones, sandstones and some conglomerates. The formation crops out in the Foothills of the Canadian Rockies, and in the subsurface it extends from Grande Prairie to Calgary. This formation has been the target of intensive exploration for hydrocarbons over many decades. Major oil fields of the Cardium are shown in Figure 1.1.

Detailed analysis of the Cardium Formation in the subsurface has been interpreted to represent sediment deposition in at least 3 different settings (Plint et al., 1986):

1) a laterally prograding shoreface and alluvial plain (Kakwa and Musreau members) that interfinger seaward with
2) a vertically aggrading offshore shelf (Nosehill, Bickerdike, and Hornbeck members). The Raven River, Dismal Rat and Karr members represent similar offshore deposits, however, their laterally equivalent shoreline facies have not yet been defined.
3) Erosively based, conglomeratic sediments (Waskahigan, Burnstick, Carrot Creek and Amundson members) were deposited during periods of lowered sea level.

The relationship and geometry of the members is shown in Figure 1.2. Episodes of lowered sea level caused sedimentation in environments 1 and 2 to cease.

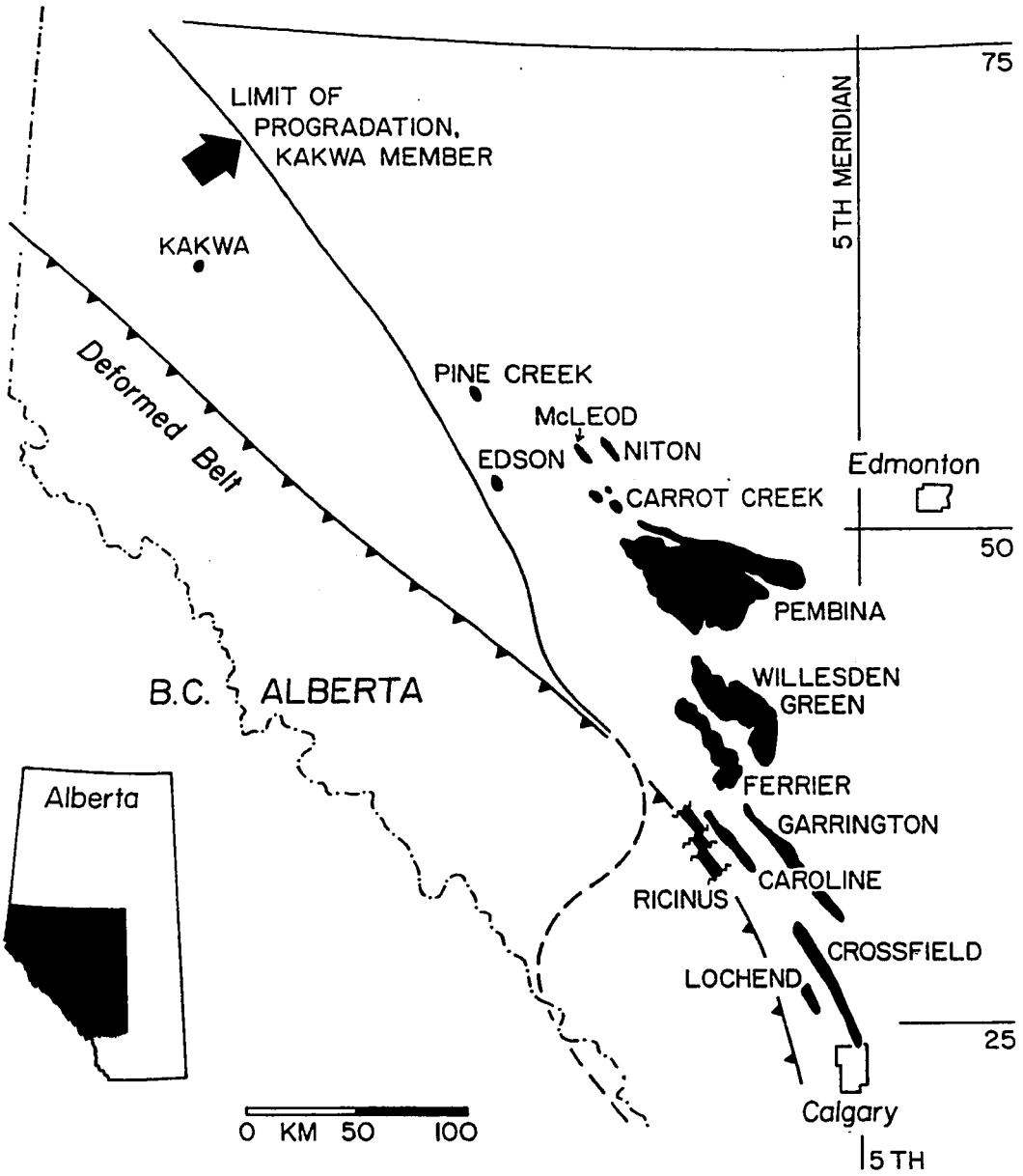

Figure 1.1 Location map of the Cardium oilfields in the Alberta Basin. (From Walker, 1986)

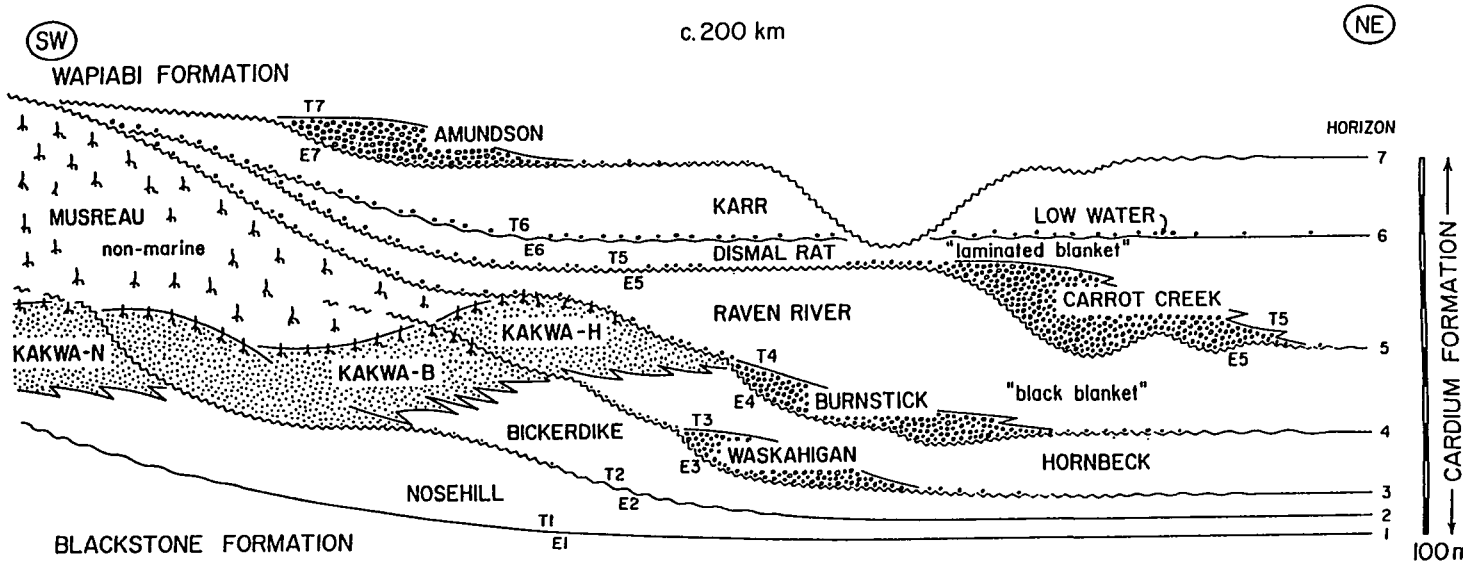

Figure 1.2 Stratigraphic relationships of the various members of the Cardium Formation in southwestern Alberta. E1 through E7 represent the erosional surfaces, and T1 through T7 represent the transgressive surfaces. (From Plint et al., 1986)

This resulted in erosion of both shoreline and offshore sediments. Gravels varying in thickness from a thin veneer of pebbles to 20m (Fig. 1.3) were deposited on these erosional surfaces (Plint et al., 1986), and host a diverse assemblage of diagenetic mineral phases. These sediments have been interpreted as representing rapid drops in relative sea level, resulting in rapid shifts of the shoreline towards and away from the center of the basin. This sedimentological history implies a series of rapid shifts in the position of the land/sea boundary. In places, the erosional surfaces were not as well developed and consist of sideritic horizons mixed with scattered grains of coarse sand or granules. These horizons are interpreted by Plint et al. (1986) to represent pauses in sedimentation with possibly minor erosion. At present, seven erosional surfaces have been identified (Fig. 1.2).

The stratigraphy of the Cardium Formation, is also discussed by Walker (1986), Rine, Helmold and Bartlett (1987), Hayes and Smith (1987), and Plint et al. (1987). Detailed sedimentologic and stratigraphic studies on individual fields of the Cardium Formation have been investigated by Walker (1983a) [Garrington, Caroline and Ricinus]; Walker (1983b) [Garrington and Caroline]; Walker (1985) [Ricinus]; Bergman (1987) and Bergman and Walker (1988) [Carrot Creek]; Bartlett (1987) and Plint and Walker (1987) [Kakwa]; Leggitt (1987) [Pembina]; Pattison (1988) [Caroline, Crossfield, Garrington and Lochend]; Eyles and Walker (1988) and Walker and Eyles (1988) [Willesden Green].

For this study, sampling was carried out on cores from the Carrot Creek and Kakwa fields. These sites are taken to represent idealized marine (Carrot Creek) and

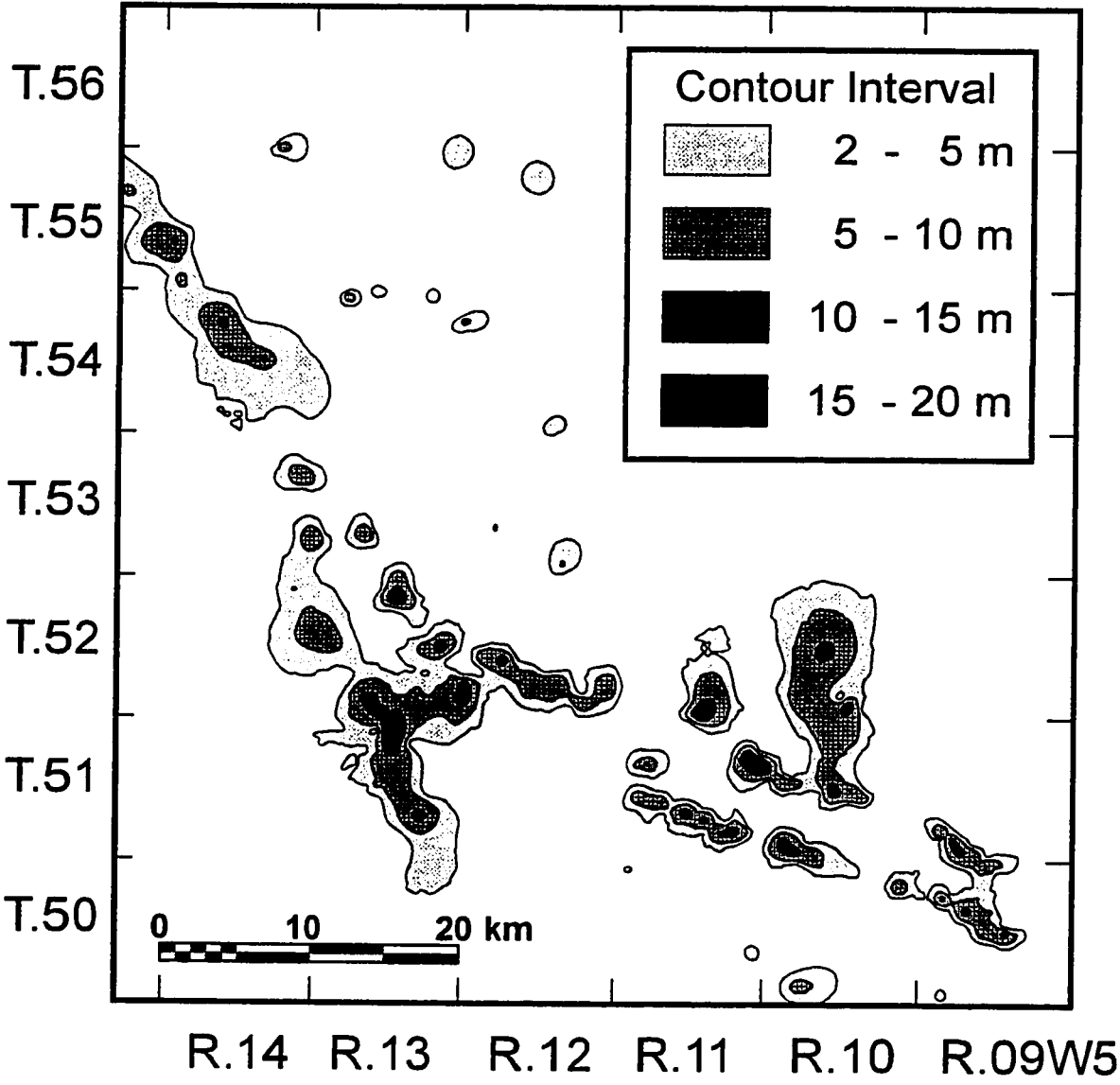

Figure 1.3 Isopach map of the Carrot Creek conglomerates within the Cardium Formation. For clarity reasons, values less than 2m were not charted.

continental/transitional (Kakwa) sediments of the Cardium Formation. Composite vertical facies sequences for Carrot Creek and Kakwa fields are shown in Figures 1.4 and 1.5. respectively.

1.2 Objective of Research

Siderite is a common mineral constituent in the Cardium Formation, and occurs both as an early pore-filling, cementing phase and as concretions in clastic sediments (conglomerate, sandstone and mudstone) of apparently marine origin. Calcite is present in lesser amounts and its occurrence is restricted mostly to the conglomeratic units. The origin of these mineral phases is extremely important in confirming the suggested models for the depositional history and in interpreting the diagenetic history of the formation. In particular, it would be extremely useful to be able to distinguish between marine and non-marine siderite, early post-depositional siderite, and diagenetically later carbonate formed as pore-filling and/or replacement phases.

The stable ($\delta^{13}C$ and $\delta^{18}O$) and radiogenic $^{87}Sr/^{86}Sr$ isotopic composition of all diagenetic minerals will be used to interpret the evolution of the pore water within the sediments. Based on our present day understanding on the formation of siderite, the isotopic and elemental data should reflect the diagenetic environment of mineral precipitation. In places where petrographic evidence indicates early siderite formation, shortly after sediment deposition, the geochemical data may be used to determine the environment of sediment deposition (ie. marine brackish or fresh water). Any correlation

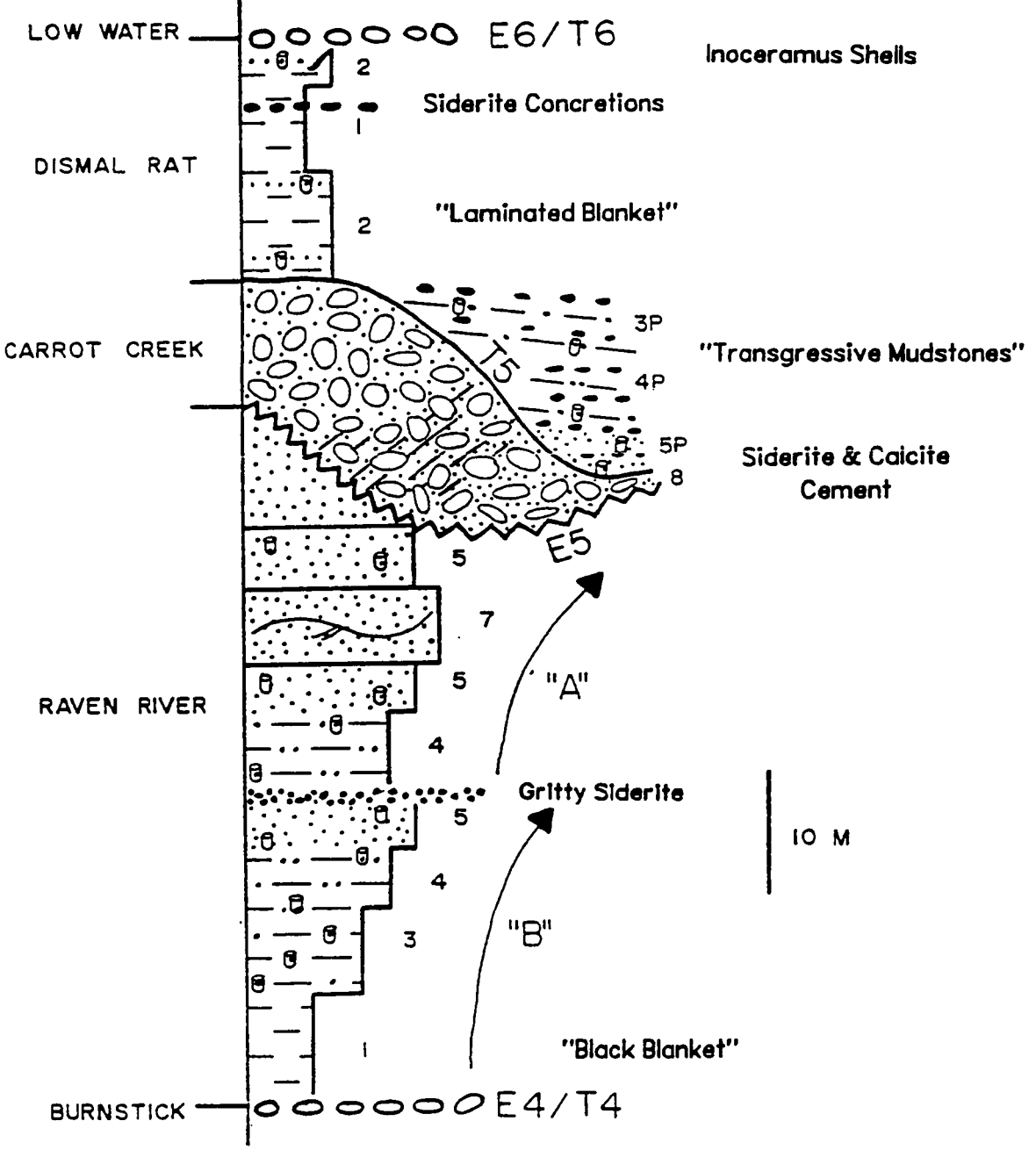

Figure 1.4 Idealized facies sequence for the Carrot Creek Member. Typical diagenetic carbonate phases are also shown. (Modified from Bergman, 1987)

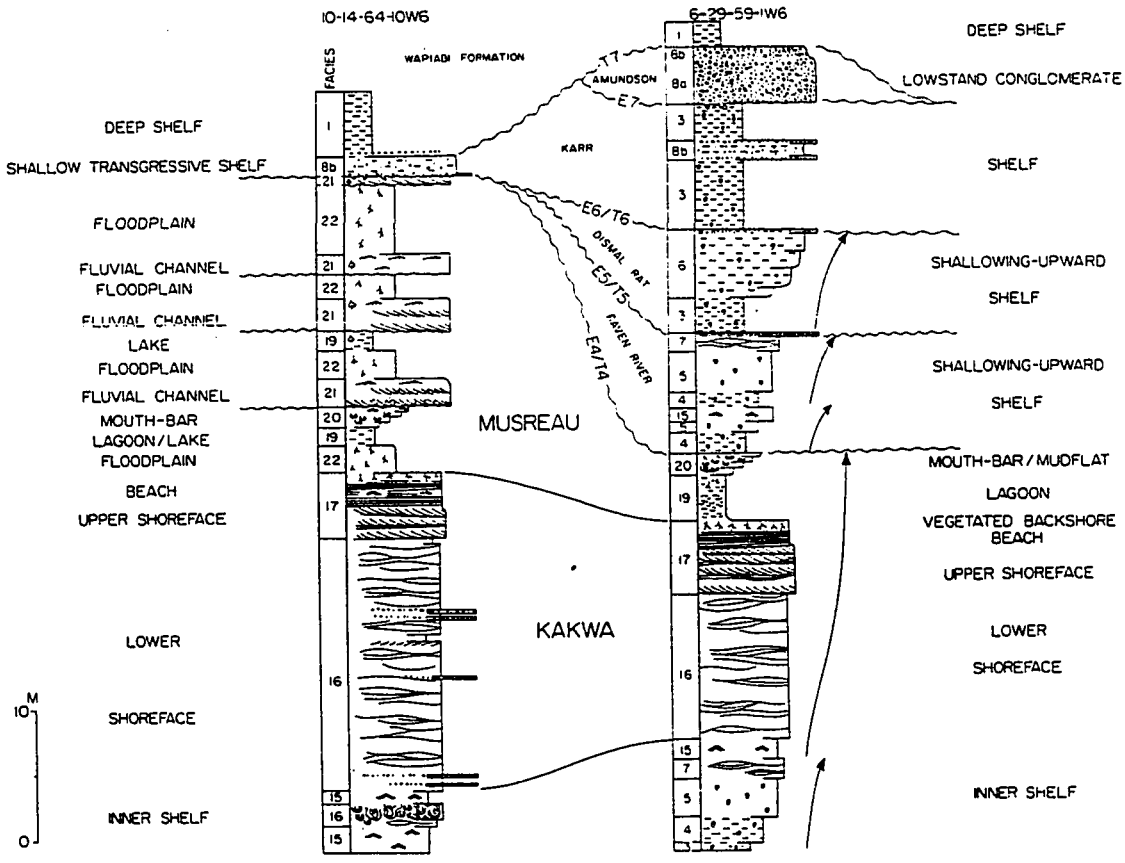

Figure 1.5 Comparison of two typical core sections from the western and eastern side of the Kakwa area. The wells are spaced 120 km apart. The numbers indicate facies. (From Plint and Walker, 1987)

between the isotopic/elemental composition of siderite and the depositional environment could be of considerable aid in future interpretation of similar clastic deposits.

It should be noted that Sr isotopic analysis of siderite-clay mixtures has not been previously documented. Doing this requires that any Sr isotopic work will deal with the development of an analytical technique for the extraction of Sr from siderite without contamination by radiogenic clay Sr.

CHAPTER 2

Formation of Siderite

2.1 Siderite Geochemistry

Siderite concretions, lenses, bands and cements occur in sediments ranging in age from Precambrian to Recent. Based on stable isotope studies, paleontological and/or lithological criteria, siderites in ancient sediments are interpreted to have formed in either marine, brackish or freshwater environments (Weber et al., 1964; Timofeyeva et al., 1976; Matsumoto and Iijima, 1981; and others). Similarly, in more recent settings, siderite formation has been noted in freshwater (Postma, 1981), brackish water (Pye, 1981) and marine water environments (Craig, 1969; Gautier and Claypool, 1984).

The conditions under which siderite will precipitate are very limited. Low Eh, low $\Sigma S^{=}$, high P_{CO_2} (ie. high dissolved inorganic carbon (DIC) concentration), high pH and high Fe^{2+} concentration (Figures 2.1, 2.2 and 2.3) favour siderite formation (Garrels and Christ, 1965; Berner, 1964 and 1971). Consider the reaction

$$FeCO_3 + Ca^{2+} \rightleftharpoons CaCO_3 + Fe^{2+} \quad (1)$$

$$K = 0.005 = a_{Fe^{2+}}/a_{Ca^{2+}} \quad (2)$$

where K is the equilibrium activity ratio. For siderite to be relatively stable over calcite, the concentration of iron (Fe^{2+}) must be greater than 0.5% that of calcium. (Woodland and Stenstrom, 1979). For average river water, the concentration of $Fe^{2+} \simeq 3.5\%$ Ca^{2+}, well within the siderite stability range. In freshwater, dissolved sulphate is also low and in such environments anaerobic oxidation of organic matter within sediments can result

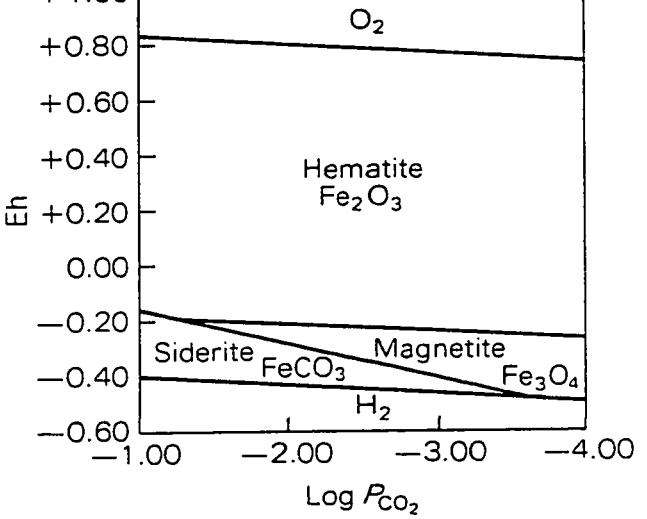

Figure 2.1 Eh-log P_{CO_2} diagram for hematite, magnetite and siderite in marine sediments. $T = 25°C$, $P_{total} = 1$ atm, $a_{Ca^{2+}} = 10^{-2.58}$ equilibrium with calcite assumed and $\Sigma S^{=}$ is assumed to be so low that pyrite and pyrrhotite do not plot stably. (From Berner, 1971)

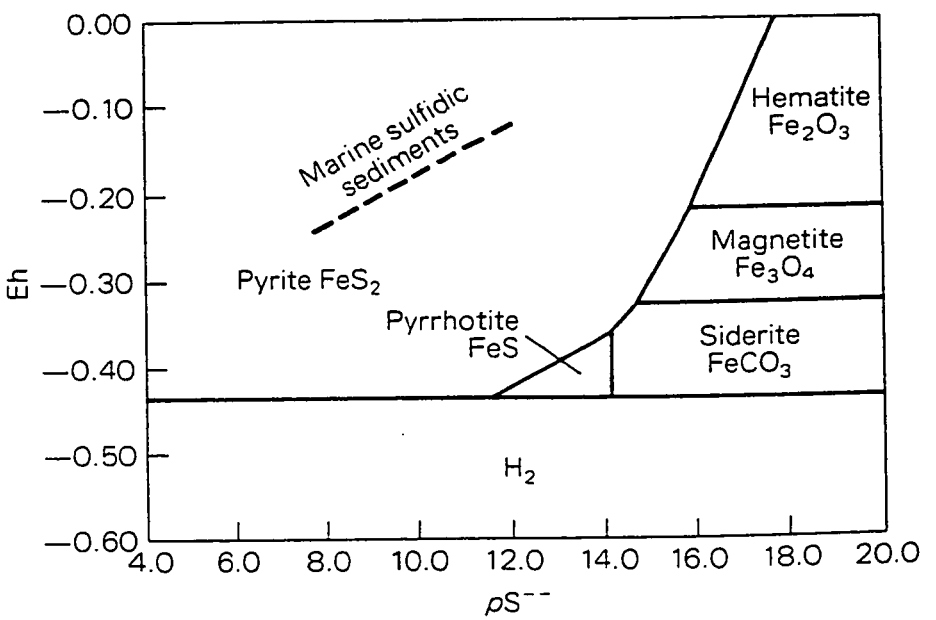

Figure 2.2 Eh-$pS^{=}$ diagram for pyrite, pyrrhotite, hematite, magnetite and siderite in water. The parameter $pS^{=}$ is the negative logarithm of the activity of sulphide ion. $T = 25°C$, $P_{total} = 1$ atm, pH = 7.37, and log $P_{CO_2} = 2.40$. (From Berner, 1964)

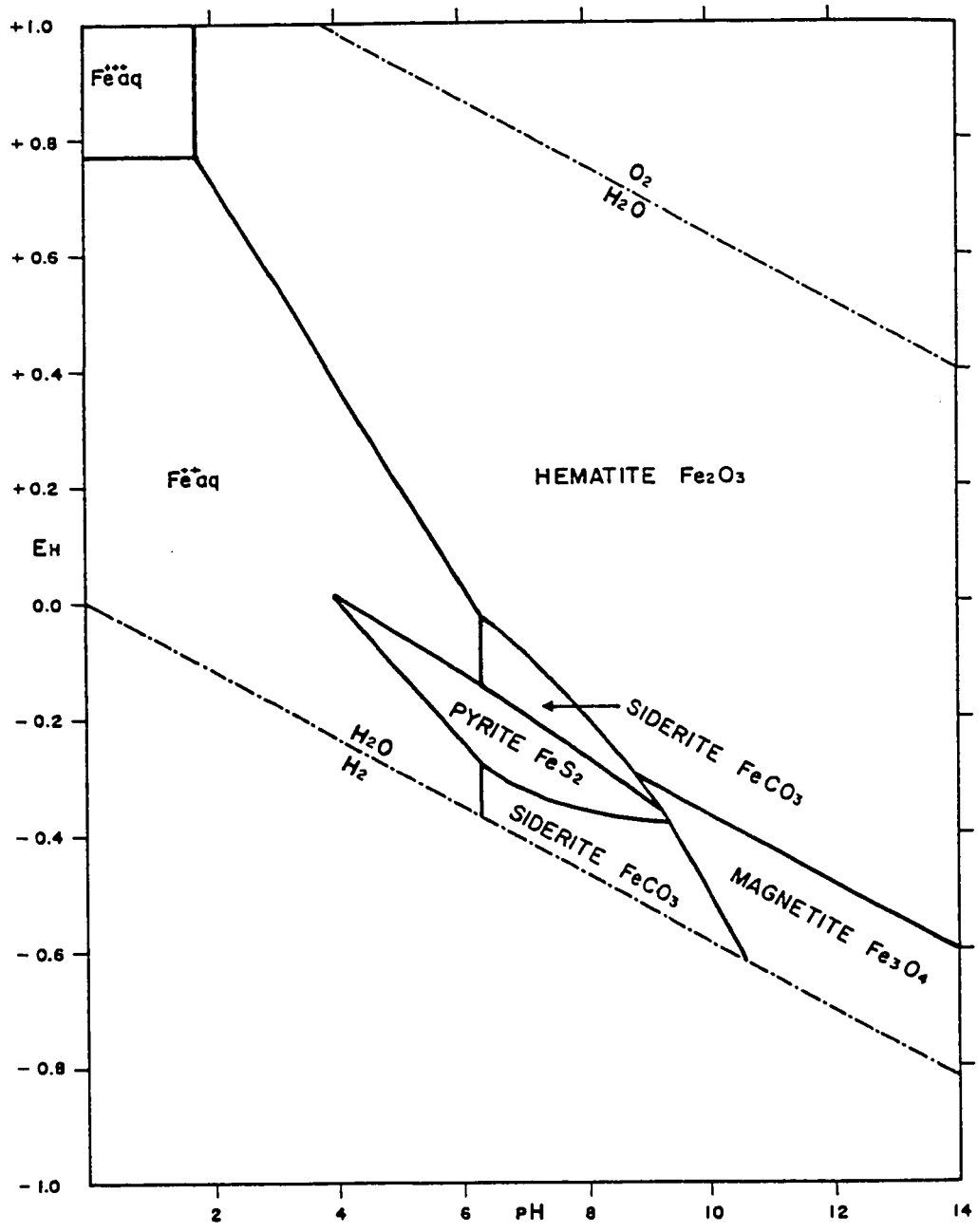

Figure 2.3 Eh- pH diagram for iron oxides, sulphides and carbonate in water. T = 25°C, P_{total} = 1 atm, total dissolved sulphur = 10^{-6}, and total dissolved carbonate = 10^{0}. (From Garrels and Christ, 1965)

in high DIC and low $\Sigma S^{=}$ concentrations. Under such conditions, siderite is stable and can precipitate in porespaces of freshwater saturated sediments.

2.2 Siderite in Marine Environments

2.2.1 Conditions for Marine Siderite Precipitation

In seawater, the concentration of $Fe^{2+} \simeq 0.002\%$ Ca^{2+}, a value so low that siderite would be considered thermodynamically unstable in such an environment (Berner, 1971; Woodland and Stenstrom, 1979). Additionally, the sulphate content is high and anaerobic oxidation of organic matter will almost certainly result in the reduction of SO_4^{2-}. Under these conditions $\Sigma S^{=}$ consists of either H_2S or HS^{-} (Figure 2.4) and pyrite will be thermodynamically more stable than siderite (Berner, 1971 and 1981). Thus it appears that siderite can precipitate from seawater only if sulphate reduction is inhibited or the dissolved sulphides are removed, and the iron concentration increased with respect to calcium. Berner (1971) notes that precipitation of siderite from seawater under conditions where sulphate reduction is inhibited, so that SO_4^{2-} will exist in a metastable form, represents an unusual situation and has never been observed in modern marine sediments. Depleting the $\Sigma S^{=}$ from the pore waters by precipitation of pyrite or other sulphide phases appears to be a less complicated mechanism for explaining subsequent siderite formation. In the Cardium Formation pyrite is ubiquitous. The very fine grained framboidal pyrite, which paragenetically precedes the siderite, indicates that the sediments initially passed through a zone of sulphate reduction.

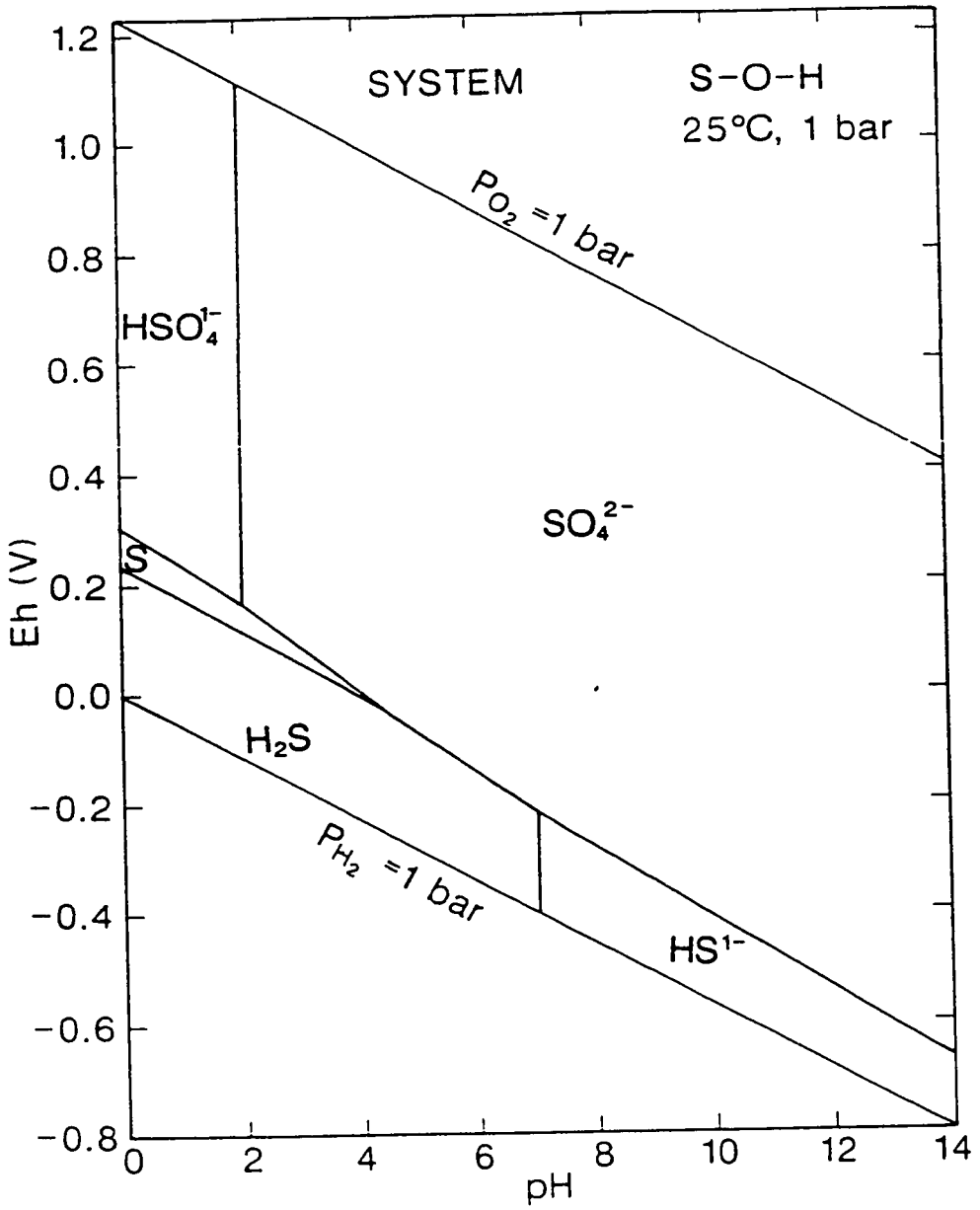

Figure 2.4 Eh-pH diagram for part of the S-O-H system. The activity of dissolved S = 10^{-3} (approx. 32 ppm). (From Brookins, 1988)

2.2.2 Organic Matter Degradation and Diagenetic Siderite Precipitation

In sedimentary environments where the rate of organic matter input exceeds the rate of its oxidation by dissolved oxygen, there will be a net accumulation of the organic material within the sedimentary pile. For marine sediments, organic matter is the main reduced constituent being oxidized. With increasing depth in the sedimentary pile, different oxidants are used in the redox reactions which govern the breakdown of organic matter. As one oxidant is consumed it is replaced by the next most efficient species (eg. Claypool and Kaplan, 1974; Froelich et al., 1979; Berner, 1980). This degradation of organic matter is usually mediated by bacteria which are ubiquitous in aqueous environments. The main processes involved in organic matter degradation and the common diagenetic mineral precipitates are shown in Table 2.1.

If under anoxic conditions sufficient organic carbon is present in the sediments, and if dissolved sulphate is present, then bacterial reduction of sulphate ensues (eg. Claypool and Kaplan,; Irwin et al., 1977). For example,

$$SO_4^{2-} + 2CH_2O \rightarrow H_2S + 2HCO_3^- \qquad (3)$$

From equation (3) it can be seen that sulphate reduction is limited by the supply of organic matter and by the availability of SO_4^{2-}. Goldhaber and Kaplan (1974) noted that the diffusion of sulphate from overlying seawater into anoxic sediments is limited by the sedimentation rate. In recent marine, organic rich sediments with slow accumulation rates, the dissolved sulphate is generally present to depths as great as hundreds of meters. However, aqueous sulphate is depleted at shallow depths in rapidly accumulating, organic rich sediments.

OXIC ENVIRONMENT	Common Diagenetic Minerals
1) Aerobic Respiration	MnO_2, Fe^{III}-oxides
$CH_2O + O_2 \rightarrow CO_2 + H_2O$	
SUBOXIC ENVIRONMENT	
2) Nitrate Reduction	CaMg-calcite
$5CH_2O + 4NO_3^- + 4H^+ \rightarrow 2N_2 + 5CO_2 + 7H_2O$	
3) Manganese Reduction	Mg-calcite, Ca-dolomite
$CH_2O + 2MnO_2 + 4H^+ \rightarrow 2Mn^{2+} + CO_2 + 3H_2O$	
4) Iron Reduction	FeMg-Calcite
$CH_2O + 2Fe_2O_3 + 8H^+ \rightarrow 4Fe^{2+} + CO_2 + 5H_2O$	
ANOXIC ENVIRONMENT	
5) Sulphate Reduction	pyrite, marcasite, rhodochrosite
$2CH_2O + SO_4^{2-} \rightarrow S^{2-} + 2\,CO_2 + 2H_2O$	
6) Methanogenesis	siderite, Fe-calcite, glauconite
$2CH_2O \rightarrow CH_4 + CO_2$	
7) Thermal Decarboxylation	Fe-calcite, siderite
$R.COOH \rightarrow RH + CO_2$	

Table 2.1 Reactions of metabolic processes involved in the degradation of sedimentary organic matter and common associated diagenetic mineral precipitates. CH_2O designates simple organic matter. The equations are written with respect to their position in a sedimentary sequence and their corresponding Gibbs free energy changes decrease down sequence. For simplicity, minor intermediate reactions were omitted. (Data compiled from Claypool and Kaplan, 1974; Irwin et al, 1977; Froelich et al, 1979; Berner, 1980; Matsumoto and Iijima, 1981; and Curtis et al, 1986.)

Below the zone of sulphate reduction, microbial methanogenesis is the dominant process involved in the continued decomposition of organic matter (Table 2.1 and Figure 2.5: eg. Claypool and Kaplan, 1974; Hennessy and Knauth, 1985; Curtis and Coleman, 1986). If the organic rich sediments also contain some Fe^{III} oxides, then the combined effect of CO_2 production (Reactions 1 to 7 in Table 2.1), iron reduction (Reaction 4 in Table 2.1) and continued organic degradation by microbial methanogenesis would result in the precipitation of siderite,

$$7CH_2O + 2Fe_2O_3 \rightarrow 3CH_4 + 4FeCO_3 + H_2O \quad (4)$$

The carbon isotopic composition of siderite should reflect this process. During methanogenesis, isotopically heavy ^{13}C siderites should form with the light carbon going into the methane (Figure 2.6; Gautier and Claypool, 1984). The inference is that siderite can precipitate soon after sediment deposition and at shallow depths in areas where the sedimentation rate is high, but is prohibited in forming, except possibly at considerable depth, in slowly accumulating sediments. Furthermore, zones of siderite formation will be controlled by microbial methanogenic processes.

The explanation given above is in agreement with the currently accepted conditions which limit siderite formation (low Eh, low $\Sigma S^{=}$, etc.). The geochemical data also agree with this interpretation and will be discussed in the succeeding chapters.

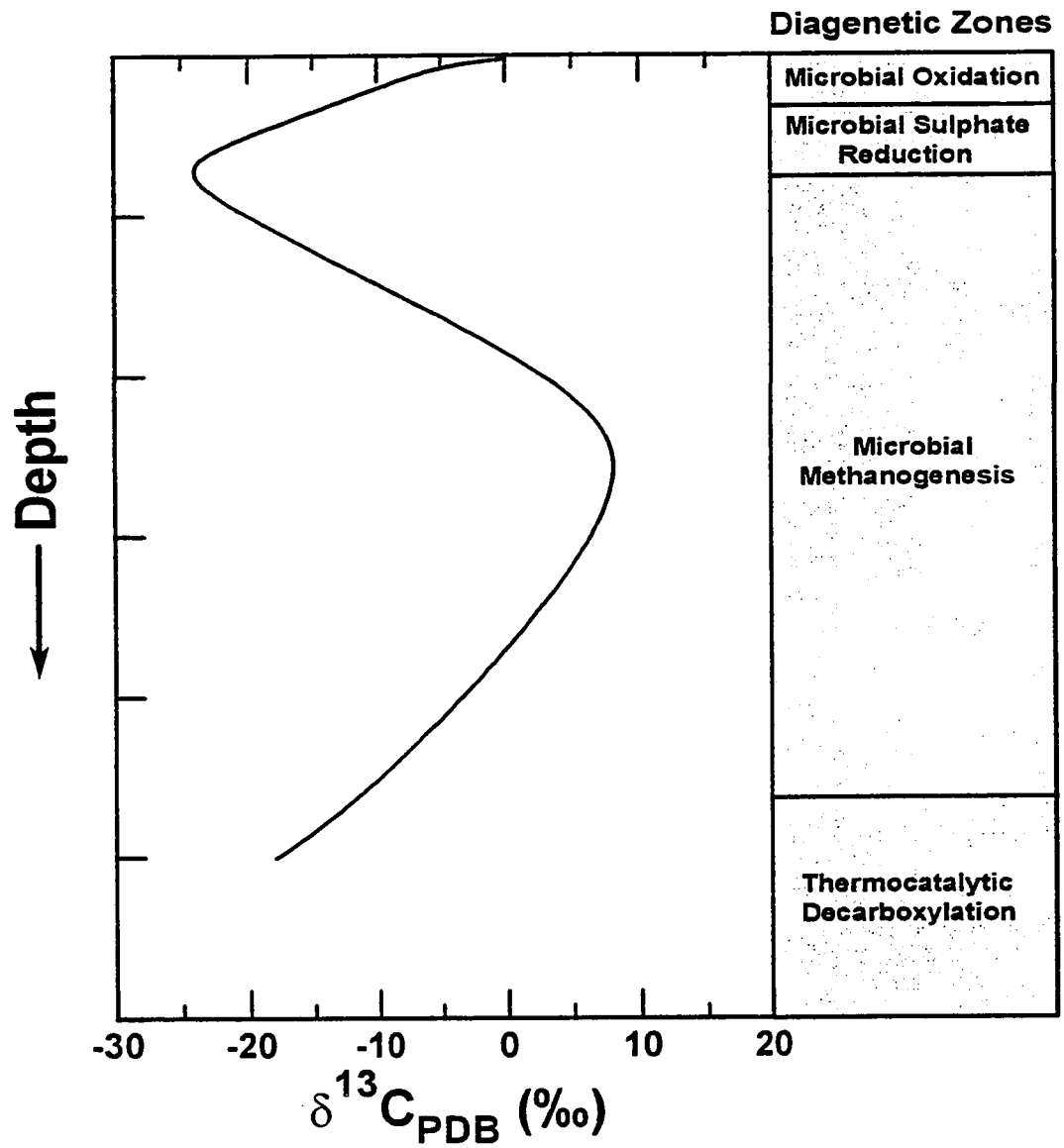

Figure 2.5 Generalized diagram showing the effects of reactions within distinct diagenetic zones on the $\delta^{13}C$ of CO_2 dissolved in pore waters of deep sea sediments. True depth intervals are not shown since they vary from site to site (being dependent on external parameters such as sedimentation rate). The profile shown is derived from Claypool and Kaplan (1974).

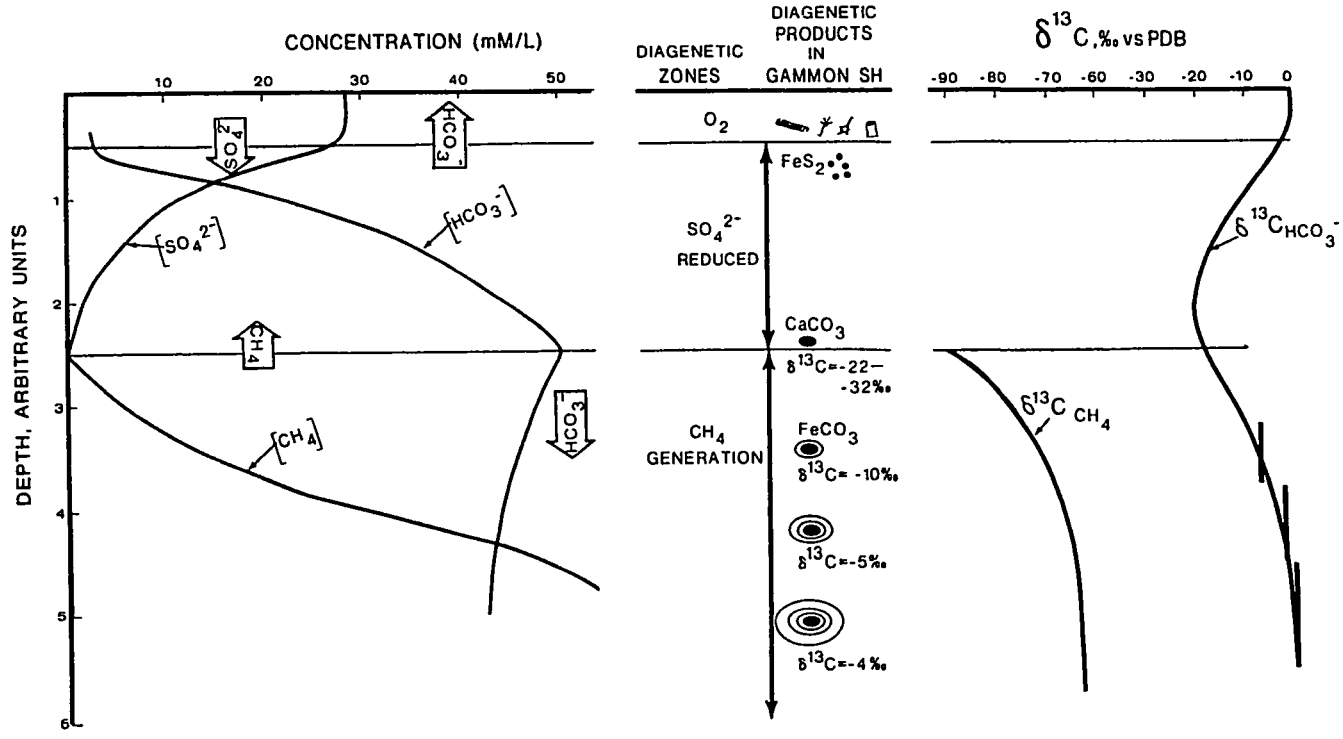

Figure 2.6 Principal chemical and isotopic trends (SO_4^{2-}, HCO_3^- and CH_4) of interstitial waters during early diagenesis of the Gammon Shale, inferred from diagenetic products. (From Gautier and Claypool, 1984)

2.2.3 Source of Iron

The conditions required for siderite formation are such that it is a product of the diagenetic environment rather than direct precipitation from overlying waters. Under such conditions there are three possible sources of iron:

1) Original pore water of the sediment
2) Migrating fluids
3) Detrital minerals

The concentration of iron in seawater and river water is low, approximately 0.01 and 0.7 ppm respectively (Blatt et al., 1980). Such concentrations in the initial pore fluids would be inadequate to account for the large quantities of siderite present. Furthermore, the high calcium activity in marine waters would favour calcite formation over siderite (Berner, 1971). Migrating continental waters such as waters draining peat bogs are relatively high in Fe^{2+} (Woodland and Stenstrom, 1979). Lateral flow of such waters could supply the iron essential for siderite formation. The effects of this lateral movement should be reflected in a higher siderite concretion population adjacent to the source area (Woodland and Stenstrom, 1979). Presently no such zonational distribution of siderite has been noted in the Cardium Formation. Goldhaber and Kaplan (1974) note that a high iron content in many marine sediments is associated with the clay fractions. This is based on a good correlation between total iron and clay mineral content. Iron oxide coatings on the surface of the clay mineral platelets are commonly produced during rock weathering and soil formation, and represents the bulk of iron transported by clay minerals (Carroll, 1958). Blatt et al. (1980) note that the Amazon River, which has an

iron content of 3 ppm, could carry a sufficient amount of ferric iron as colloids and adsorbed on clays and organic matter to form a major iron formation in 176,000 years. Therefore, it is likely that under anoxic conditions iron from the continentally derived sediments can be mobilized as ferrous iron, increasing the concentration of Fe in the pore water to the point where siderite will be more stable than calcite (ie. $Fe > 0.005Ca$).

2.2.4 Iron and Microbial Processes

As discussed in the above section, diagenetic reactions in pore water of deep-sea sediments are closely related to numerous bacterial processes which vary with depth in the sedimentary pile (Table 2.1, Figures 2.5 and 2.6; Claypool and Kaplan, 1974). In general, strains of *Disulfovibrio* and methanogenic bacteria are associated with zones of sulphate reduction and methane production respectively. Since siderite can precipitate in the zone of methanogenesis, it is possible that siderite formation is directly related to these bacterial processes.

Several bacteria have been observed in laboratory experiments and in natural sediments to precipitate siderite and magnetite by dissimilatory iron reduction (Bell et al., 1987; Ellwood et al., 1988; Lovley et al., 1987). A bacteria, GS-15, found in sediments of the Potomac River, effectively couples organic matter oxidation to ferric iron reduction during growth under anaerobic conditions (Lovley et al., 1987). Each mole of acetate that GS-15 oxidizes, results in the production of two moles of CO_2 and the reduction of eight moles of ferric iron (Fe^{3+}) to ferrous iron (Fe^{2+}). Furthermore, Lovley and Phillips (1987) demonstrated that in the presence of reactive iron, such as

coatings of amorphous iron(III) oxyhydroxide on clays, Fe-reducing bacteria will significantly inhibit the activity of sulphate-reducing bacteria and methanogens. Depending upon the form of the organic substrate, Fe(III) form, Eh, pH and other microenvironmental conditions, Fe^{2+} produced during dissimilatory iron reduction can form a variety of iron minerals, including siderite (Bell et al., 1987). The common occurrence of siderite throughout the Cardium formation suggests that Fe^{3+} reduction may have been an important microbial process during the early stages of diagenesis. The ability of Fe-reducing bacteria to drastically inhibit the activity of sulphate-reducing bacteria and the rapid sedimentation rate (which will hinder the diffusion of sulphate into the sedimentary pile) explains why siderite is so dominant compared to pyrite in the Cardium Formation. Sedimentary siderites in the Kuparuk Formation of Alaska are also attributed to have formed via Fe^{3+} reducing microbial processes (Mozley and Carothers, 1992).

It is not in the scope of this research to verify the pathway that iron takes in the formation of siderite. However, bacterial processes can be temperature sensitive, and if microbial activity was involved in the production of Fe^{2+} and any subsequent siderite precipitation, then one can conclude that siderite formed at relatively low temperatures (ie. $<65^{\circ}C$, Surdam et al., 1984; $<80^{\circ}C$, Carothers and Kharaka, 1980), and therefore at "shallow" depths.

2.2.5 Modern-Day Examples from the DSDP

Siderite is a common mineral in ocean sediments investigated by members of the Deep Sea Drilling Project (DSDP). There are over 240 references to siderite in the 96 volumes of the Initial Reports of the Deep Sea Drilling Project (See Appendix, for a summary on some DSDP sites where siderite was more than just a trace mineral in these sediments). The age of siderite bearing sediments are not restricted to any specific time period. Oceanic sediments containing siderite range in age from Lower Cretaceous through to the Pleistocene.

Macroscopically, the mode of occurrence of siderite in oceanic sediments can range from fine grains disseminated throughout the sediment (Lancelot and Ewing, 1972; Lancelot et al., 1972) to more concentrated cement (Einsele and von Rad, 1979) or assemblage of well-sorted, silt-sized grains (Beall et. al, 1973) to zones of predominantly sideritic nodules, lenses and bands up to 6 cm thick (Hollister et al., 1972a; Lancelot and Ewing, 1972; Basov et al., 1979; Arthur, 1979). The concentration of siderite ranges from sediments with only trace amounts to concentrated zones where it can reach 95 volume percent of the sediment (Hollister et al., 1972b).

Microscopically, siderite occurs as well-crystallized rhombs in hemipelagic sediments (Lancelot and Ewing, 1972), minute spherulites which measure about 0.005 to 0.010 mm in a muddy matrix of a sandstone (Laughton et al., 1972), assemblages of silt-sized spherulites (Beall et al., 1972), microsparitic cement in a terrigenous silt layer (Einsele and von Rad, 1979), and bands, lenses and nodules composed of siderite grains of diverse concentration, size (up to 0.1 mm) and crystal perfection (Basov et al., 1979).

The occurrence of siderite in oceanic sediments has been interpreted four different ways:

1) Peterson et al. (1970) noted siderite frequently associated with rhodochrosite ($MnCO_3$) and cristobalite (SiO_2) and they suggested that it is a recrystallization product formed as a result of some hydrothermal alteration of pre-existing tuffs. Although this may be a possible explanation for siderite formation at this site, it is not a common process at other sites.

2) Siderite found in coarse terrigenous sediments is also terrigenous in origin (Beall and Fischer, 1969).

3) Siderite in the sediments is diagenetic in origin and formed as a result of dissolution/replacement of pre-existing calcite (either skeletal or early diagenetic) by siderite (Hollister et al., 1972c; Lancelot and Ewing, 1972; Laughton et al., 1972; Einsele and von Rad, 1979; Arthur, 1979). The replacement of a carbonate precursor by siderite is evident in the sediment at site 106 (Lower Continental Rise) where there is a negative correlation between the amounts of siderite and calcareous microfossils (Hollister et al., 1972c).

4) Authigenic or diagenetic precipitation of siderite without a calcite precursor (Beall et al., 1973; Einsele and von Rad, 1979; Chamley et al., 1979; Basov et al., 1979). In Lower Cretaceous sediments near Galicia Bank (west of Spain), siderite distribution shows a direct correlation with the concentration of organic matter in clayey pelites (Basov et al., 1979). This would imply that bacterial reduction of

organic matter in the sediment would produce the required carbonate for siderite precipitation.

The general consensus appears to be that siderite in oceanic sediments is of an authigenic or diagenetic nature. Pyrite is a common constituent in these sediments and indicates that the sediments have passed through a stage of sulphate reduction. Further pyrite formation was hindered by rapid sedimentation rates which prevented sulphate diffusion into the sedimentary pile and maintained anaerobic conditions very close to the sediment water interface. Reported sedimentation rates where siderite is common range from 4.3 cm/1000 yrs (Peterson et. al., 1970) to 7.5 cm/1000 yrs (Arthur, 1979) to as high as 20 cm/1000 yrs. (Lancelot and Ewing, 1972). The high DIC concentration required for siderite formation appear to be site specific and is either due to bacterial reduction of organic matter or dissolution of carbonate present in or near the sediments. Finally, the iron (high Fe/Ca ratio) necessary to produce siderite is either adsorbed on pelagic clays in the sediments (Basov et al, 1979; Matsumoto, 1983) or there may be local carbonate-poor terrigenous sediments with high Fe/Ca ratios (Arthur, 1979).

CHAPTER 3

Petrography and Diagenesis of the Cardium Formation

3.1 Petrographic Description of Diagenetic Phases

These petrographic descriptions are based on thin sections predominantly from the Carrot Creek field plus a few from the Kakwa, Pembina, and Garrington fields. Petrographic investigation reveals that there are at least 5 different types of siderite, 3 or more types of calcite and several other diagenetic minerals. The following is a summarized description of the main diagenetic minerals.

Siderite:

Siderite is a common mineral in many units of the Cardium Formation. It can be found in very fine grained mudstones through to very coarse grained conglomerates; in bioturbated and undisturbed sediments; and in marine (Carrot Creek), brackish and freshwater (Kakwa) sediments. The mineral can be found dispersed in sediments with concentrations ranging from $< 1\%$, to zones up to 40 cm thick composed almost entirely of siderite. There is no lateral or vertical control over siderite distribution, however, it appears more prevalent near and within the conglomeratic units. Siderite in the Cardium Formation can be generalized to occur as follows:

I) Gritty, bioturbated, sideritic mudstone ("gritty siderite"), of regional extent.

II) Homogeneous concretionary layers up to 0.4 m thick, within mudstones and sandstones.

III) Concretionary layers <10 cm thick, within slightly bioturbated sands and conglomerates, less homogeneous, increased grit content, of local extent.

IV) In the conglomerate as matrix, pore-filling, pore-lining cements, and replacing clasts.

V) Rip-up, sideritic clasts in sandstone or conglomerate.

Microscopic investigations reveal that the siderite has six distinct types of mineral forms. A detailed description of these forms is as follows:

A) Very fine grained (micritic) siderite which occurs most commonly as light brown seams (less than 3 cm thick) and as matrix material within the conglomerate and sandstone (Fig. 3.1A). The grains are dominantly anhedral, but may contain spherulitic and granular (microspar) forms. Quartz grains less than 0.15mm and clay minerals are dispersed throughout the micritic siderite seams/matrix.

B) Spherulitic pore-filling siderite 0.015 to 0.4 mm in diameter. The coarser fraction may exhibit a characteristic "iron cross" extinction. There is commonly a nucleus which consists of either a poorly to well developed rhombic siderite crystal, a fine grained clast, or a very fine grained opaque mineral (Fig. 3.1B). A detailed analysis of the inclusions reveals that they are sideritic in composition (unpublished data, pers. comm., Suchecki, 1988). This phase is common in siderite nodules/bands of varying thickness and as conglomerate cement.

C) Granular (or saccharoidal) pore-filling siderite 0.02 to 0.25 mm in diameter. The grains are equidimensional and differ from the spherulites in that a nucleus is not present, or at least not very distinct (Fig. 3.1C). The fine grained fraction grades

Figure 3.1 Six common siderite forms found in the Carrot Creek conglomerate of the Cardium Formation.

A) Very fine grained, micritic siderite. 5-36-52-13W5, 1587.3m

B) Spherulitic siderite with dark fine grained sideritic nucleus. 16-2-54-12W5, 1397.4m

C) Granular siderite. 5-36-52-13W5, 1587.1m

D) Rhombic siderite crystals on clast surfaces. 5-36-52-13W5, 1587.1m

E) Sheaf-like siderite bundles seeded on the surface of clasts. 10-35-52-13W5, 1593.5m

F) Sparry siderite filling pore space between clasts. 16-30BQ-53-13W5, 1560m

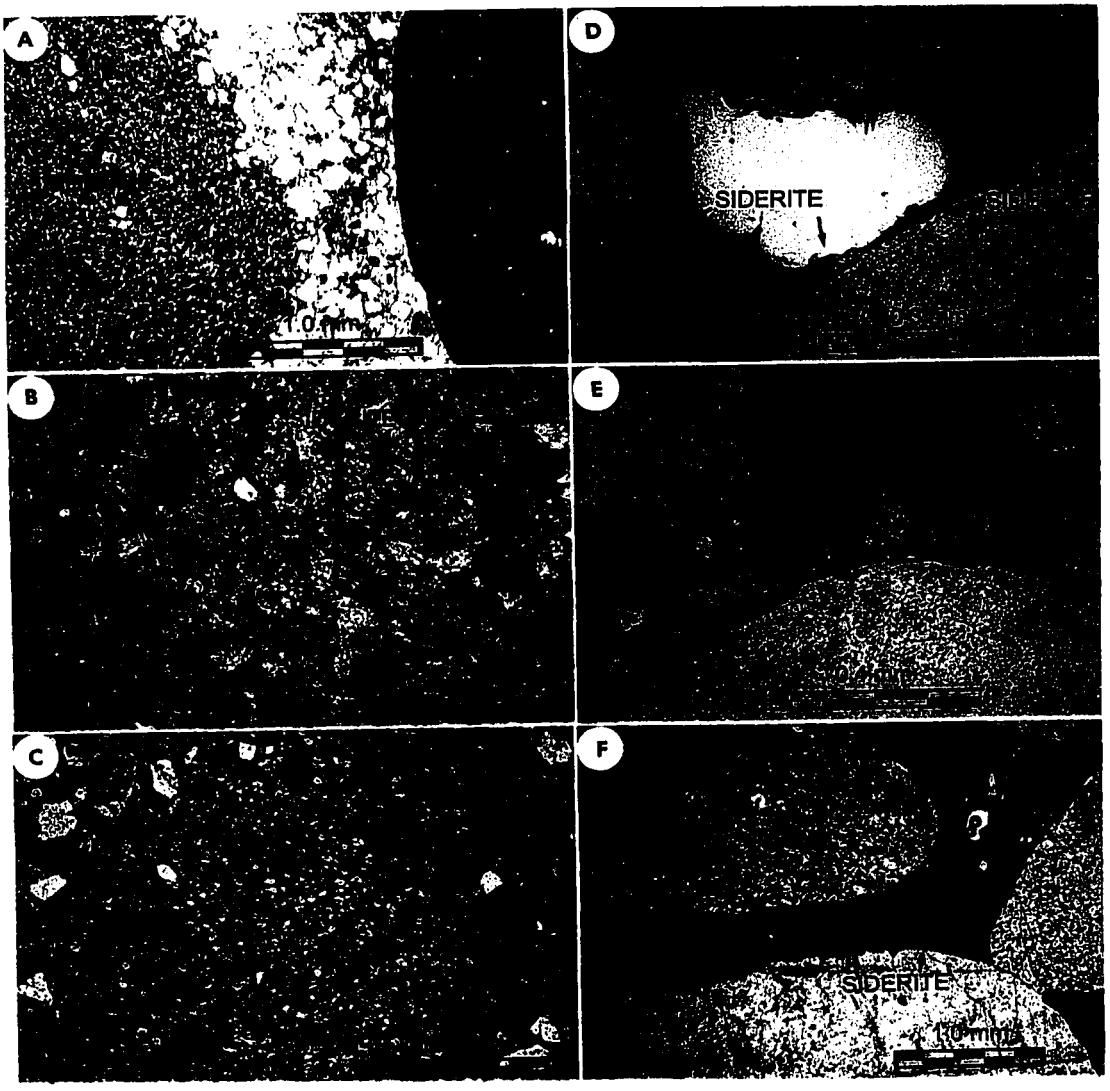
A
1.0 mm
D
SIDERITE
B
E
C
F
SIDERITE
1.0 mm

into the micritic siderite. This phase may be a microspar equivalent of the micritic siderite. It is commonly found in siderite nodules/bands and as conglomerate cement.

D) Elongated rhombic siderite 0.06 to 0.4 mm in diameter. This lozenge shaped siderite occurs along the rims of clasts, as a pore-lining cement and as isolated crystals disseminated in porespaces within the sandstone and conglomerate facies (Fig.3.1D). Occasionally these rhombs may surround clasts in tight clusters yielding a druse cement type of texture. This siderite form represents a very minor phase.

E) Sheaf-like bundles of rhombic siderite 0.2 to 1.5 mm in diameter. This form generally occurs seeded on the rims of clasts and as pore-lining cement. Occasionally these siderite bundles can be so tightly clustered that they totally surround the clasts (Fig. 3.1E). The siderite is commonly found in the sandstone and conglomerate. A common characteristics of this siderite is its association with areas of the conglomerate lacking a mud matrix, and during its growth the pore-lining cement only partially occluded the primary porosity.

F) Sparry siderite 0.2 to 1.7 mm in length. Some have a characteristic iron cross extinction (Fig. 3.1F). The siderite occurs as a pore-filling cement in the conglomerate and sandstone facies. It appears to be associated with regions of the conglomerate that were void of matrix material.

The mineral form appears to be related to the porespace available during mineral precipitation. Where the conglomerate is matrix supported and porespace is low, the mineral forms are type A, B, C, and D. In clast supported conglomerates, the dominant mineral forms are type D, E and F. In nodules/bands the forms tend to be B and C.

Calcite:

Compared to siderite, calcite is less abundant and does not display as variable a mineral form as does the siderite. Staining of the samples for Fe indicates that all calcites are ferroan. Due to the ferroan composition of the calcites, cathodoluminescence and staining techniques are of limited use in distinguishing the different phases. There may exist several calcite phases, but only 3 types are present in significant amounts for isotopic analysis.

1) Sparry ferroan calcite (I). It occurs commonly as a sparry pore-filling cement in the conglomerate (Fig 3.2A). The calcite postdates the pyrite and conglomeratic siderite. Where the calcite cement is present, there are generally less sutured contacts between clasts, and the calcite is sometimes strained. In hand specimen the calcite has a clear to white color.

2) Sparry ferroan calcite (II). The calcite occurs as a sparry pore-filling cement in the conglomerate facies. In places it appears to be a replacement of the conglomeratic siderite (Fig. 3.2B). Occasionally relict siderite phases can be seen in large plates of this calcite cement. In hand specimen it has a grey to pale brown color.

3) Vein filling calcite (III). The calcite is a late stage, ferroan sparry calcite which occurs in vugs and cross cutting veins. Well developed, very coarse grained rhombic crystals (Fig. 3.2C) which have grown perpendicular to cavity walls are common. It can also occur as a pore-filling cement in the conglomerate, where it is distinguished from the sparry ferroan calcite (I) and (II) by its cross-cutting nature

Figure 3.2 Calcite, pyrite and quartz diagenetic phases in the conglomeratic unit of the Cardium Formation

A) Framboidal pyrite crystals on clast surfaces. Sparry ferroan calcite (I) fills the pore spaces. 4-28-51-11W5, 1648.2m

B) Sparry ferroan calcite (II) filing pore space between clasts. Relict siderite (brown) is evident within the calcite. Note the quartz overgrowth on the siliceous clast, giving it an angular appearance. 9-3-52-11W5, 1571.5m

C) Fracture filling calcite in a gritty mudstone unit. 13-35-38-7W5 (Ferrier)

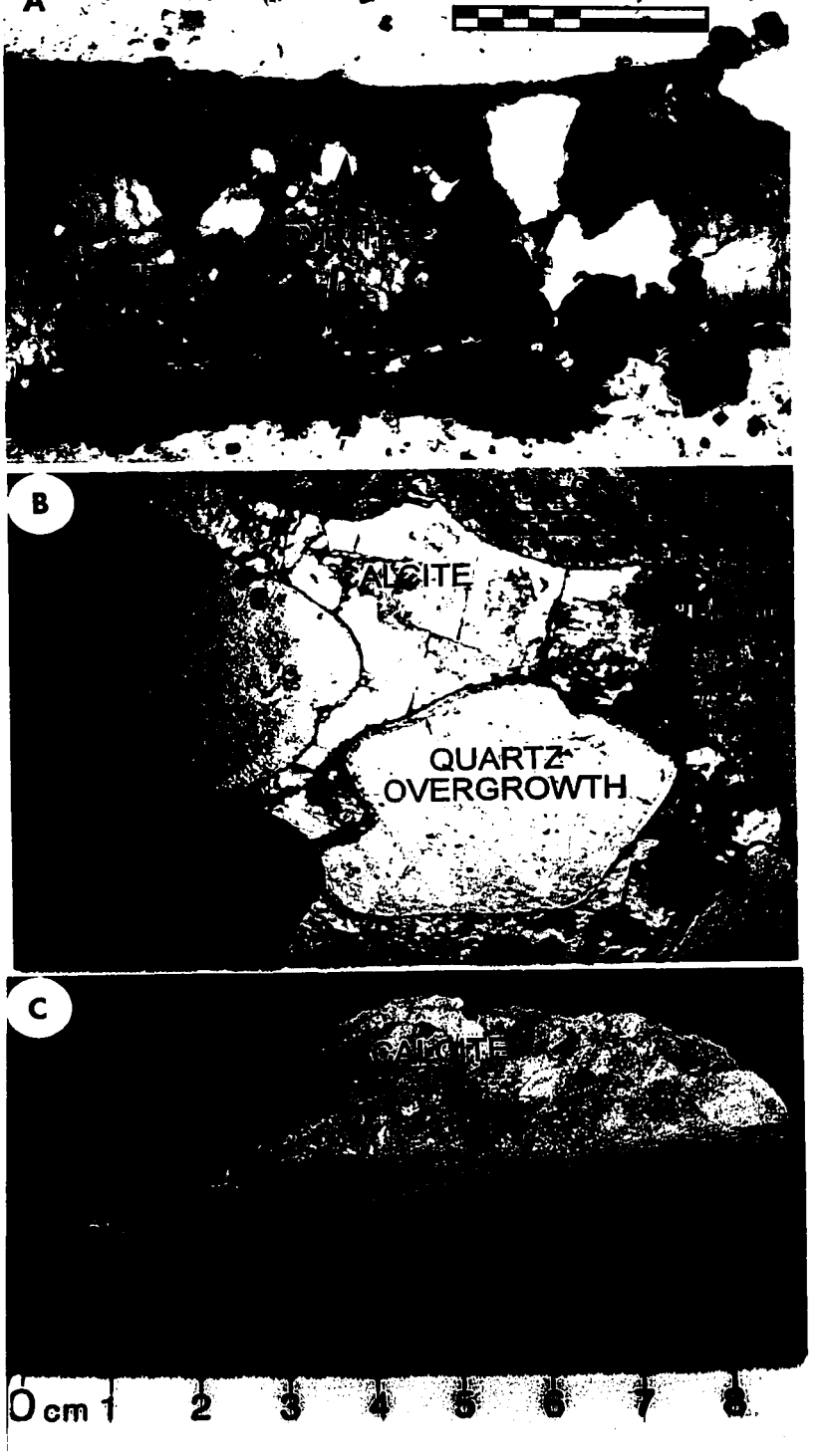
A
B
CALCITE
QUARTZ
OVERGROWTH
C
CALCITE
0 cm 1 2 3 4 5 6 7 8

(ie. filling fractures within clasts and previously formed siderite seams) and by its isotopic signature.

Kaolinite:

Secondary kaolinite occurs as very fine grained aggregates (<0.06 mm) in porespace of conglomerates (Fig. 3.3A), and in isolated pockets of the conglomerate "mud" matrix. The kaolinite formed later than the siderite and sparry ferroan calcite (I) and (II) but earlier than the vein filling calcite. In areas where kaolinite and calcite are found in contact, there appears to have been dissolution of calcite and precipitation of kaolinite. The kaolinite in the isolated pockets of the conglomeratic matrix probably formed as an alteration product of an alumino-silicate mineral grains such a feldspar.

Pyrite:

Except for one rare occurrence where a pocket of conglomerate matrix consists of mostly pyrite, it is not usually visible in hand specimen. However, microscopic observation indicates that pyrite is a common mineral in all lithologic units, including siderite horizons. The pyrite is usually not noticed due to its fine grain size (0.05 to 0.06 mm) and its disseminated distribution. Its opaque optical property also makes it hard to distinguish from the fine grained organic fragments in the sediment. The most common form of the pyrite is framboidal (Fig. 3.2A), although cubic, octahedral and anhedral forms may also be present. Many organic fragments with cell-like structures, when observed under reflecting light, indicate that they have been partially or completely

Figure 3.3 Kaolinite, quartz and organic debris in the conglomerate unit of the Cardium Formation.

A) Kaolinite filling pore space between clasts. Where calcite and kaolinite are in contact, the calcite has an corroded appearance and is partially replaced by kaolinite. 2-29-52-13W5, 1660.4m

B) Organic clast preserved in the conglomeratic unit. These fragments can be partially or completely replaced by pyrite. 2-29-52-13W5, 1661.1m

C) Quartz overgrowth on a conglomeratic clast. The overgrowth has formed an complete crystal with definable faces. 8-35-51-13W5, 1824.9m

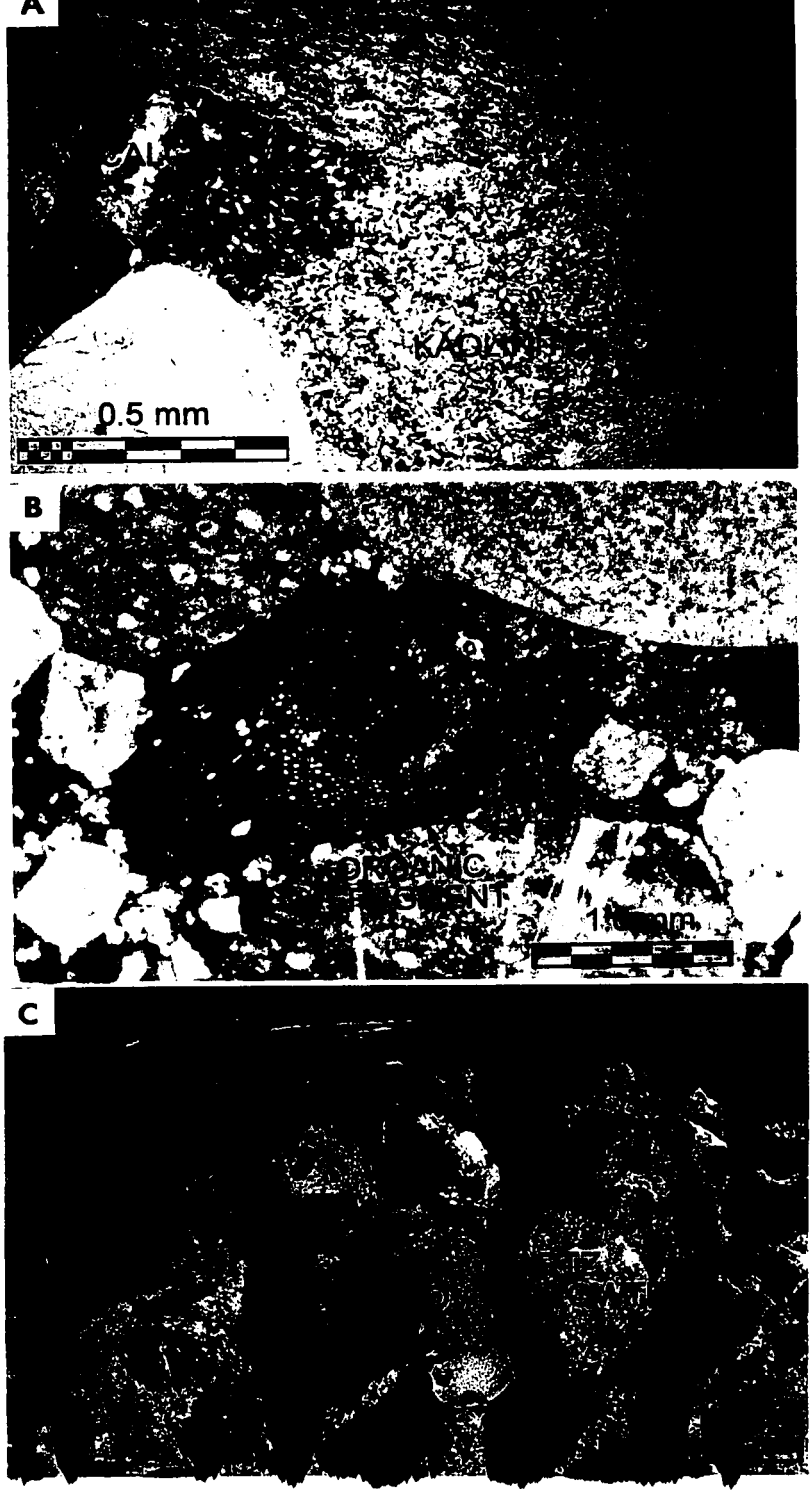
A
AL
KAOLIN
0.5 mm
B
C

replaced by pyrite. In the conglomerate facies the pyrite framboids can be found rimming clasts, and siderite (or calcite) cement may radiate outward from the pyrite. This suggests that pyrite precipitated at an early stage and predates siderite formation.

Quartz:

Secondary quartz is confined to the cherty clasts and grains in the conglomerate and sandstone. The clasts may be recrystallized to varying degrees and minor quartz overgrowths may also be common (Fig. 3.2B and 3.3C). Cavity filling chalcedony may occur filling vugs in the conglomerate or sandstone but more commonly it is found filling microcavities in large chert clasts which have undergone dissolution.

3.2 Petrographic Description of Detrital Phases

Quartz:

Monomineralic quartz grains <0.15mm in size are scattered throughout the conglomerate matrix and within the gritty siderite horizons. Although the conglomerates overly quartz rich sandstone units, abundant sand-sized quartz grains are lacking in the conglomerate matrix.

Feldspar:

Plagioclase is found in only a few thin sections. Trace amounts are evident from XRD spectra. Minor occurrences in the Cardium have also been noted by Staley (1987), Sweeney (1983) and Griffith (1981).

Organic Matter:

Organic matter is scattered throughout the sediments. In the conglomerate and sandstone facies it is usually preserved as fragments up to 1.6 mm in length (Fig. 3.3B). In a few isolated cases pockets of conglomerate with a coaly matrix can be found. The organic fragments are replaced by pyrite to varying degrees. Sediments rich in organic carbon such as coal seams up to 35 cm thick, black nonmarine mudstones, and carbonaceous black mudstones and sandstones have also been reported by Plint and Walker (1987). Organic fragments can also be found within siderite nodules/bands.

Clays Minerals:

Based on observation of Upper Cretaceous sediments by Longstaffe (1989), Staley (1987) and others, there is no doubt that various clay minerals formed during the diagenetic history of the Cardium Formation. These minerals are very fine grained and occur disseminated throughout the units. Due to extraction and cleaning problems that would be encountered, they were not considered for chemical analysis. XRD whole rock analysis suggests that the dominant clay mineral is a degraded illite/mica.

Rocks:

The clasts within the conglomerate are predominantly chert, with varying amounts of volcanic, mudstone, siltstone and siderite clasts. In regions of the conglomerate where cementation occurred very early, the rounded form of the clasts tend to be preserved. In other regions where cementation was late or nonexistent, the clasts

exhibit concavo-convex and sutured contacts and varying degrees of fracturing, internal recrystallization to chalcedony and replacement by pyrite, siderite and/or calcite. Several clasts show well preserved weathering rinds, indicating that they were exposed to air after an earlier depositional event. Subsequent reworking and further transportation of clasts must have been limited for it would have destroyed the weathering imprint. This is also supported by the presence of locally derived siderite clasts, which due to their more fragile nature cannot endure lengthy transport distances. A two-step depositional cycle may also account for the absence of sand-sized particles in some conglomerate matrices (ie. the sand-sized particles were selectively removed at the first deposition site).

3.3 Diagenesis in the Cardium Formation

Previous diagenetic studies on the Cardium Formation have been carried out by Griffith (1981; Ferrier field), Sweeney (1983; Ricinus, Caroline and Garrington fields), Staley (1987; Cardium & Viking Formations), Machemer and Hutcheon (1988; Pembina field), Almon (1979; Ricinus field), Hart et al. (1992; Nosehill, Kakwa and Musreau Members), and others.

Figure 1.3 represents an isopach map of the Carrot Creek field. The striking feature of the isopach map is that the conglomeratic unit does not represent a sedimentary unit of uniform thickness and continuity, but rather is made up of isolated conglomeratic pods. These conglomeratic pods are capped above by mudstones and below by sandstone and mudstone. Considering the lateral distribution of the conglomeratic units across the entire Cardium Formation (Figure 1.1 and 1.2), it would be unlikely that the diagenetic

sequence of events was the same for all conglomerate units. It is more likely that several different diagenetic "microenvironments" existed in the Cardium, each being dependent on the proximity to the continental source, amount of organic matter in the surrounding sediment, composition of the conglomerate matrix, porosity, sediment deposition rate, encroachment of meteoric water from the continent, and several other factors. For example, a detailed analysis of conglomerate core samples from the Carrot Creek field reveals a considerable matrix diversity: clast supported with open porespace; clast supported with a monomineralic pyrite, siderite or calcite matrix; clast supported with a variable mixtures of pyrite, siderite, calcite and kaolinite matrix; clasts with a mud supported matrix and no cement; clasts with a mud supported matrix and siderite cement; and clasts with a coaly matrix.

Due to the diversity of the mode of occurrence of the diagenetic mineral phases in the Cardium Formation, the proposed paragenetic sequence is idealized for the Carrot Creek Member. The paragenetic sequence for Carrot Creek is shown in Figure 3.4.

Factors such as siderite clasts of local origin, weathering rinds on some clasts, the lack of any sand-sized grains in the conglomerate matrix, and a diverse matrix composition suggest that the conglomeratic units represent reworked sediments. This implies that the gravels were originally deposited nearshore and during a later event were retransported along with newer local material to their present depositional sites. Shells of dead marine organisms (Inoceramus and oysters) were incorporated into the sediment and preserved in the mudstones. These shells represent carbonate precipitation directly from marine or brackish waters.

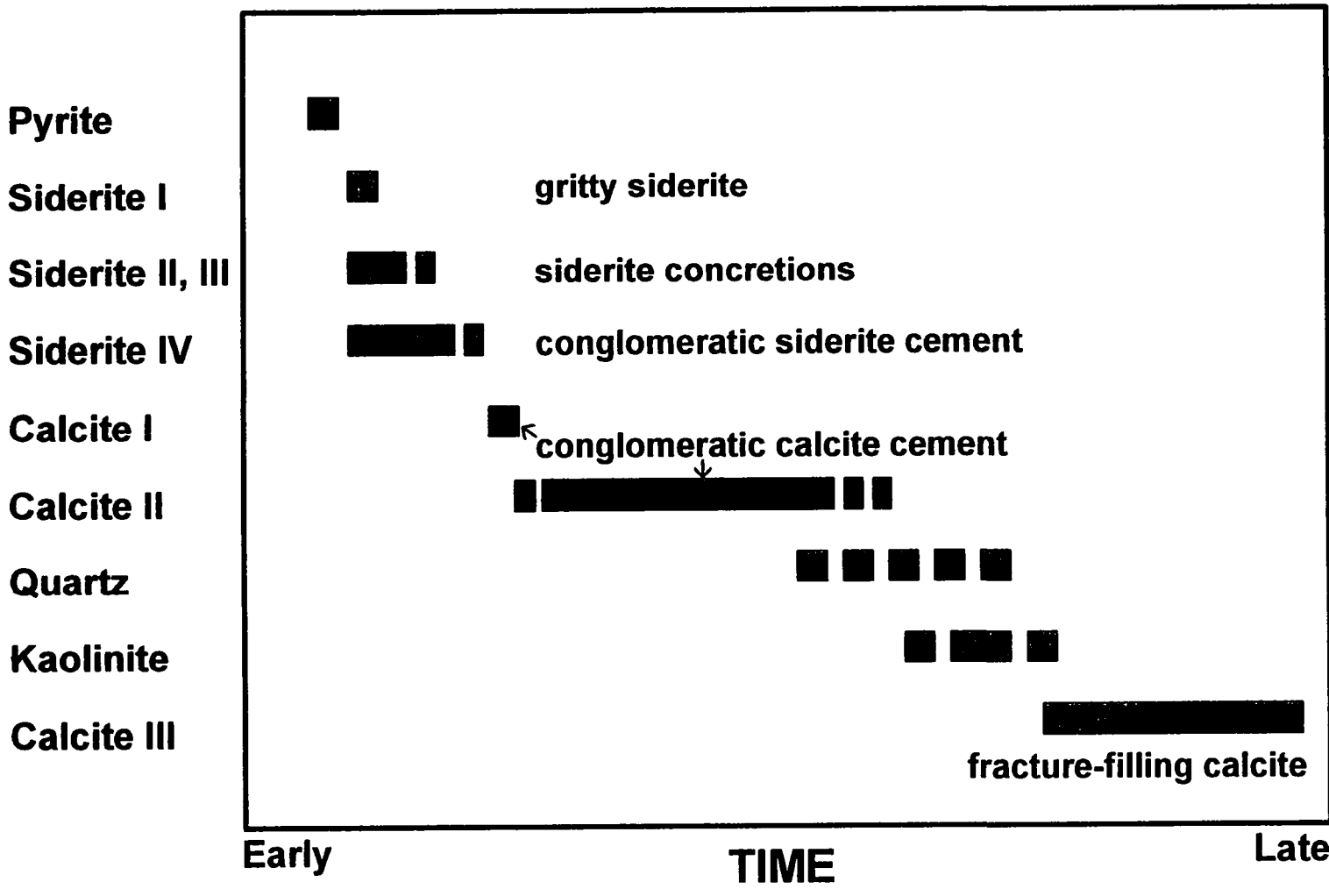

Figure 3.4 Paragenetic sequence for the Cardium Formation. Based predominantly on petrography of the Carrot Creek field.

The pyrite framboids found on clast surfaces and replacing organic fragments represent the first diagenetic precipitates after sediment deposition. The result of this precipitation of pyrite mediated by bacterial processes, along with a continued rapid sedimentation rate would be to deplete the porewaters of SO_4^{2-}. The rapid sedimentation rate prevents diffusion of more SO_4^{2-} from seawater. Where pyrite is found coexisting with siderite and calcite, the pyrite is found seeded on clast surfaces and is surrounded by either pore-lining siderite, pore-filling siderite or pore-filling ferroan calcite cement. The onset of siderite precipitation indicates total sulphate depletion, high DIC content and a high Fe/Ca ratio in the porewaters. Reducing conditions in the sediment would cause iron adsorbed on clay particles to go into solution until the Fe/Ca ratio is reached where siderite is preferentially stable over calcite. Continued bacterial degradation of organic matter in the sedimentary pile would increase the CO_2 content of the porewater. The siderite precipitated in the conglomerate either as a mud matrix/clast replacement, pore-lining cement or pore-filling cement. In mudstones the siderite precipitated as concretionary nodules or bands. The observed variability in siderite form appears to be related to the initial porosity, or more accurately, the initial "size" of the pores in the conglomerate matrix. Where the matrix is high, micritic, granular and spherulitic siderite is common. In clast supported conglomerates, with low matrix and abundant large pore-spaces, rhombohedral crystals, sheaf-like bundles and sparry siderite predominate. Due to the absence of large porespaces in the fine grained mudstones, the dominant siderite forms of concretionary nodules/bands are micritic, granular and spherulitic. There is no

clear petrographic evidence to differentiate the timing of the three different types of siderite (gritty, concretionary and conglomeratic) in the sediments.

In thin sections where both siderite and calcite coexist, the siderite is found as individual grains on clasts surfaces or as clusters forming a pore-lining cement, with the ferroan calcite filling the center porespaces. The transition from siderite to ferroan calcite precipitation is more than likely a result of lower Fe/Ca ratios in the porewaters, either due to iron depletion as a result of pyrite and siderite formation, or dilution by migrating iron poor waters. Calcite (I) precipitated first and is usually found as sparry plates between closely spaced clasts, or in the "corners" of touching clasts (as in Figs. 3.2A and 3.3A). Calcite (II) precipitated next and fills entire porespaces or totally surrounds clasts with optical continuity (Fig. 3.2B). In several areas there are eroded and relict siderite grains surrounded by calcite (II) which suggests that the calcite may be a replacement product of siderite. It appear that calcite (I) and (II) were precipitated prior to extensive compaction, whereas the later fracture filling calcite (III) postdates compaction. Clasts in conglomeratic zones with siderite and calcite (I) and (II) cement (matrix or cement supported) show very little sign of alteration other than surface replacement by the carbonates. In clast supported regions, the clasts have concavo-convex and sutured contacts, fracturing, and extensive recrystallization in chert clasts.

Kaolinite precipitated after the sparry calcite cement. In areas where kaolinite is found in contact with calcite, the latter has a corroded appearance, which suggest replacement (Fig. 3.3A). Kaolinite can also be found as islands within the mud matrix of conglomerates. These kaolinitic "islands" are interpreted as alteration product of

aluminosilicate mineral clasts such as feldspar. Quartz precipitated sometime after the sparry calcite cement, but before the fracture filling calcite. Fracture filling calcite can be found in fractured clasts that have been recrystallized to chalcedony. The paragenetic relationship between kaolinite and quartz is not known. However, in one instance kaolinite was found in a fracture of a clast. If quartz precipitation and recrystallization is related to the compactional event, then the kaolinite may be post compaction.

Fracture filling calcite (III) is the last diagenetic carbonate precipitated. This calcite is easily recognized by its cross-cutting nature, particularly in the mudstones. In the conglomerate it is somewhat harder to see, but is identifiable when found in fractures of clasts.

The observed change in diagenetic mineral precipitation with time is indicative of a varying porewater chemistry. The elemental and isotopic composition of these mineral precipitates is analysed in the next chapters and will be used to resolved the nature of the porewaters.

CHAPTER 4

Strontium Isotopes

4.1 Strontium in Seawater

The $^{87}Sr/^{86}Sr$ ratio of seawater has been observed to change throughout the Phanerozoic, in a consistent fashion through all the oceans of the world (Fig. 4.1, Burke et al., 1982; Peterman et al., 1970). Based on the comparison of $^{87}Sr/^{86}Sr$ ratios of modern seawater and marine carbonates of the same age derived from different parts of the world, it is concluded that Sr in the oceans has been isotopically homogeneous throughout Phanerozoic time (Faure, 1986). The reason for this Sr isotopic homogeneity in the oceans is due to the long residence time of Sr (5×10^6 years) compared to the mixing time of the oceans (approx. 10^3 years). Additionally the concentration of Sr in the oceans is high (7.7 μg/ml) compared to the average continental river water (0.068 μg/ml) (Faure, 1986). Through time, the $^{87}Sr/^{86}Sr$ ratio in seawater is regulated by mixing of strontium derived from three different sources (Burke et al., 1982; Veizer, 1989):

1) Old sialic rocks of the continental crust with average $^{87}Sr/^{86}Sr = 0.720$. The Sr enters the oceans via groundwater and river discharge, with a mean $^{87}Sr/^{86}Sr = 0.7101 \pm 5$ (Goldstein and Jacobsen, 1987).

2) Young volcanic rocks with average $^{87}Sr/^{86}Sr = 0.704$. The Sr enters the ocean via hydrothermal waters discharged from vents at mid-oceanic ridges. These hot waters have a $^{87}Sr/^{86}Sr \approx 0.7035 \pm 5$ (Albarède et al., 1981; Elderfield and Grieves, 1981; Piepgras

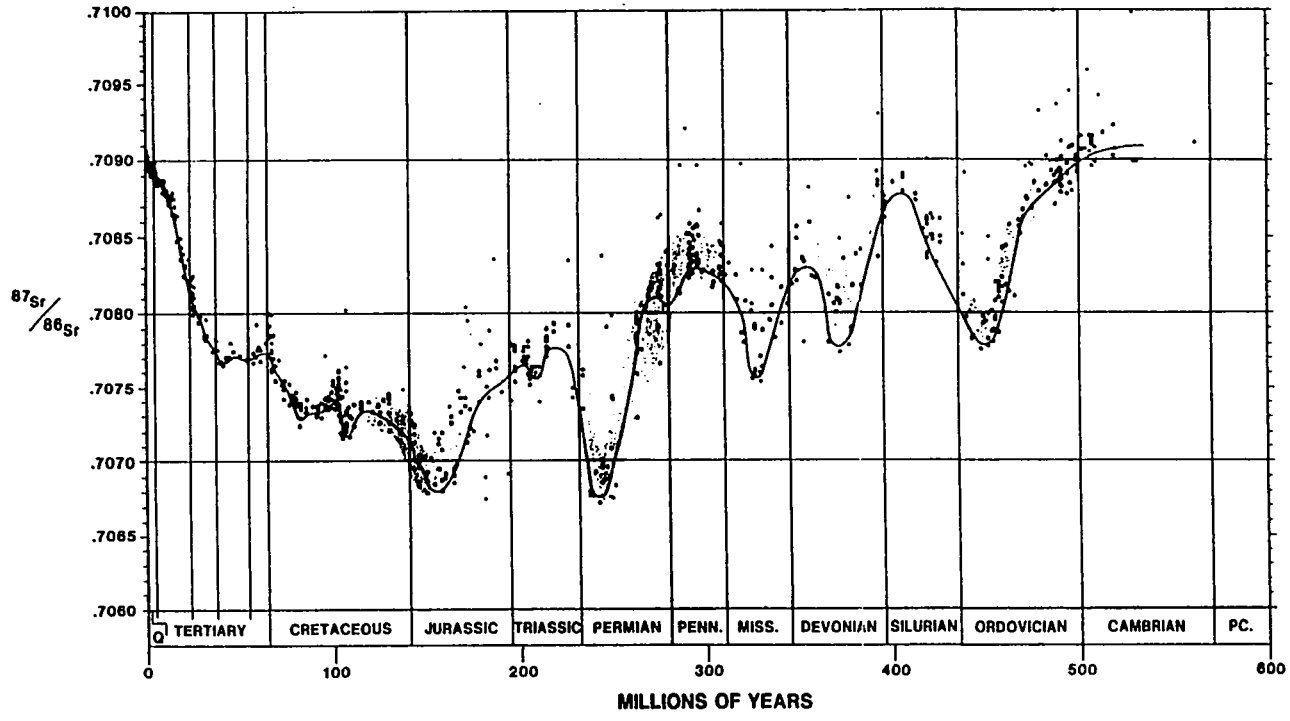

Figure 4.1 Plot of $^{87}Sr/^{86}Sr$ vs. age for 744 of 786 marine samples. The line represents the best estimate of seawater ratio versus time. (From Burke et al., 1982)

and Wasserburg, 1985). Sr is also incorporated from diagenetic waters, modified by reactions of volcanic material in the ocean crust, with a $^{87}Sr/^{86}Sr = 0.7064$ (Palmer and Elderfield, 1985).

3) Phanerozoic marine carbonate rocks with an $^{87}Sr/^{86}Sr$ ratio range of 0.7067 - 0.7091. The Sr enters the ocean by diagenetic waters and has an average $^{87}Sr/^{86}Sr \approx 0.7087$ (Elderfield and Gieskes, 1982; Palmer and Elderfield, 1985).

The shape of the strontium isotopic curve, therefore represents changes of influx of Sr into the ocean from the above three sources. Periods of increased seafloor spreading would result in lower $^{87}Sr/^{86}Sr$ ratios in the oceans, whereas higher rates of continental weathering would raise the strontium isotopic ratio of the oceans (Burke et al., 1982).

The ratio in Sr-bearing marine carbonates reflects the strontium isotopic composition of the coeval seawater from which the minerals precipitated. The present $^{87}Sr/^{86}Sr$ value for seawater is 0.70907 ± 0.00004, and during Turonian time the range was between 0.7072 and 0.7075 (Fig. 4.2, Koepnick et al., 1985). Strontium isotopic composition of molluscan fossil shell material from the Western Interior Basin of North America (Whittaker and Kyser, 1993), fall within the global seawater values and therefore reflect the exchange of seawater between the open oceans and the Western Interior seaway. If siderite in the Cardium Formation precipitated from seawater trapped in the pore space of the sediments relatively early, then it should reflect the $^{87}Sr/^{86}Sr$ ratio of Turonian age seawater.

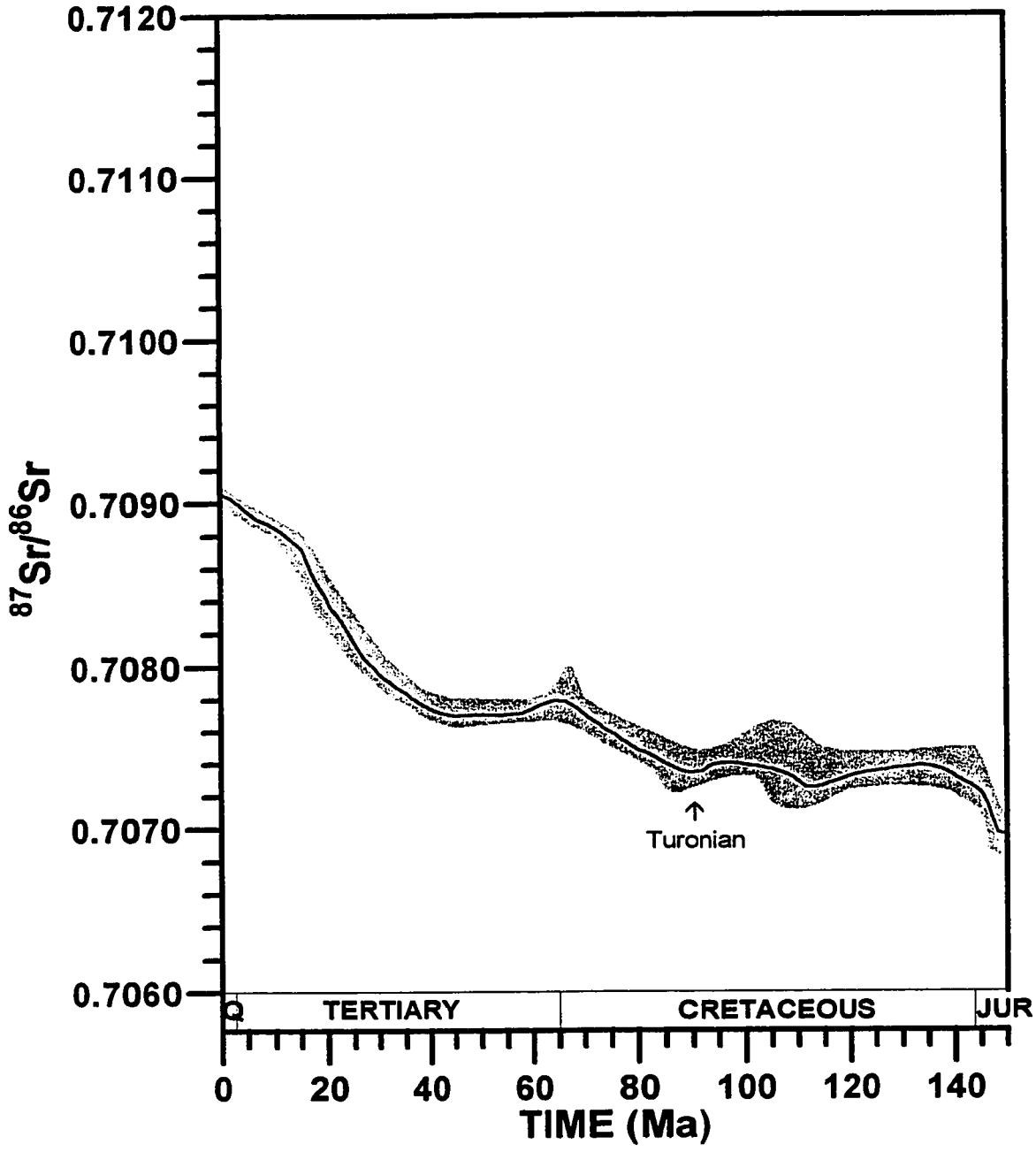

Figure 4.2 Plot of $^{87}Sr/^{86}Sr$ vs. age for Cenozoic, Cretaceous and Late Jurassic. Band defines the upper and lower limit that encloses more than 98% of the Cenozoic and Cretaceous data. For any given time, the correct seawater ratio probably lies within the band. The line drawn through the band is the estimate of seawater ratio vs. time. (From Koepnick et al., 1985)

Elderfield and Gieskes (1982) analysed the Sr isotopic composition of interstitial sea waters of cores from 37 Deep Sea Drilling Project sites. Their data demonstrate that the major processes affecting the $^{87}Sr/^{86}Sr$ distribution in interstitial waters of deep sea sediments are the alteration of volcanic matter dispersed in the sediments and the recrystallization of carbonates. Furthermore, the effects of alteration of continental debris are minimal. However, during late stage burial diagenesis, transformation of detrital clay minerals to more stable phases may introduce significant amounts of radiogenic strontium. High $^{87}Sr/^{86}Sr$ ratios may also result if radiogenic Sr is brought in by migrating fluids expelled from shales or other sediments rich in continental debris (Stueber et al., 1984).

Siderite cement in the conglomerate units and the concretionary nodules/bands in the mudstone units of the Cardium Formation were analysed for their Sr isotopic composition. Since volcanic matter and carbonate deposits are non-existent in the Cardium Formation, and since the effect of alteration of continental debris is minimal, early formed siderites should reflect the Sr isotopic composition of the pore fluids from which they precipitated. The mudstone hosted siderites should therefore reflect a marine $^{87}Sr/^{86}Sr$ ratio of Turonian age seawater. The conglomerates, although deposited in a marine environment and capped by marine mudstones (Plint et al., 1986), rest on subaerial erosive surfaces cut into sandy units. The sandstone units may have been capable of introducing meteoric water into the porespace of the conglomerates. If so, the Sr isotopic composition of the carbonate cements should have a more radiogenic signature than the contemporaneous seawater. However a marine $^{87}Sr/^{86}Sr$ signature in the early

diagenetic mineral phases, would suggest that there was no encroachment of continental waters into the basin.

4.2 Analytical Procedure for Analysis of Sr Isotope Ratios in Siderite

4.2.1 Introduction

To date only 3 papers have been presented on the strontium isotopic composition of siderite. Frimmel (1988) analysed the $^{87}Sr/^{86}Sr$ ratios in metasomatized Paleozoic sediments of the Eastern Alps, containing magnesite, siderite and ankerite mineralization. Cortecci and Frizzo (1993) looked at the $^{87}Sr/^{86}Sr$ ratios of stratiform and vein siderite deposits in northern Italy. In both cases the siderites deposits are relatively massive, clean samples, and are associated with hydrothermal fluid alteration processes. Faure and Jones (1969) analysed the strontium isotopic composition of a mixture of authigenic minerals in Red Sea sediments. The authigenic mixture of iron oxide, siderite, calcite, rhodochrosite and quartz were found 90 to 740 cm below the sediment-seawater interface. Individual mineral phases were not analysed.

To the author's knowledge, clastic sedimentary hosted authigenic or diagenetic siderites have never been analysed for their $^{87}Sr/^{86}Sr$ ratios. The main reason for this is that sedimentary siderites are relatively impure, containing abundant clay minerals, other carbonate fractions and other detrital or diagenetic "contaminants". These contaminants have a high Sr concentration (>1000 ppm) compared to the siderite (75 to 275 ppm). The clays in particular have high radiogenic strontium signatures and will more than likely mask the primary signature of the siderites. For the $^{87}Sr/^{86}Sr$ ratios of sedimentary

siderites to be of any significance, a cleaning technique needs to be developed to remove any isotopic overprints associated with the impurities.

4.2.2 Sample Cleaning

A sample of concretionary siderite from the marine mudstone facies of the Cardium Formation was used as a standard for all initial Sr extraction experimentations. Due to extensive experimentation, a second standard was required as the first was consumed. The siderite standard was crushed and sieved through a 200 mesh screen. Normally, the next step is to dissolve the carbonate with an acid such as HCl. However, doing so with siderite would not only dissolve the carbonate, but also any associated calcite as well as leachable Sr from the clay minerals. Another complication is that siderite is not as reactive with acids as are other carbonates such as calcite or even dolomite. If the acid concentration or reaction time is increased, more contaminating Sr will be introduced in the process.

To demonstrate the effect that various clays impurities can have on the $^{87}Sr/^{86}Sr$ ratio of siderite, various percentages of pure siderite were mixed with common clay minerals such as montmorillonite, bentonite, illite and kaolinite. A modern day marine calcite was mixed with montmorillonite for comparison. These carbonate-clay mixtures were then dissolved in 0.5M HCl for 30 minutes. The Sr was extracted and the $^{87}Sr/^{86}Sr$ ratios of these mixtures were analysed (Fig. 4.3). As the graph shows, certain calcite-clay mixtures can contain as much as 90% clays without any effect on the carbonate $^{87}Sr/^{86}Sr$ ratio. For siderite, even a 5% contamination by clays (particularly

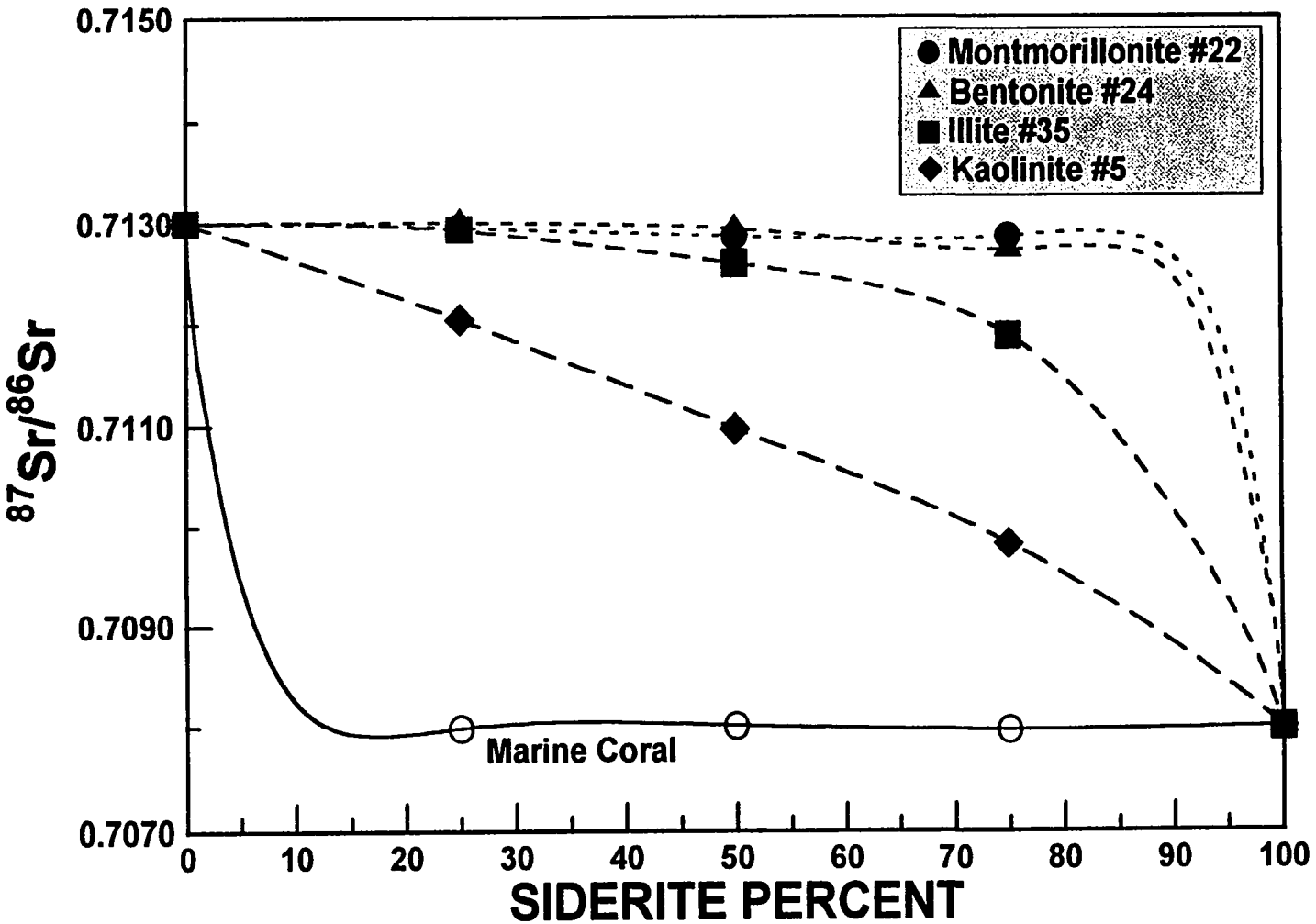

Figure 4.3 Plot of $^{87}Sr/^{86}Sr$ ratios for various clay-siderite mixtures. A modern marine carbonate coral (normalized to the same Sr ratio as the siderite) is included for comparison.

montmorillonite/bentonite), can have a significant effect on determining its strontium isotopic composition. A method is therefore required to remove most of the clays from the samples or to leach away any exchangeable strontium within the clay mineral structure. It should be noted that the clay-siderite mixtures in Figure 4.3 do not share diagenetic or time related events, hence the contamination effect may be more exaggerated than would a contemporaneous siderite-clay mixture.

A typical clay (montmorillonite) structure is shown in Figure 4.4. The formula for the montmorillonite group is

$$(½Ca,Na)_{0.7}(Al,Mg,Fe)_4[(Si,Al)_8O_{20}](OH)_4 \bullet nH_2O$$

Substitutions in the octahedral and tetrahedral sites upsets the charge balance which is neutralized by the addition of an equivalent number of interlayer cations (Na, Ca, and to a lesser extent K, Ce, Sr, Mg, H and others) — all of which are to varying degrees exchangeable (Deer et al., 1966).

There appears to be a general consensus, based on different experiments, that for the dominant clay mineral phases, mainly one or two exchange sites occur (Farrah et al., 1980; Kralik, 1984). In kaolinite, a dominant detrital phase, the primary capacity to fix cations (such as Sr^{2+}), are at broken bond surfaces normal to the layer plane. Fixation on these sites is pH dependent and bound cations can easily be leached at a low pH (Yariv and Cross, 1979). In illites, marginal sites can easily exchange, whereas the more central sites in the interlayer positions of the crystal structure are less susceptible to exchange. The exchangeable sites in the expanded frayed edges, which contain the most recently exchanged ions from the late diagenetic fluids or from passing weathering

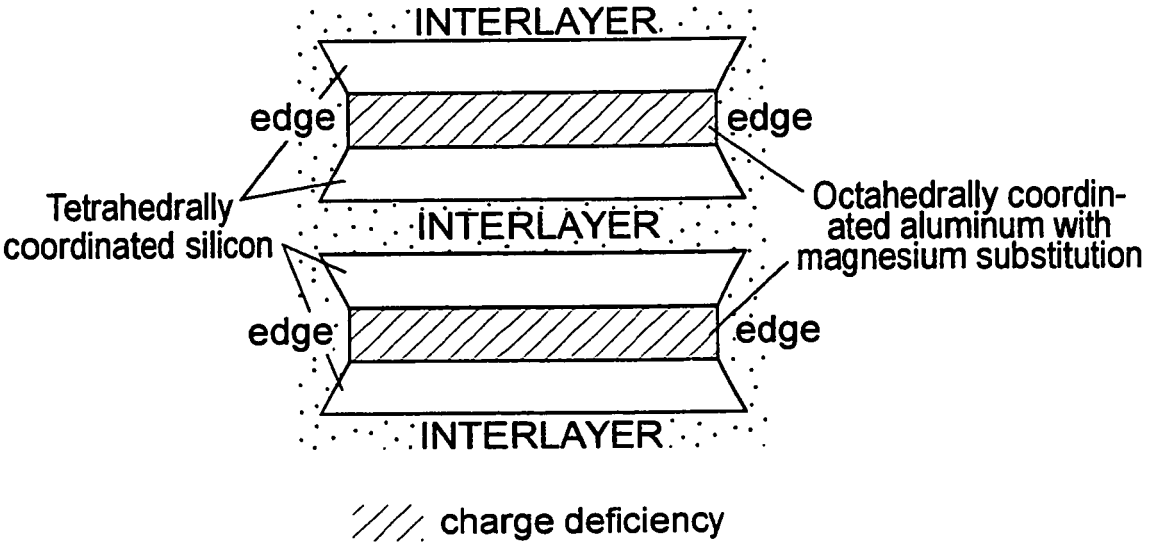

Figure 4.4 Schematic of a montmorillonite layer structure. (From Carroll and Starkey, 1971)

solutions is easily leached with an ion-exchange resin. Ions in the more sluggishly exchangeable core sites, which may have formed or exchanged during diagenesis, can be leached by HCl (Kralik, 1984). Acid dissolution experiments on glauconite by Thompson and Hower (1973) demonstrated that if an ion is bonded in two or more different structural sites with different activation energies, then the ion will be removed at two different rates.

Although HCl can readily leach the contaminating Sr from the periphery and core sites of clay minerals, it would also dissolve the siderite. The first approach would be to physically remove as much of the clay minerals from the siderite as possible. Siderite has a density of 3.5 - 3.96, whereas clays have an average density of 2.65 (Deer et al., 1966). Two different separation methods were tried, gravimetric sediment settling and heavy liquid mineral separation. In the first method, 200 mesh powdered siderite samples were dispersed in a water-filled cylinder and the siderite was separated from the clays by the timed sediment settling method. For the second method, the siderite powders were mixed with a heavy liquid solution and centrifuged for 30 minutes to separate the silicates from the siderite. The heavy liquid solution ($\rho = 3.0$ g/ml, $Sr_{conc} < 1$ppm) was prepared by mixing 850g of the inorganic salt sodium polytungstate ($3Na_2WO_4 \bullet 9WO_3 \bullet H_2O$) with 150 g of distilled water. A comparison between the two clay mineral separation methods and their effect on the strontium isotopic composition of the sedimentary siderite is shown in Figure 4.5. The lower $^{87}Sr/^{86}Sr$ ratio of the siderite extracted by heavy liquid mineral separation, indicates that this method is more

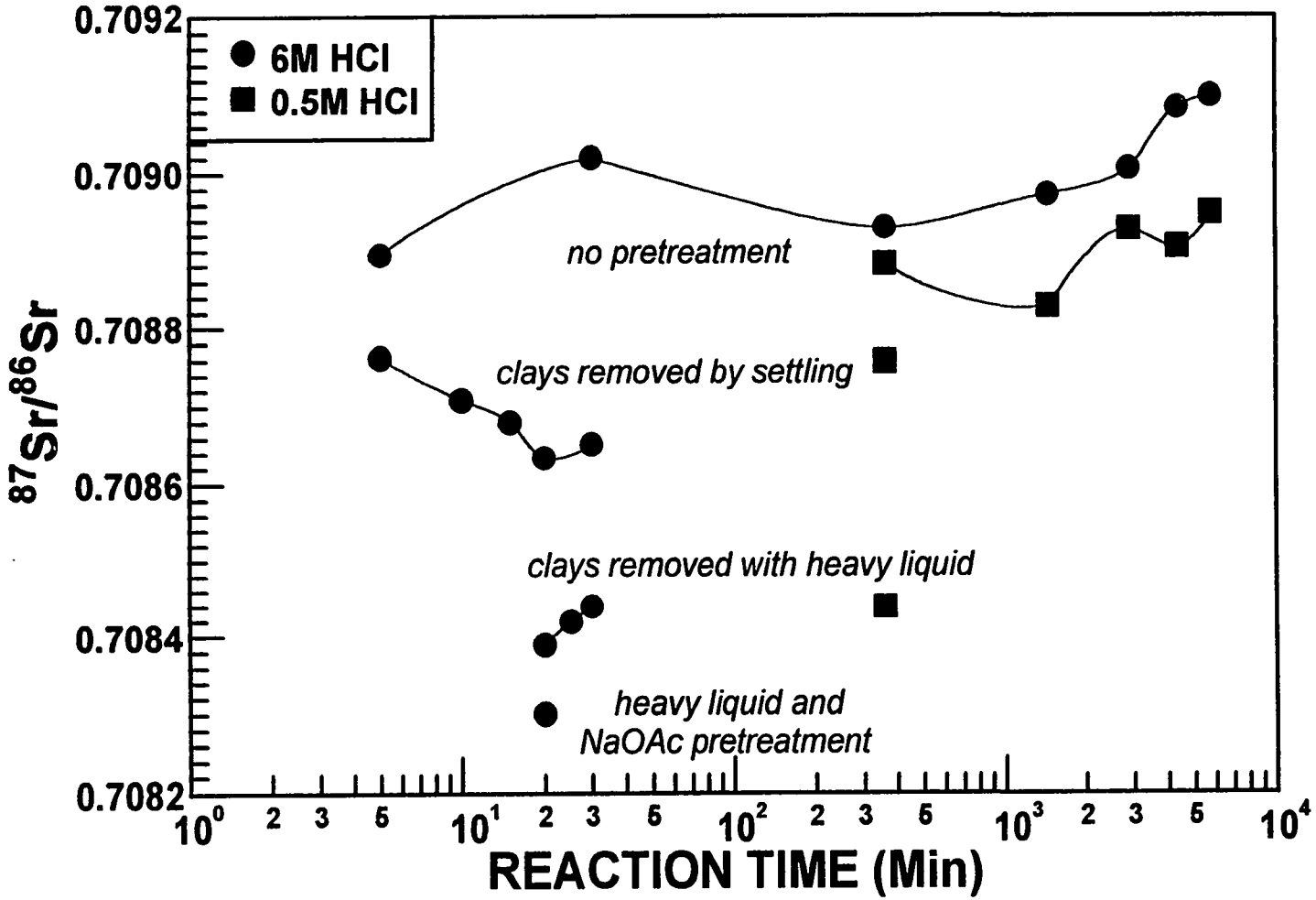

Figure 4.5 Different sample pretreatment and dissolution methods and their effects on the $^{87}Sr/^{86}Sr$ ratio of siderite. Lower Sr isotopic ratios approach the Turonian seawater range of 0.7072 to 0.7075.

effective in removing the silicate contaminants (continental silicates have higher Rb and radiogenic Sr concentrations, which increases the Sr isotopic signature).

Following the heavy liquid separation, two leaching methods were applied to remove any Sr that may be present in clays interlocked with the siderite. Many different reagents have been used to separate carbonates from clays or to liberate exchangeable metals from clays. Reagents such as hydrochloric acid (HCl), acetic acid (HOAc), ammonium acetate (NH_4OAc), sodium acetate (NaOAc), magnesium chloride ($MgCl_2$) and sodium hydroxide (NaOH) have been used in various soil and sediment analysis studies (Jackson, 1969; Carroll and Starkey, 1971; Tessier et al., 1979; Morton, 1985). Figure 4.6 summarizes the results of the various pretreatment methods and their effects on the Sr isotopic composition of siderite. Treatment of the siderite samples with 1M $MgCl_2$ (pH=7.0, for 2 hrs.) and 3M NaOH (for 1-6 days) yielded $^{87}Sr/^{86}Sr$ ratios that were higher than untreated samples. Although these reagents were prepared from "spec-pure" products, they contained sufficient Sr to yield a Sr isotopic signature. The Sr isotopic ratios of these two reagents were found to be >0.711, and is assumed to be the cause of the higher ratios in the treated samples. Siderite samples treated with 1M NaOAc (pH=5.0, for 2 hrs.) and 1M NH_4OAc (pH=4.0, for 1-6 days), resulted in lower Sr isotopic signatures than did untreated samples. Both reagents had insufficient Sr to allow us to determine their Sr isotopic signatures. NaOAc treated samples consistently yielded lower $^{87}Sr/^{86}Sr$ signatures than did those treated with NH_4OAc. Continued experimentation with NaOAc showed that a 2 hr. leach was optimal for siderite-clay samples (Fig. 4.7).

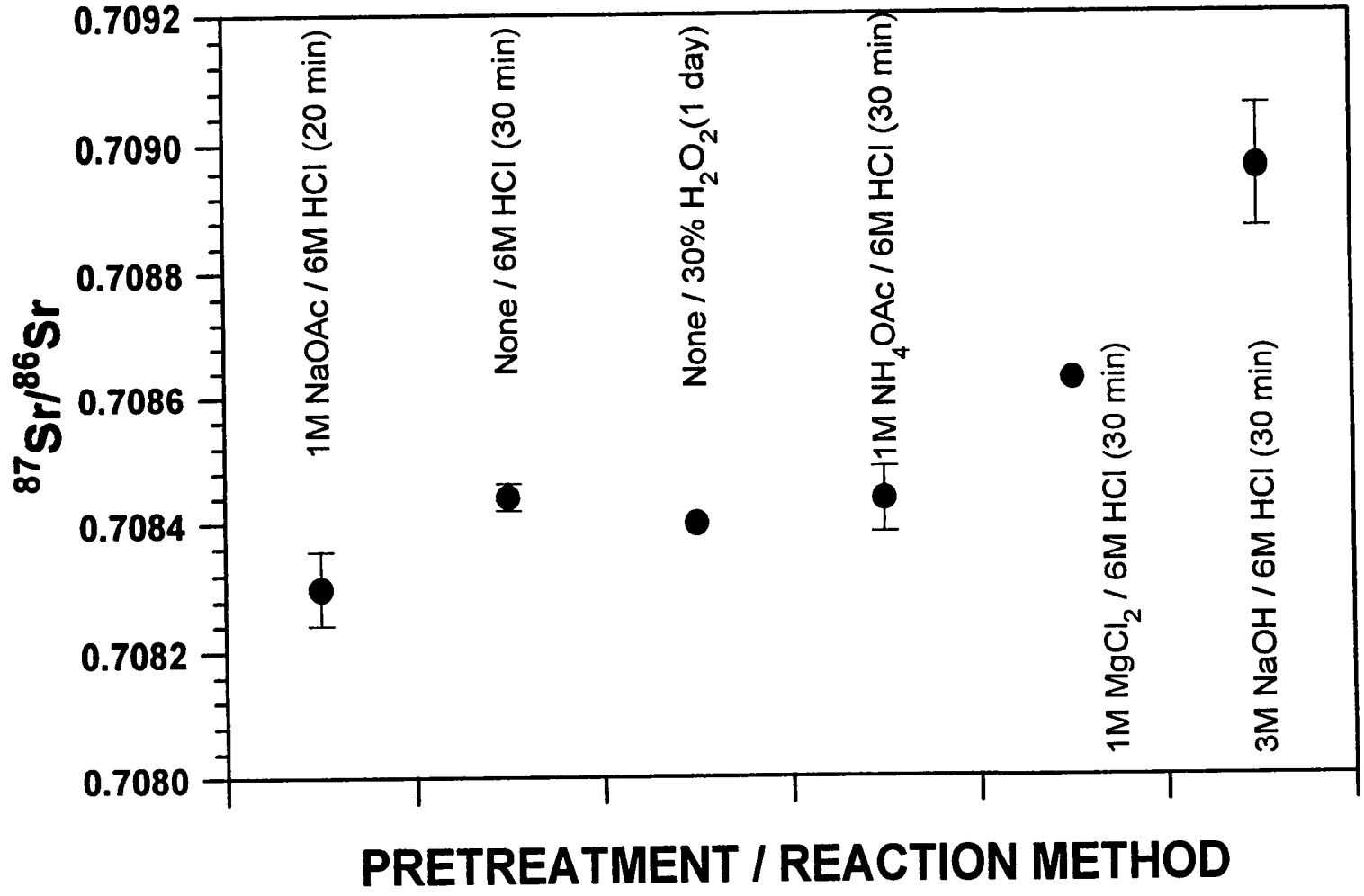

Figure 4.6 Sample pretreatment methods and their effects on the Sr isotopic composition of siderite. All sample were additionally treated with 0.5M HCl for 20 min. prior to acid dissolution. Error bars are 2σ (sample replicates).

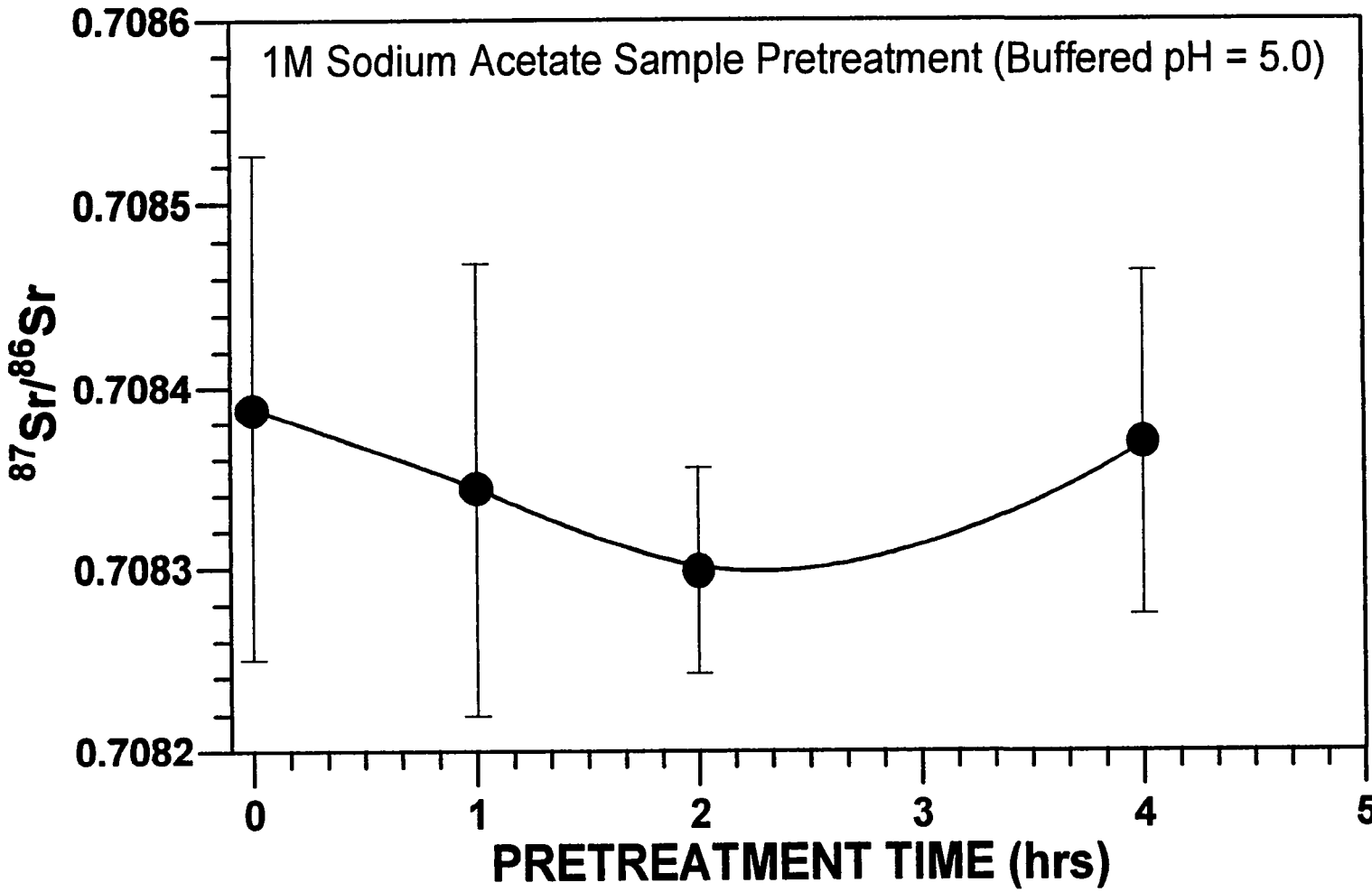

Figure 4.7 Timed sample pretreatment with 1M sodium acetate solution buffered to a pH of 5.0 with acetic acid. Lower $^{87}Sr/^{86}Sr$ ratios of the treated clay-siderite mixture, represent better response to the the pretreatment method. Error bars are 2σ for sample replicates (n=3).

After the sodium acetate treatment, a second leach with 0.5M HCl was applied. Ostrom (1961) and Carroll and Starkey (1971) noted that a clay mineral's reaction to acid, though varying with the kind of clay mineral, is noticeably stronger with HCl than acetic acid. The siderite samples were reacted with 0.5M HCl for 20 min. This final HCl acid treatment should progressively remove any remaining Sr at clay edge surfaces and interlayers sites. This HCl leach will also remove any calcite (which has considerably higher Sr concentration than siderite) that may be present in the sample with minimal siderite removal.

The siderite samples at this stage are ready for acid dissolution for Sr analysis. The siderites are only partially dissolved to prevent any contamination by Sr in clays that are wholly surrounded by siderite. Siderite dissolution experiments were performed with 6M HCl for relative short periods of time (15 to 30 min.) and 0.5M HCl for a longer duration (4 - 7 hrs.). For siderite-clay mixtures, the optimal reaction time appears to be 20 min. with 6M HCl (Fig. 4.8). Siderite samples reacted with 6M HCl over a shorter time period consistently resulted in a lower $^{87}Sr/^{86}Sr$ ratio. It appears that lowering the contact time between the acid and siderite-clay mixture results in the least amount of Sr clay contamination. The siderite was also reacted with 30% H_2O_2 for 1 day. The highly exothermic reaction resulted in slightly lower Sr isotopic values compared to the 6M HCl reaction (Fig. 4.6). However, only 1 out of 3 reactions yielded enough Sr for an isotopic analysis. It may be that the Sr is being partitioned into the iron oxides/hydroxides precipitated during the reaction. Time did not permit us to continue experimentation with

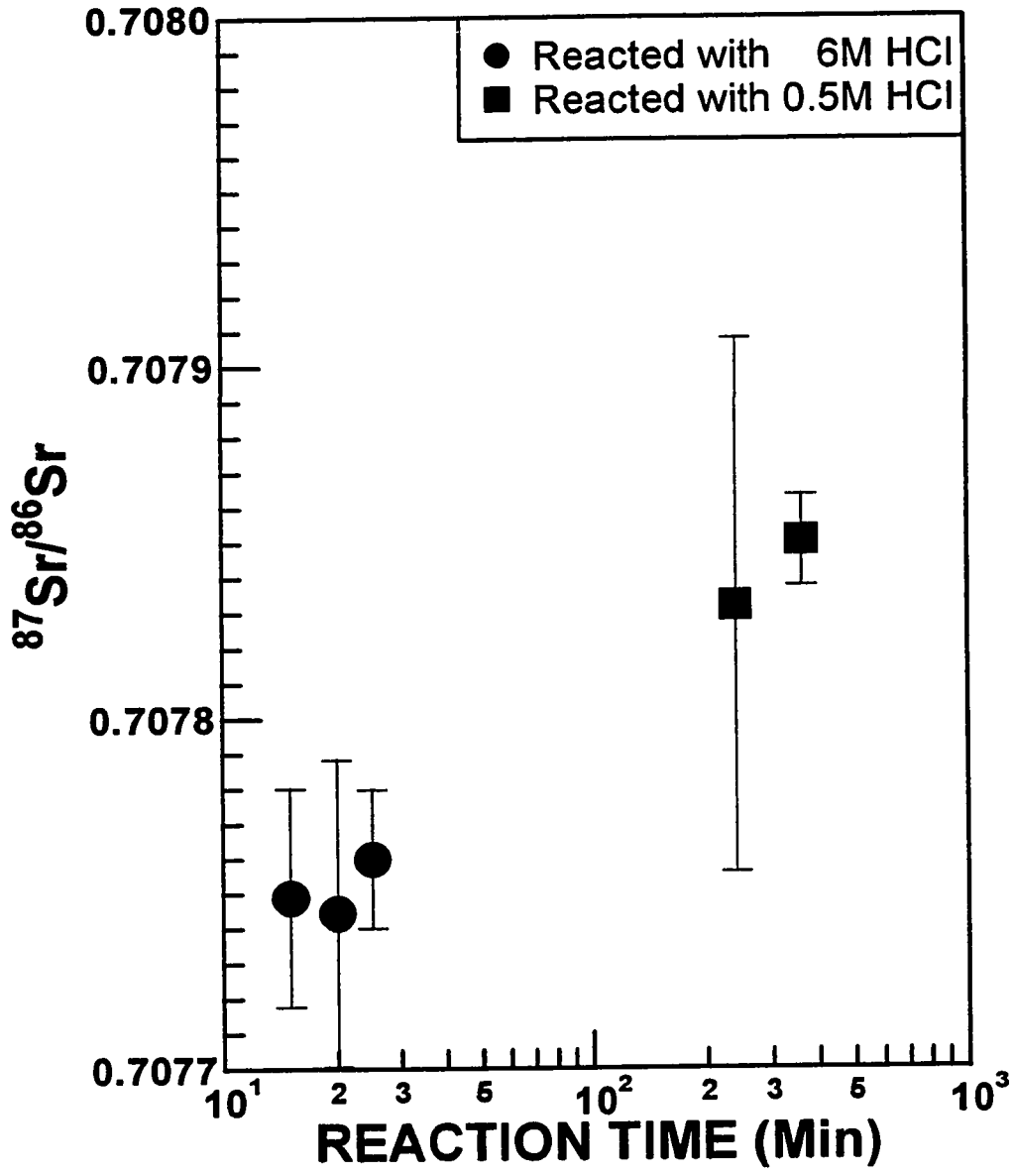

Figure 4.8 Acid concentration and reaction time and its effects on the Sr isotopic composition of siderite. Error bars are 2σ for sample replicates.

the hydrogen peroxide reactions, but changing the concentration and reaction time could lead to more precise $^{87}Sr/^{86}Sr$ ratios than the 6M HCl reaction.

A comparison between the different pretreatment and leaching methods and their effect on the $^{87}Sr/^{86}Sr$ ratio of siderite is shown in Figure 4.5. A flow chart for the cleaning and leaching procedure of siderite is shown in Figure 4.9. Calcite samples did not require any special treatment since they were relatively clean and their Sr isotopic signature is not affected by the presence of clays, even at high percentages (Fig. 4.3). Some relict siderite grains may be present within the sparry calcite. To prevent any Sr dissolution from siderite within the calcite, the calcite was reacted with a lower acid concentration and over a very short period of time. Fifty to 100 mg of calcite was reacted with 10 ml of 0.5M HCl for 5 min. The solution was centrifuged to settle any particulate matter and split into one 6 ml aliquot for Thermal Ionization Mass Spectrometry (TIMS) analysis and one 3 ml aliquot for Inductively Coupled Plasma Mass Spectrometry (ICPMS) analysis.

4.2.3 Column Chemistry and Mass Spectrometry

After the siderite was dissolved, 6 ml of the solution were removed and evaporated by heat lamps. The samples were then acidified with 2 ml of 2.5M HCl. The samples were centrifuged to settle any suspended matter and loaded into the cation exchange columns. The ion-exchange resin used was Bio-Rad AG50W, 200-400 mesh, H^+ form. The columns were calibrated by introducing a 2 ml Rb and Sr solution into the columns, washing-in with 4 ml of 2.5M HCl and eluting with 46 ml of 2.5M HCl.

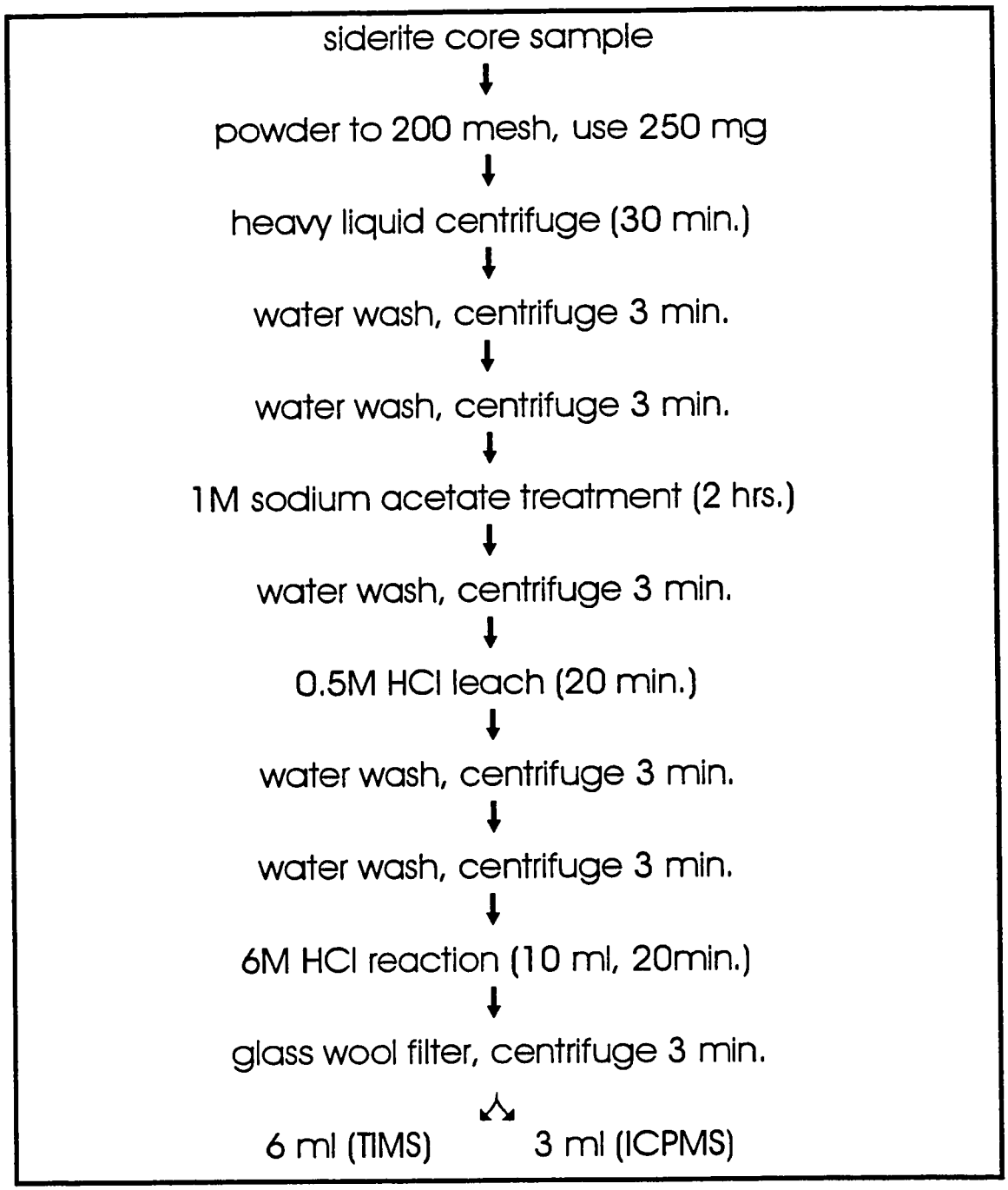

Figure 4.9 Flow chart for the preparation of sedimentary siderites for Sr isotopic analysis.

Eluted samples were collected at 2 ml intervals and analysed for Rb and Sr with ICPMS. The calibration curve for the columns is shown in Figure 4.10. For Sr analysis, 9 ml were collected from the exchange columns and evaporated to dryness.

The Sr samples were dissolved in 1 μL of 0.3M H_3PO_4 and loaded onto single Ta filament beads. The samples were analysed on a VG354 thermal ionization mass spectrometer (TIMS). Fourteen samples and 2 standards were loaded on a barrel and mounted into the mass spectrometer. All Sr isotope ratios were normalized to $^{86}Sr/^{88}Sr=0.1194$. The standard used during the course of the experimentation and sample analysis was NBS 987. The NBS 987 data is presented in Figure 4.11, and for 67 analyses the mean $^{87}Sr/^{86}Sr$ ratio is 0.71020 ± 0.00004 (2σ). This value is within error of the value reported in the 1986 VG354 technical manual (0.710232). Two procedural blanks were run to measure the amount of sample contamination introduced during wet chemistry and mass spectrometry. The blanks yielded values of 0.282 and 0.098 ng of Sr. These values are negligible compared to the Sr content in the calcite and siderite samples (15,000 to 600,000 ng). For additional information on Sr column chemistry and solid source mass spectrometry, refer to Dickin (1995) and Potts (1987).

4.3 Strontium Isotopic Composition of Diagenetic Mineral Phases

The Sr isotopic composition of the diagenetic mineral phases found in the Cardium Formation is shown in Figure 4.12. As expected the marine calcite shells plot in the Turonian seawater field, since they represent contemporaneous precipitates. The brackish water shells have a higher $^{87}Sr/^{86}Sr$ ratio due to continental influences. All other

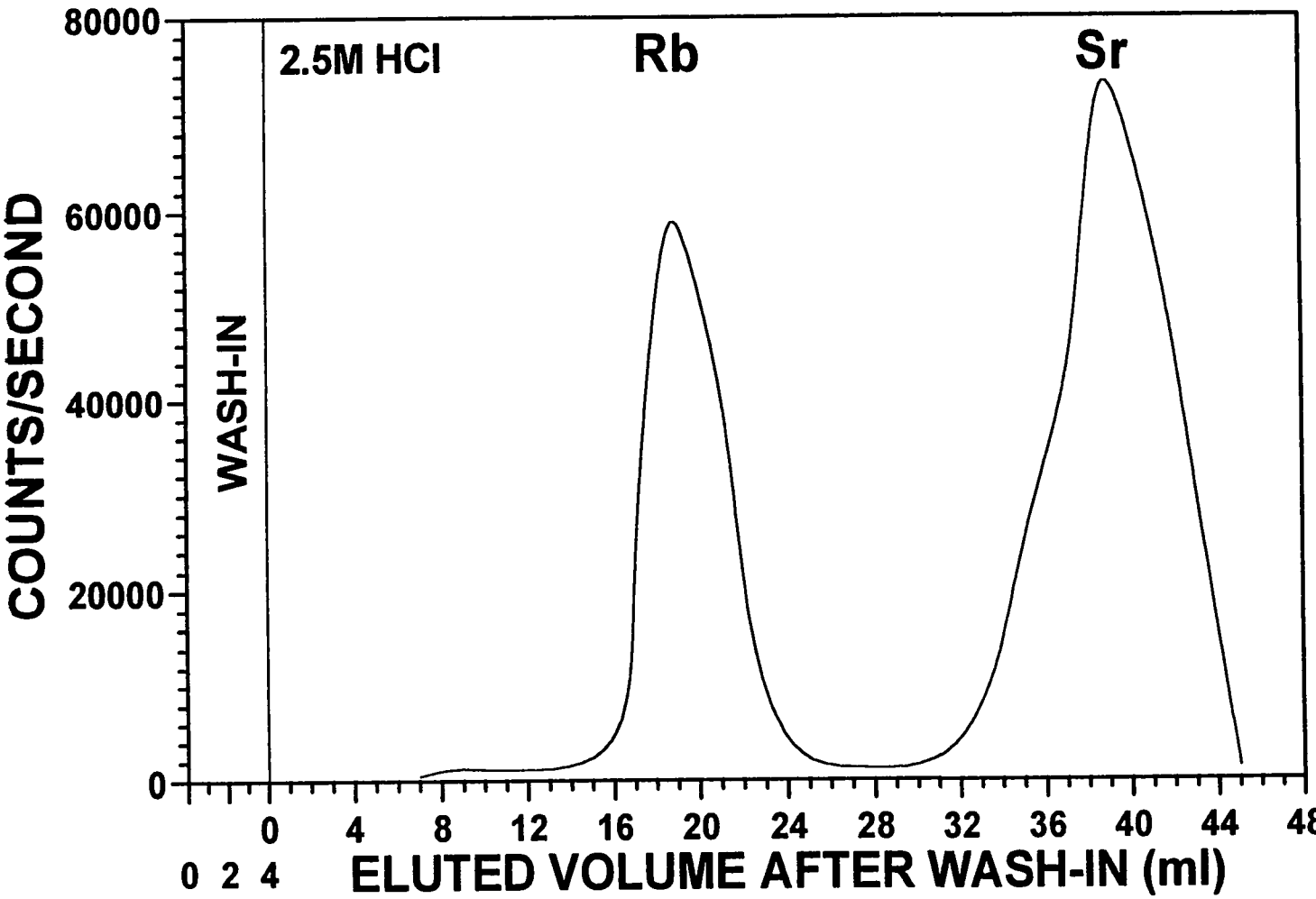

Figure 4.10 Ion exchange column calibration for the extraction of Rb and Sr. The column resin used was Bio-Rad AG50W, 200-400 mesh, H^+ form.

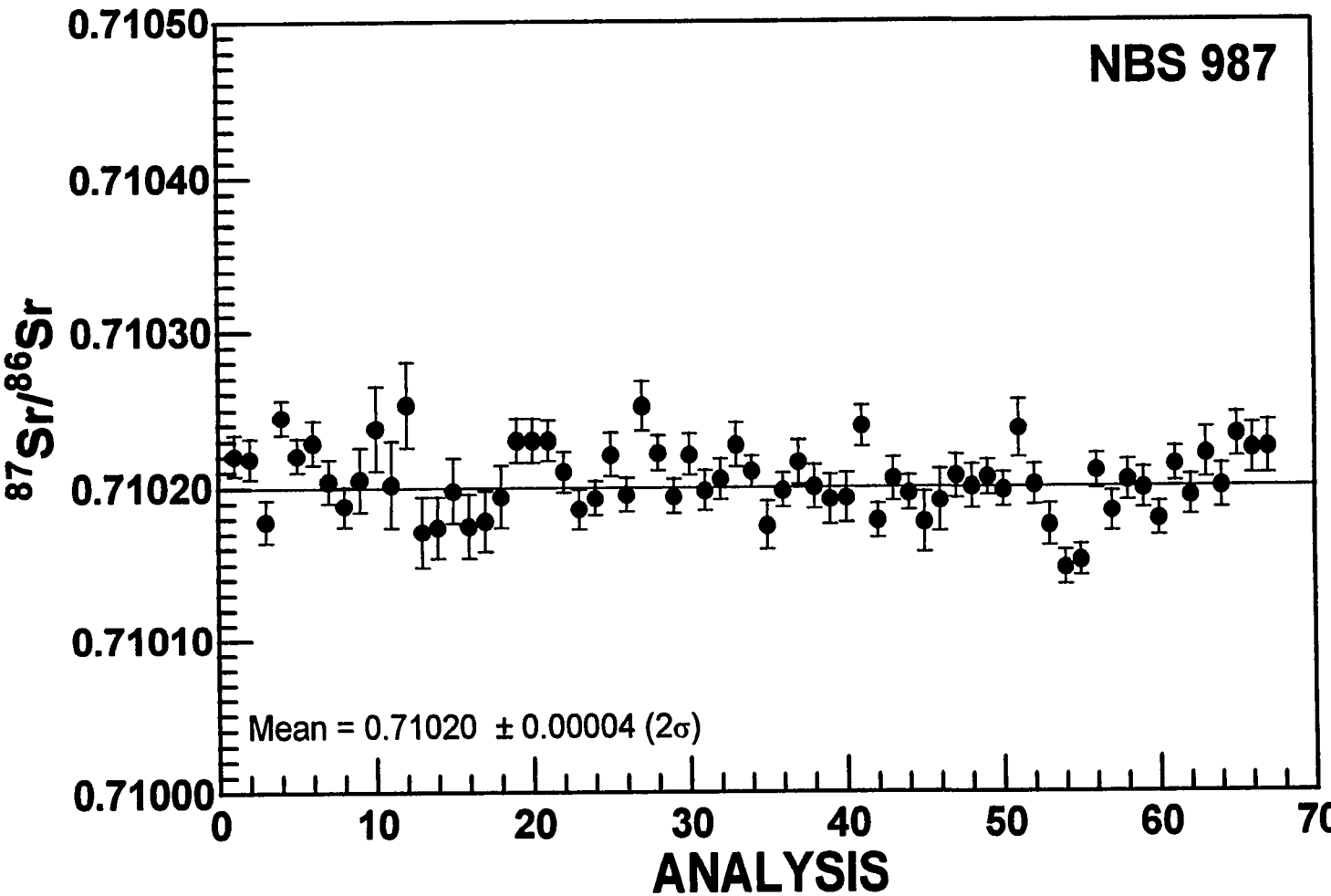

Figure 4.11 $^{87}Sr/^{86}Sr$ ratios of the NBS 987 standard generated during the course of this study. The 2σ error bars represent the instrumental error.

Figure 4.12 $^{87}Sr/^{86}Sr$ ratios of diagenetic mineral phases in the Cardium Formation. Symbol represent the mean Sr isotopic composition and the vertical bars represent the range in the data. Numbers in parenthesis are the sample numbers for each group. Solid symbols represent minerals from marine sediments and open symbols from continental/brackish water sediments.

⬢ - clay minerals (exchangable Sr)

⬟ - kaolinite

◇ - oyster shells, brackish water

◆ - Inoceramid shells, marine

◆ - gritty siderite

● - concretionary siderite nodules/bands, marine

○ - concretionary siderite nodules/bands, continental/brackish

■ - conglomeratic siderite cement

▼ - conglomeratic calicte I

▲ - conglomeratic calcite II

✖ - fracture filling calcite

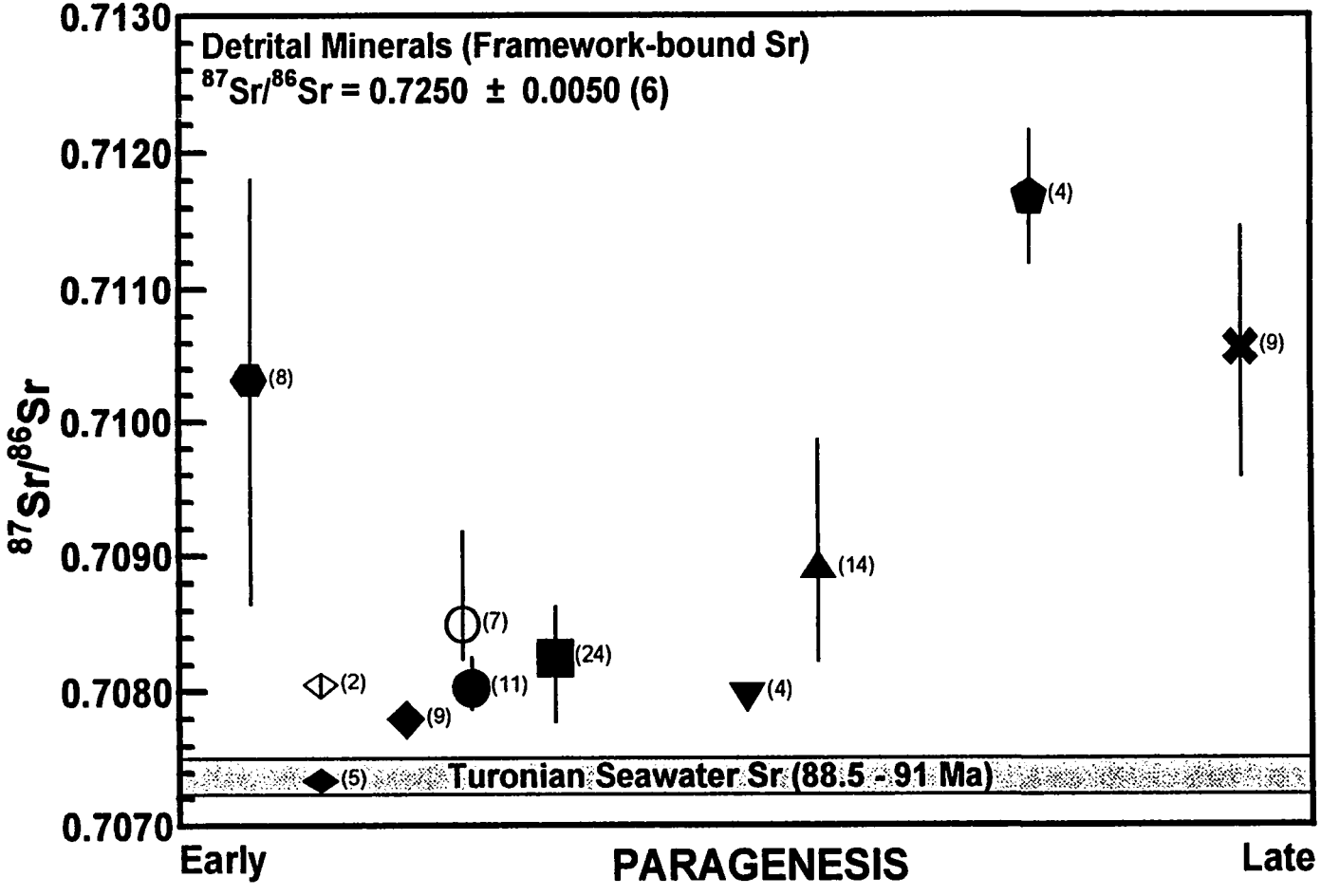
Detrital Minerals (Framework-bound Sr)
$^{87}Sr/^{86}Sr$ = 0.7250 ± 0.0050 (6)
0.7130
0.7120
0.7110
0.7100
0.7090
0.7080
0.7070
$^{87}Sr/^{86}Sr$
(8)
(4)
(9)
(14)
(7)
(24)
(2)
(11)
(9)
(4)
(5)
Turonian Seawater Sr (88.5 - 91 Ma)
Early
PARAGENESIS
Late

diagenetic phases have a Sr isotopic signatures that are not characteristic of Turonian marine precipitates. However, when one compares siderite concretions within marine mudstones and continental/brackish water sediments, the siderites associated with marine sediments exhibit lower $^{87}Sr/^{86}Sr$ ratios. The fact that the marine hosted siderites and conglomerate calcites have higher Sr isotopic values than Turonian seawater, is an indication that they precipitated from diagenetically modified waters sometimes after bacterial sulphate depletion in the sediment pore spaces. Continental clays with exchangeable Sr sites, could have altered the Sr isotopic composition of the porewater to more radiogenic values. The main feature to note in Figure 4.12 is that the Sr isotopic composition of the diagenetic mineral precipitates increases with their position in the paragenetic sequence. Early formed carbonates have Sr isotopic signatures slightly higher than Turonian seawater and the late fracture-filling calcites have continental signatures. The high Sr isotopic composition of kaolinite is probably related to the feldspar precursor. This trend can be attributed to dissolution of continental derived material within the sediments during diagenesis, meteoric water encroachment, or both. Oxygen isotopic data could help to resolve this problem.

CHAPTER 5

Stable Isotopes

5.1 Introduction

The oxygen isotopic composition of a carbonate mineral is determined by the isotopic composition of the water from which it precipitated and by the temperature of the water. If we assume that the isotopic composition of the Western Interior Seaway in late Cretaceous was similar to present seawater, and since temperature can be assumed to have been close to normal for Cretaceous surface conditions (typical of tropical climates today), then $\delta^{18}O$ values of early precipitated carbonate would be near 0 to -2‰ (PDB). Mineral precipitation in freshwaters would result in more negative values due to the lighter isotopic composition of meteoric water. In brackish water, which represents mixed waters of the above two environments, early formed carbonates should display transitional values between the two endmembers.

A slightly lower oxygen isotopic composition of the Interior Seaway, due to dilution by meteoric waters has been suggested by Tourtelot and Rye (1969). If so, then early precipitated marine carbonates may have more depleted $\delta^{18}O$ values (possibly as low as -5‰, PDB). Kyser et al. (1993) also reported low $\delta^{18}O$ values of -5 to -8‰ in carbonate shells from planktonic and benthic faunas from Turonian age sediments at the northern portion of the Western Interior Basin. Such low values in the carbonates would require seawater temperatures in excess of 30°C — a rather unacceptably high value. Kyser et al. (1993) concluded that during Cenomanian and Turonian time the Interior

Seaway had lower $\delta^{18}O$ values (due to meteoric runoff) and higher temperatures than those of the coeval open oceans. Oxygen isotopic studies of tests of foraminifera and nanofossils from Cretaceous age deep sea cores and outcrop sections, indicate that Cretaceous age oceans were 15°C warmer than modern day oceans (Douglas and Savin, 1975; Barron, 1983). A consequence of the elevated temperatures during this time period would have been lower $^{18}O/^{16}O$ ratios of the oceans due to a lack of glacial activity (Shackleton, 1967; Barron, 1983), but the effect would only result in a maximum shift of -1.3‰ in $\delta^{18}O$ of the oceans (Savin and Yeh, 1981).

Late stage marine siderites which formed at greater depths may exhibit more negative $\delta^{18}O$ values. This is a reflection of increasing temperatures with depth of burial. Therefore, zoned concretions which formed over a wide depth range should reveal increasingly lighter $\delta^{18}O$ from the core to the edge (assuming that the system remained more or less closed). Such decreasing oxygen isotope trends in various concretions have been observed by several authors (Timofeyeva et al., 1976; Irwin, 1980; Hennessy and Knauth, 1985).

In the Cardium formation, the oxygen isotopic composition of early formed siderites may most accurately reflect the depositional environment. Carbonate samples from continental-transitional (Kakwa) and marine sediments (Carrot Creek) were analysed for $\delta^{18}O$ to see if a meaningful correlation exists between the oxygen and strontium isotopic composition of siderite and the expected environment of deposition. The $\delta^{18}O$ of calcite cements, a late carbonate phase in the conglomerates can yield additional information regarding post depositional events during burial diagenesis.

Carbonates precipitating from seawater generally have a carbon isotopic composition ($\delta^{13}C$) of 0 $\pm$ 4 ‰ (Keith and Weber, 1964). If siderite is a diagenetic product, then biogenic carbon dioxide released during oxidation of organic matter will control the carbon isotopic composition of the carbonate. With depth in the sediment column, bicarbonate ions formed from the biogenic CO_2 will increase in concentration and the original HCO_3^- will be of lesser importance. It therefore appears that for siderite, the carbon isotopic composition is indicative of the diagenetic process rather than the environment of formation (Fritz et al, 1971).

Irwin et al. (1977) noted that in organic rich marine sediments, 4 major diagenetic depth related zones could be recognized (Fig. 5.1; see also Fig. 2.6, Gautier and Claypool, 1984). The relative importance of each zone is dominantly controlled by rate of burial. Degradation of organic matter in the zone of bacterial oxidation and bacterial sulphate reduction results in isotopically lighter bicarbonate ($\approx$-25‰, PDB) compared to the marine bicarbonate reservoir ($\approx$ 0‰, PDB). Carbonates precipitating in these zones will have low $\delta^{13}C$ values. However, siderite is unstable under such diagenetic conditions and cannot possibly precipitate in zone I and II.

If degradation of organic matter occurs through the process of microbial methanogenesis (zone III, Fig. 5.1), then the resulting CO_2 will be enriched in ^{13}C compared to CH_4. Carbonates precipitating from such waters will reflect the high $\delta^{13}C$ of the CO_2. Irwin et al. (1977) note that carbonates with $\delta^{13}C$ values as high as +15‰ are possible under such conditions. High $\delta^{13}C$ values in marine siderites has been reported by Gautier and Claypool (1984). Continental siderites analysed by Fritz et al.

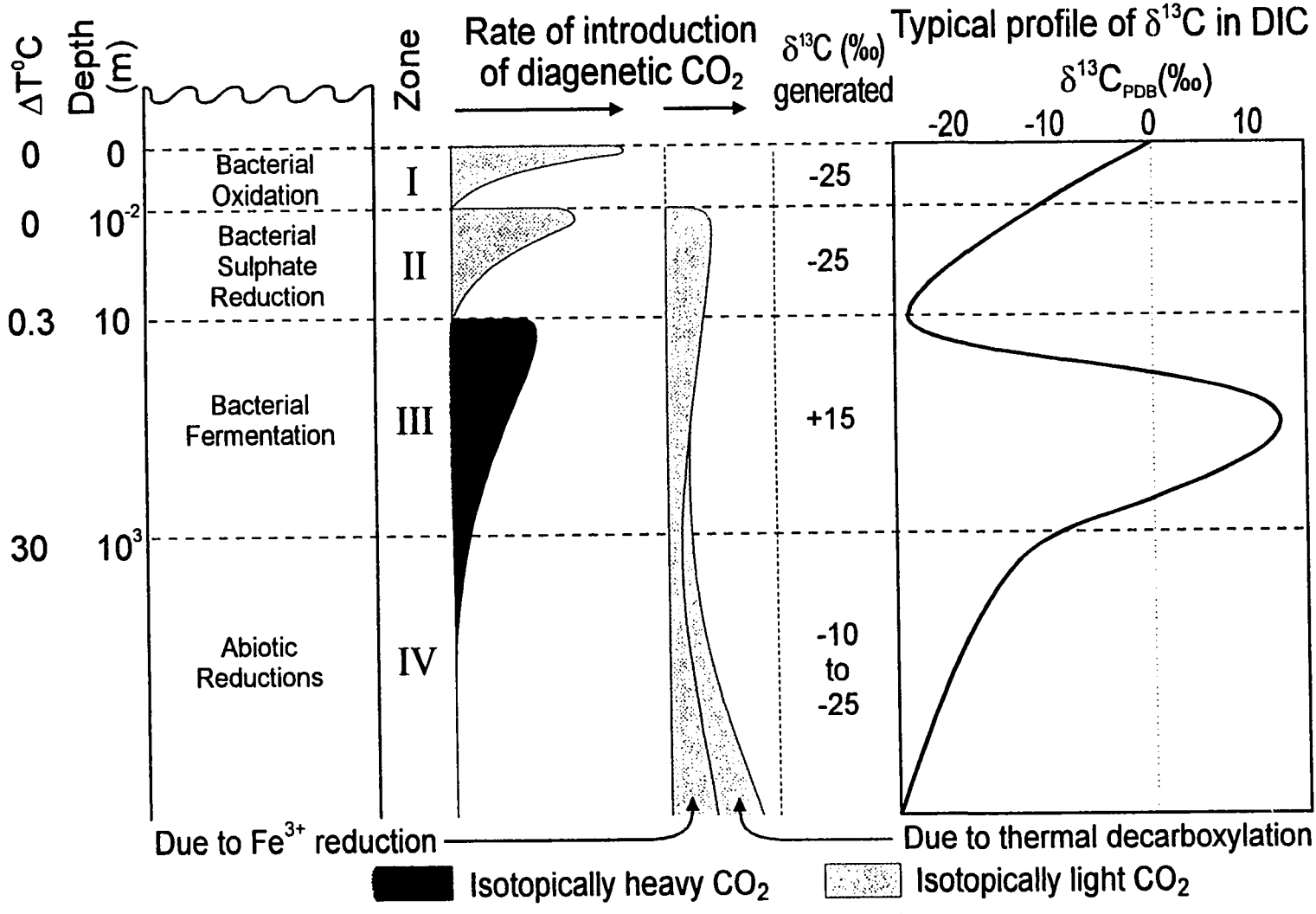

Figure 5.1 Variation in the carbon isotopic composition of diagenetic CO_2 introduced within different diagenetic zones (Modified from Irwin and Curtis, 1977). $\delta^{13}C$ profile is derived from Claypool and Kaplan (1974).

(1971) and Gould and Smith (1979) also show high $\delta^{13}C$ values. In both cases the heavy carbon isotope values are attributed to bacterial decomposition of organic matter where heavy CO_2 and light methane are formed.

Oxidation of earlier formed methane, will result in bicarbonate depleted in ^{13}C (as low as -50‰, Curtis and Coleman, 1986). Under such conditions isotopically light siderite can precipitate. Light $\delta^{13}C$ values in siderites from the Cardium Formation has been reported by Staley (1987).

Abiotic reactions such as thermal decarboxylation (zone IV, Fig. 5.1) is more important at greater depths and carbonates precipitating in this zone should have low $\delta^{13}C$ values (-10 to -25‰, PDB; Irwin et al., 1977).

As pointed out by Fritz et al. (1971) and Irwin et al. (1977), the $\delta^{13}C$ of siderite will not be indicative of the environment of sediment deposition. However, the carbon isotopic data may indicate which diagenetic environment(s) dominated at the time of siderite formation.

5.2 Oxygen Isotopic Fractionation

Equilibrium isotope fractionation for divalent metal carbonates can be described in terms of isotope exchange reactions. The oxygen isotope exchange between calcium carbonate and water, for example, is dependent upon the equilibrations in the following reactions (eg. Carothers et al. 1988):

$$CO_2 + H_2O \rightleftharpoons H_2CO_3 \quad (1)$$

$$H_2CO_3 \rightleftharpoons HCO_3^- + H^+ \quad (2)$$

$$HCO_3^- \rightleftharpoons CO_3^{2-} + H^+ \quad (3)$$

$$Ca^{2+} + CO_3^{2-} \rightleftharpoons CaCO_3 \quad (4)$$

Due to the overwhelming amount of water relative to carbon dioxide in the natural environment, the oxygen isotopic composition of the water controls the oxygen isotopic composition of the dissolved carbonate.

The oxygen isotopic exchange between $CaCO_3$ and H_2O can be written so that only one atom is exchanged:

$$\tfrac{1}{3}Ca^{16}CO_3 + H_2{}^{18}O \rightleftharpoons \tfrac{1}{3}Ca^{18}CO_3 + H_2{}^{16}O \quad (5)$$

and the fractionation factor is

$$\alpha_{CaCO_3\text{-}H_2O} = ({}^{18}O/{}^{16}O)_{CaCO_3}/({}^{18}O/{}^{16}O)_{H_2O} \quad (6)$$

The fractionation factor (α) is related to the equilibrium constant (K) by

$$\alpha = K^{1/n} \quad (7)$$

where n is the number of atoms exchanged. For equation 5, only one atom is exchanged, so $n = 1$, and therefore $K = \alpha$

The isotopic fractionation factors which are close to unity (1.00x), can make use of the mathematical approximation,

$$10^3 \ln(1.00x) \simeq x \quad (8)$$

The isotopic fractionation factor between two phases A and B, expressed in permill notation, can therefore be approximated by the following relationship,

$$\Delta_{A\text{-}B} = \delta_A - \delta_B \simeq 10^3 \ln\alpha_{A\text{-}B} \quad (9)$$

Experimental studies of oxygen isotopic fractionation between solids and water over wide temperature ranges (see for example, O'Neil et al., 1969; Friedman and O'Neil, 1977), has established to following relationship:

$$10^3 \ln\alpha = A \cdot 10^6/T^2 + B \qquad (10)$$

where A and B are constants and T is the temperature (°K). The constants have been derived for numerous common mineral-water phases found in the natural environment. O'Neil et al. (1969) demonstrated that water of the same isotopic composition and temperature, can precipitate different divalent metal carbonates, with slight differences in their isotopic composition. They concluded that both the cationic size (predominantly its effect on the internal vibrations of the anion) and mass (which affects the lattice vibrations) are important in the isotopic fractionation.

Oxygen isotope fractionation between siderite and water have been reported by Becker and Clayton (1976), Golyshev et al. (1981) and Carothers et al. (1988). The fractionation equations for siderite-water and calcite-water are given below:

$$10^3 \ln\alpha_{(\text{calcite-water})} = 2.78 \times 10^6 T^{-2} - 2.89 \quad \text{(Friedman \& O'Neil, 1977)} \qquad (11)$$

$$10^3 \ln\alpha_{(\text{siderite-water})} = 2.89 \times 10^6 T^{-2} - 2.81 \quad \text{(Becker \& Clayton, 1976)} \qquad (12)$$

$$10^3 \ln\alpha_{(\text{siderite-water})} = 3.18 \times 10^6 T^{-2} - 5.86 \quad \text{(Golyshev et al., 1981)} \qquad (13)$$

$$10^3 \ln\alpha_{(\text{siderite-water})} = 3.13 \times 10^6 T^{-2} - 3.50 \quad \text{(Carothers et al., 1988)} \qquad (14)$$

Equation (14) consistently yields a 2‰ heavier value than equations (12) and (13). Over the temperature range of 15 - 30°C and $\delta^{18}O_{water}$ = 0‰ (SMOW), siderite would precipitate with a heavier oxygen isotopic composition relative to calcite by approximately 1.4‰ (eqns. 12 & 13) to 3.3‰ (eqn. 14). However, as stated in Section

5.1, the oxygen isotopic composition of the Cretaceous Interior Seaway contained a significant meteoric water component (Tourtelot and Rye, 1969; Kyser et al., 1993), and Cretaceous oceans were warmer than modern oceans, so we can expect early marine precipitated calcite and siderite to have lower $\delta^{18}O$ values than expected under normal marine conditions.

5.3 Analytical Procedure

The technique for the reaction of carbonates with 100% phosphoric acid at 25°C to liberate CO_2 for isotopic analysis is described by McCrea (1950). During the phosphoric acid and carbonate reaction, a temperature dependent fractionation of the oxygen isotope occurs, since only ⅔ of the carbonate's oxygen is liberated as CO_2 gas. For each carbonate mineral type reacted at a specific temperature, a phosphoric acid liberated CO_2–carbonate fractionation factor (α), is used in the conversion of raw mass spectrometry data to correct for the oxygen isotope fractionation.

Phosphoric acid reaction of siderite at 25°C is extremely slow and may require more than 6 months to attain high CO_2 yields for reliable results. However, Becker and Clayton (1976) stated that >99% yields are not necessary for accurate isotopic analysis of siderite. Phosphoric acid liberated CO_2–siderite fractionation factors for elevated temperature reactions have been reported by Rosenbaum and Sheppard (1986) and Carothers et al. (1988). The following fractionation factors were used during this study:

Calcite: 1.01050, for 2 hrs. reaction at 25°C (Land, 1980),

Siderite: 1.01079, for 7 day reaction at 50°C (Carothers et al., 1988),

Siderite: 1.00771, for 1½ hr. reaction at 150°C (Rosenbaum and Sheppard, 1986).

The technique used for the liberation of CO_2 gas for stable isotopic analysis is as follows. A calcite or siderite powder is placed in a glass pedestal sample holder and inserted into a 1 cm wide glass tube approximately 22 cm in length containing 2 ml of phosphoric acid (Fig. 5.2a). The reaction tube is mounted on a vacuum line and after a good vacuum is establish, it is sealed with a torch. The vacuum sealed reaction tube is placed in a 50°C oven for 2 hrs. to bring up the temperature of the phosphoric acid before reacting with the siderite sample. The reaction tube is inverted to mix the siderite with phosphoric acid (Fig 5.2b) and the reaction is left to proceed in the furnace for 7 days at 50°C (for comparative purposes, several siderite samples were also reacted at 150°C for 1½ hrs). The heating procedure is omitted for calcite as these reactions are performed at 25°C. After 7 days, the reaction tube is cooled to room temperature and placed inside a glass tube cracker attached to the mass spectrometer intake line (Fig 5.2c) for carbon and oxygen isotopic analysis. A siderite standard was reacted at regular intervals to monitor temperature stability of the furnace and for sample reproducibility measurements. A total of 14 siderite standards were analysed yielding values of $\delta^{13}C = -12.3 \pm 0.06‰$ and $\delta^{18}O = -19.6 \pm 0.11‰$. All samples were analysed on a VG602D double collector mass spectrometer and a VG-SIRA triple collector mass spectrometer at McMaster University.

Figure 5.3 shows a plot of $\delta^{13}C$ values for several siderites from the Cardium Formation. The values were derived by reacting each sample at 50°C and 150°C as described above. Carbon isotopes do not undergo any fractionation effects during

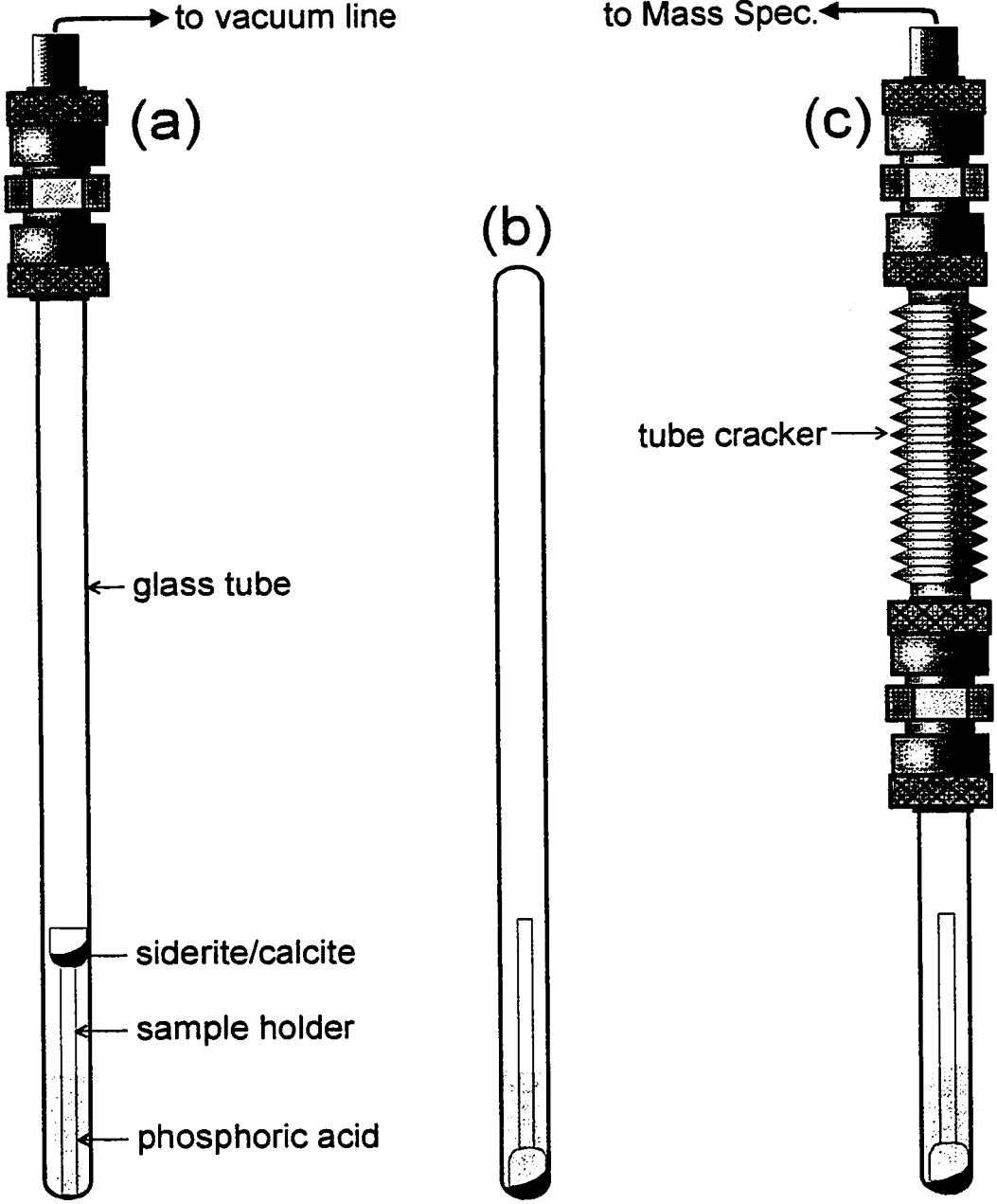

Figure 5.2 Procedure for liberating CO_2 from carbonates for stable isotope analysis. A glass reaction tube containing 2 ml of phosphoric acid and carbonate powder suspended in a sample holder (a). The vacuum sealed reaction tube is inverted to mix the carbonate with phosphoric acid (b), and after required reaction time is placed inside a glass tube cracker attached to the mass spectrometer intake line (c) for isotopic analysis.

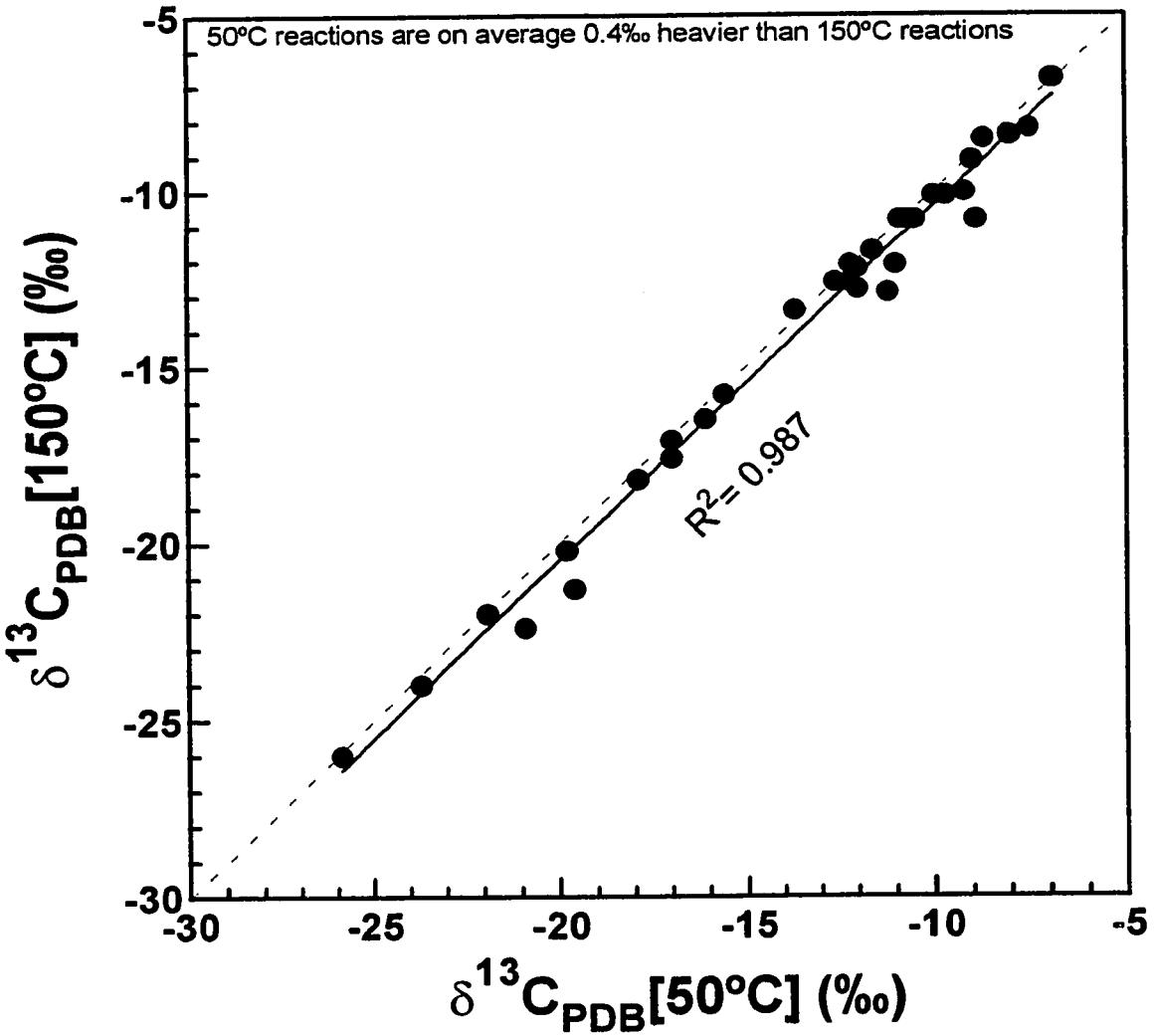

Figure 5.3 Comparison of the carbon isotopic composition of siderites reacted with phosphoric acid at 50°C and 150°C.

liberation of CO_2 by reaction of carbonates with phosphoric acid. However, the 50°C reactions generated carbon isotopic values 0.4‰ heavier than the 150°C reactions. The nature of this effect is not known but it may be related to differences between the 50°C and 150°C phosphoric acid liberated CO_2–siderite fractionation factor. The fractionation factor applies a correction to $\delta^{18}O$, but $\delta^{13}C = 1.0676\delta^{45} - 0.0338\delta^{18}O$ (for a double collector mass spectrometer; Craig, 1957). For additional information on correction factors for mass spectrometric analysis of CO_2 refer to Craig (1957) and Deines (1970).

A comparison of the oxygen isotopic composition of various siderite samples from the Cardium Formation is shown in Figure 5.4. The siderites were reacted with phosphoric acid at 50°C and 150°C. Figure 5.4a shows considerable scatter in the data and represents the analysis generated by both the VG602D and VG-SIRA mass spectrometers. There is a considerable reduction in scatter of the data when the analysis from the VG602D mass spectrometer are not included (Fig. 5.4b). Half of the siderite samples in Figure 5.4b, were mixed with the phosphoric acid before they were brought up to the 50°C and 150°C reaction temperature. Figure 5.4c shows the isotopic composition of the siderites derived by heating the phosphoric acid to its reaction temperature prior to mixing with the siderite and the liberated CO_2 gas was analysed by one mass spectrometer (VG-SIRA). The fact that the 50°C and 150°C reacted siderites plot on a line with unity slope, indicates that the phosphoric acid liberated CO_2–siderite fractionation factor of Carothers et al. (1988) and Rosenbaum and Sheppard (1986) will both yield comparable results. For consistency, all samples in this study were analysed with the VG-SIRA mass spectrometer, and the siderites were reacted with 50°C

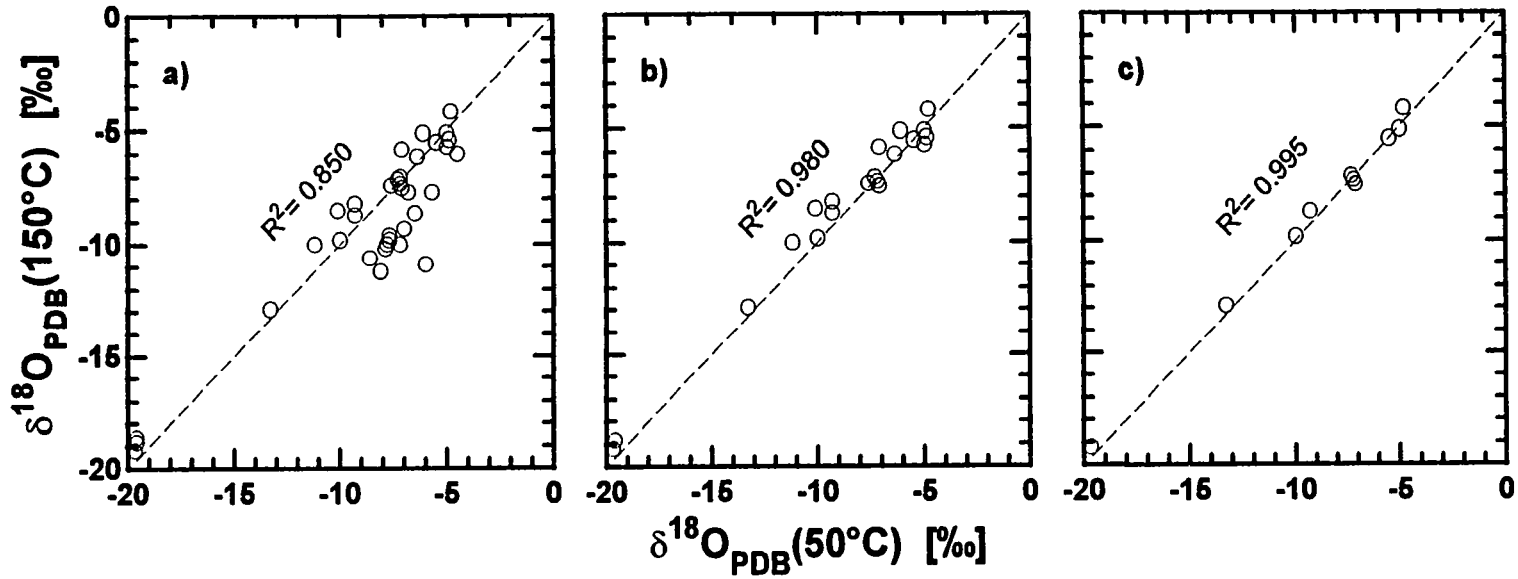

Figure 5.4 Comparison of the oxygen isotopic composition of siderites reacted with phosphoric acid at 50°C and 150°C. (a) Represents data analysed with VG602D and VG-SIRA mass spectometers. (b) Represents data analysed with VG-SIRA mass spectometer, but half the siderites were mixed with phosphoric acid before the acid attained the required reaction temperature. (c) Represents data analysed with VG-SIRA mass spectometer and the phosphoric acid was heated to the appropriate reaction temperature prior to mixing with siderite.

phosphoric acid for 7 days. All carbonate isotopic values are relative to PDB and all references to the isotopic composition of water are relative to SMOW.

5.4 Carbon and Oxygen Isotopic Composition of Main Diagenetic Minerals.

The carbon and oxygen isotopic compositions of the main diagenetic carbonate phases in the Cardium Formation are shown in Table 5.1 and Figure 5.5. The Inoceramid shells (from marine mudstones) and oyster shells (lagoonal muds) which precipitated directly from marine and brackish waters respectively, exhibit unusually low oxygen isotopic values. Based on the calcite-water fractionation factor, and a maximum temperature of 30°C, the Inoceramid shells would have precipitated from waters with an oxygen isotopic composition of -3.3 to -6.8‰ (SMOW). Kyser et al. (1993) also reported Turonian age Inoceramids with $\delta^{18}O_{PDB}$ values in the range of -5 to -8‰, which would suggest precipitation from marine waters having a lower oxygen isotopic composition (approx. -4‰, SMOW), based on average temperature of 25°C for the Late Cretaceous Western Interior Seaway (Kyser et al., 1993). Although diagenesis may generally drive whole-rock $\delta^{18}O$ to more negative values, studies by Pratt et al. (1993) indicate that the calcite and aragonite of Inoceramid bivalves and other aragonitic components of the Western Interior fauna have preserved original $\delta^{18}O$ values.

The brackish water oyster shells have an oxygen isotopic composition of -12.8‰, which would require precipitation from waters with $\delta^{18}O_{SMOW}$ = -10‰. Glancy et al. (1993) estimated that the precipitation runoff during Late Cretaceous time

Sample Type	$\delta^{18}O_{PDB}$ (‰)	$\delta^{13}C_{PDB}$ (‰)
Siderite Concretions, Marine	-4.0 - -7.5	-5.0 - -12.7
Siderite Concretions, Transitional	-9.0 - -14.3	2.3 - -9.5
Conglomeratic Siderite, Marine	-4.5 - -8.1	-6.9 - -25.9
Gritty Siderite	-7.1 - -10.2	-7.4 - -12.2
Inoceramid Shells, Marine	-6.1 - -9.5	2.7 - 5.0
Oyster Shells, Transitional	-12.8 - -12.9	-0.8 - 1.0
Conglomeratic Calcite I	-15.2 - -15.7	-2.5 - -11.8
Conglomeratic Calcite II	-15.6 - -17.9	-15.5 - -18.1
Fracture-Filling Calcite	-14.7 - -17.5	-9.0 - -16.2

Table 5.1 Range of carbon and oxygen isotopic values for major carbonate phases in the Cardium Formation.

Figure 5.5 Carbon and oxygen isotopic composition of various calcite and siderite phases in the Cardium Formation.

◇ - oyster, brackish water

◆ - Inoceramid shells, marine

◆ - gritty siderite

● - concretionary siderite nodules/bands, marine

○ - concretionary siderite nodules/bands, continental/brackish

■ - conglomeratic siderite cement

▼ - conglomeratic calicte I

▲ - conglomeratic calcite II

✖ - fracture filling calcite

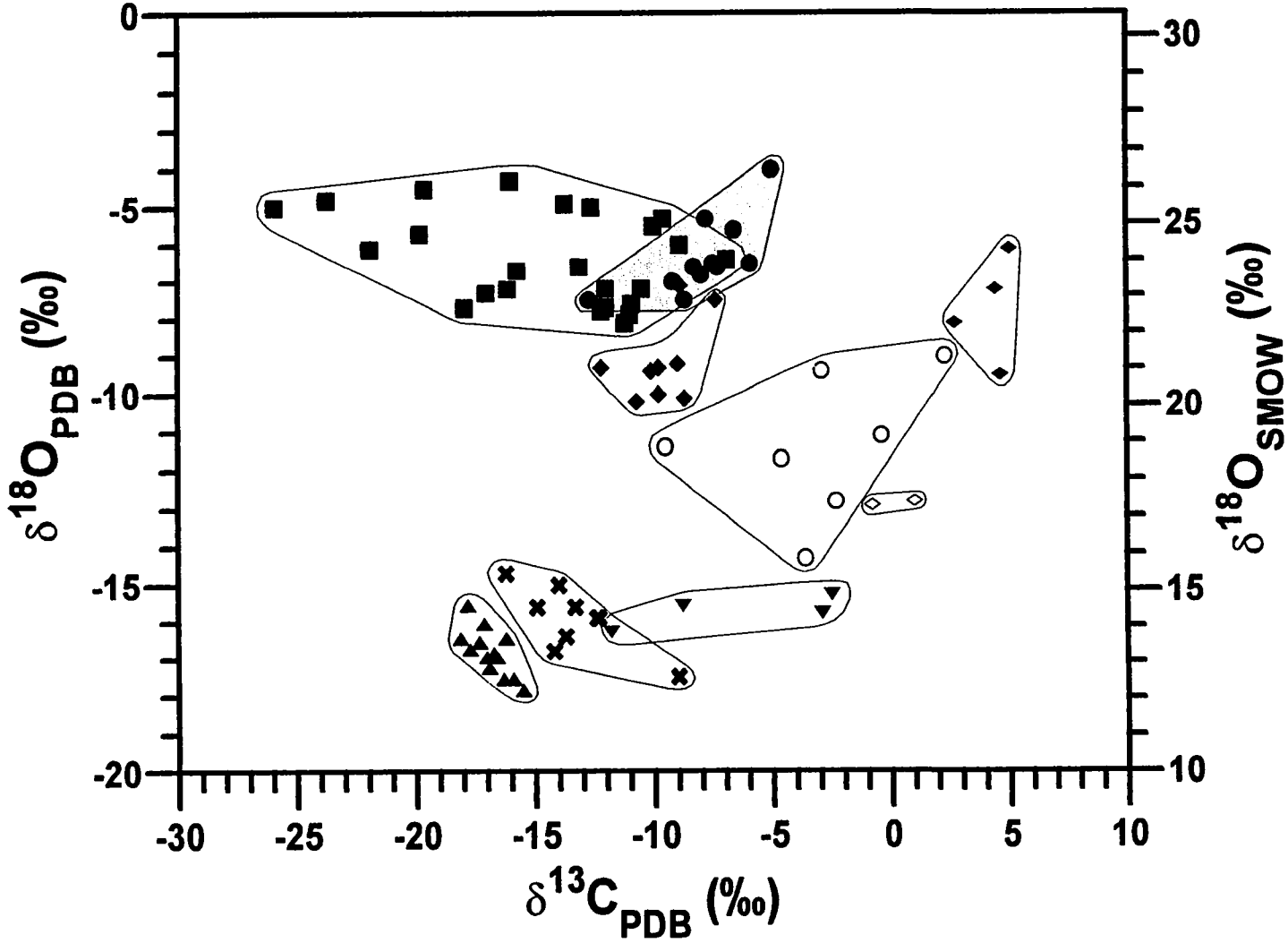
0
-5
-10
-15
-20
30
25
20
15
10
-30
-25
-20
-15
-10
-5
0
5
10
δ18OPDB (‰)
δ18OSMOW (‰)
δ13CPDB (‰)

in the Western Interior region was in the range of -8 to -21‰, with a modal value near -20‰. Today's precipitation in the region range from -12 to -20‰ (Yertsever, 1975).

The carbon isotopic composition of the shell samples ranges from -0.8 to 5.0‰. These values are within the expected isotopic range for samples precipitating from waters dominated by a marine carbonate reservoir.

There is a distinct isotopic difference between the marine (Carrot Creek) and brackish water (Kakwa) siderites (Table 5.1 and Fig. 5.5). The marine siderite concretions have $\delta^{18}O$ values of -4.0 to -7.5‰ and the conglomeratic siderite cements have $\delta^{18}O$ = -4.5 to -8.1‰. These early formed siderites would have precipitated from marine waters of similar oxygen isotopic composition as the Inoceramids. The continental/brackish water siderite concretions ($\delta^{18}O$ = -9.0 to -14.3‰) would have precipitated from waters of lighter oxygen isotopic composition, in the range of $\delta^{18}O_{SMOW}$ = -7.6 to -13.0‰.

The carbon isotopic composition of the brackish water siderites ($\delta^{13}C$ = 2.3 to -9.5‰), is no longer controlled by the overlying water reservoir, since they are shifted towards more negative $\delta^{13}C$ values as a result of bacterial oxidation, bacterial reduction and bacterial fermentation processes within the sediment. The marine siderite concretions have $\delta^{13}C$ values of -5.0 to -12.7‰, characteristic of sedimentary zones where bacterial methanogenesis dominates (Fig. 5.1). The conglomeratic siderite cements have a broader carbon isotopic range (-6.9 to -25.9‰). These values would be typical of post bacterial sulphate reduction and bacterial methanogenic processes. The conglomeratic siderites cements have a wider carbon isotopic range than the mud locked

marine siderite concretions due to the higher permeability and porosity of the conglomerates (ie. there is a potential for greater degree of mixing between diagenetic zones).

The gritty siderites are believed to have formed in bioturbated silts and muds with coarse chert grains, during a stillstand (Bergman, 1987). The oxygen isotopic composition of these gritty siderites is lower than the other marine siderites (-7.1 to -10.2‰) and would have precipitated from waters having $\delta^{18}O_{SMOW}$ = -5.6 to -8.8‰. This represents a significant input of meteoric water into the shallow region of the Western Interior Seaway.

The oxygen isotopic composition of the conglomeratic calcites ($\delta^{18}O$ = -15.2 to -17.9‰), which postdate the conglomeratic siderites, denotes a significant change of the water reservoir ($\delta^{18}O_{SMOW} \approx$ -13‰) within the marine sediments.

The oxygen and carbon isotopic composition of the siderites is within the range of those found in other parts of the Cardium Formation (For example, Staley, 1987; Machemer and Hutcheon, 1988; Hart et al., 1992). Unique to all of these siderites is their depleted $\delta^{18}O$ values. A compilation of the carbon and oxygen isotopic composition of numerous siderites by Mozley and Wersin (1992) and Mozley and Burns (1993), show anomalously depleted $\delta^{18}O$ values, considering their marine origin. Possible explanations for this depletion are recrystallization, water-sediment interaction, precipitation at anomalously high temperatures, mixing with meteoric water and variation in seawater composition. Mozley and Burns (1993) considered the most likely explanation to be either mixing of meteoric water and marine waters in marine shelf sediments or mineral-

water interaction during early diagenesis (ie. precipitation of ^{18}O enriched minerals which would cause a net depletion of $\delta^{18}O$ in the porewater).

Isotopic studies on the Pembina Member of the Cardium formation by Machemer and Hutcheon (1988) showed that there is a systematic change in the isotopic composition of calcite and siderite from $\delta^{13}C$ = -25 to -30‰ and $\delta^{18}O$ = 0‰ for early cements, to $\delta^{13}C$ = 0 to -5‰ and $\delta^{18}O$ = -15‰ for late stage cements. Although the marine unit was deposited a considerable distance offshore on a shallow shelf, they attributed the isotopic shift to invasion of meteoric water into the unit as a result of a 1 m drop in the sea level, which would push the freshwater-seawater interface 100 km seaward.

To address the problem of depleted ^{18}O values of the siderites and shell sample one must look at the isotopic composition of the early formed mineral phases. Figure 5.6 shows the probable oxygen isotopic composition of the waters that may have precipitated the early formed carbonates. These oxygen isotopic values are based on the isotopic composition of the mineral, the mineral-water fractionation factors as discussed in Section 5.2 and a Cretaceous Western Interior Seaway maximum temperature of 30°C (Kyser et al. (1993), reported an average temperature of 25°C). The siderite-water fractionation factors of Becker & Clayton (1976) and Golyshev et al. (1981) were used as it agreed more favourably with the Inoceramid derived isotopic water composition. The siderite-water fractionation factor of Carothers et al. (1988) consistently yielded 2‰ lighter oxygen isotopic water values.

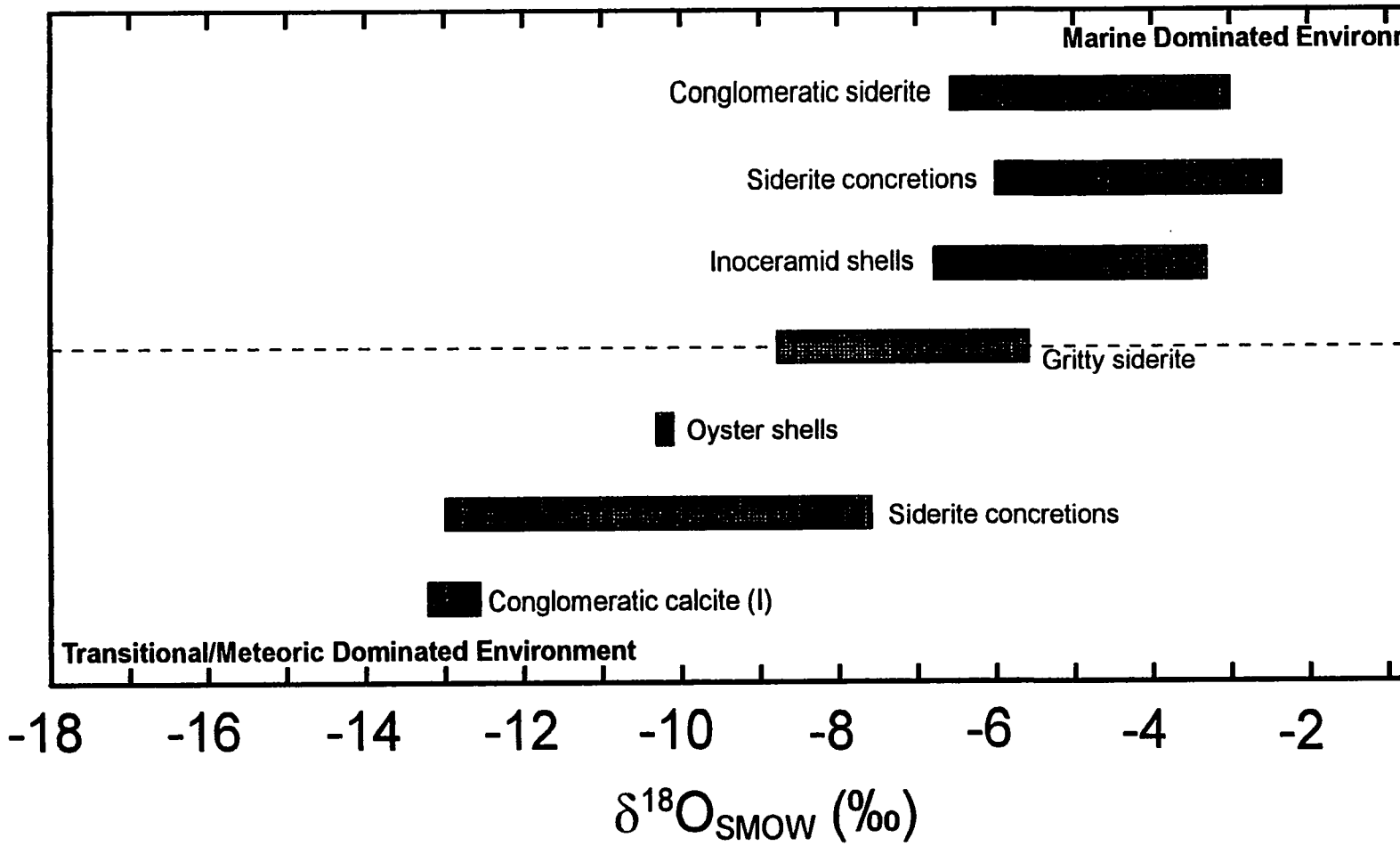

Figure 5.6 Calculated $\delta^{18}O$ values for waters which precipitated contemporaneous and early diagenetic mineral phases in the Cardium Formation. The maximum temperature of the Turonian Interior Seaway was assume to be 30°C.

The two marine siderite phases and the Inoceramid shells suggests that they were precipitated from marine waters having an oxygen isotopic composition of -2.4 to -6.8‰ (Fig. 5.6). The gritty siderites, considered to have formed during a stillstand, precipitated from marine waters with a strong meteoric influence ($\delta^{18}O_{SMOW}$ = -5.6 to -8.8‰). The continental/brackish water oyster shells and siderite concretions precipitated from considerably isotopically lighter waters in the range of $\delta^{18}O_{SMOW}$ = -7.6 to -13‰. Although the conglomeratic calcites are within marine sediments, the oxygen isotopic composition for the earliest phases suggests that the original marine pore waters were flushed with meteoric waters of $\delta^{18}O_{SMOW} \approx$ -13‰. The oxygen isotopic composition of this meteoric water is in agreement with the $\delta^{18}O$ of the waters that precipitated some of the continental/brackish water siderites. The validity of these findings will be compared to the strontium isotopic data of Chapter 4 and is discussed in Chapter 7.

CHAPTER 6

Elemental Composition of Calcite and Siderite

6.1 Introduction

Pearson (1974a, b), Matsumoto and Iijima (1981), Curtis and Coleman (1986) Curtis et al. (1986) and Mozley (1989) observed that there is a considerable variation in the Mg, Ca, Mn and Fe composition of siderites. Freshwater siderites tend to have a lower Mg/Ca ratio and are compositionally higher in Fe and Mn than marine siderites (Fig. 6.1). Additionally, early formed siderites have higher Mn and lower Mg concentrations (Fig. 6.2) than diagenetically later siderites (Curtis and Coleman, 1986; Curtis et al., 1986; Mozley and Carothers, 1992). In siderite concretions this diagenetic trend can be distinguished by an Mn rich core with increasing Mg concentration outwards. The elemental and isotopic compositional difference between marine vs freshwater siderites, and early vs late diagenetic siderites is due to the chemistry of the waters from which the carbonates precipitated. For example, marine precipitated carbonates will have high ^{18}O and Mg/Ca levels with respect to freshwater carbonates, since ^{18}O and Mg/Ca ratio are higher in seawater relative to freshwater.

High Mg siderites can also form in a freshwater environment (Matsumoto and Iijima, 1981). The high Mg content is related to diagenetic modification of Mg-clays during late stages of sediment compaction (Pearson, 1974b; Curtis et al., 1986). These high Mg continental siderites will have a low $\delta^{18}O$ (freshwater) and low initial porosity (due to compaction) and are thus distinguishable from their marine counterparts.

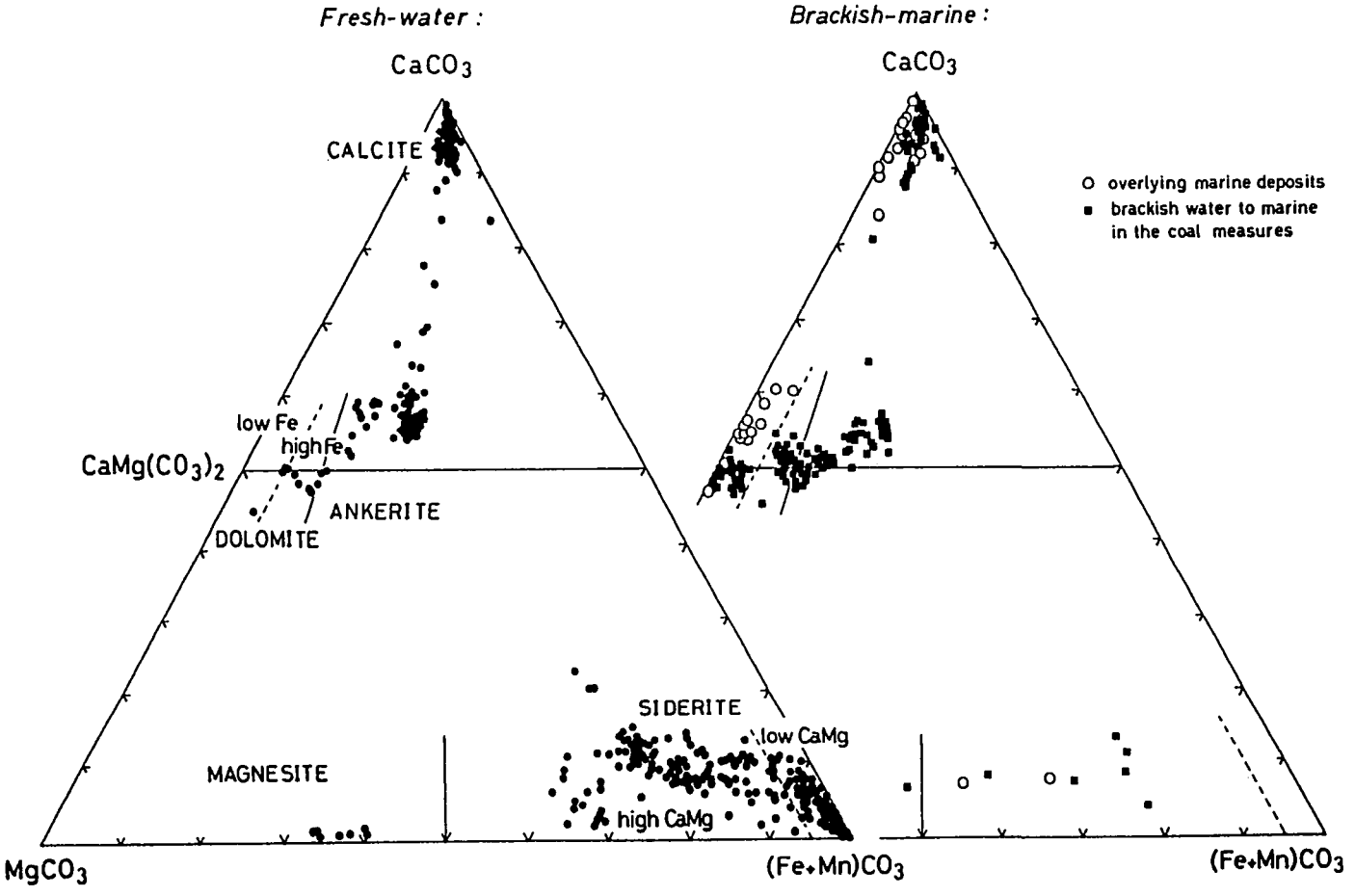

Figure 6.1 $CaCO_3$-$MgCO_3$-$(Fe+Mn)CO_3$ ternary diagrams of authigenic carbonates in Pleistocene, Paleogene and Upper Triassic coalfields of Japan. The diagram on the left shows freshwater carbonates, and that on the right shows brackish-marine carbonates. (From Matsumoto and Iijima, 1981)

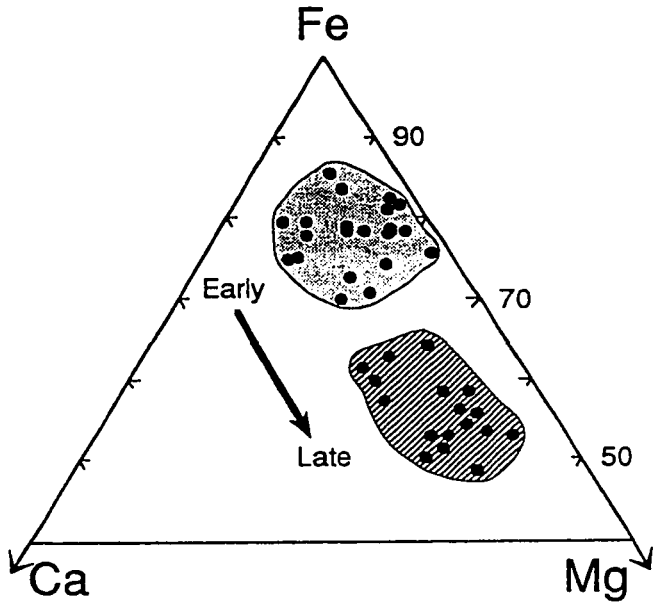

Figure 6.2 Ternary diagram illustrating the elemental composition of authigenic siderites in the Kuparuk Formation (Neocomian). Highlighted areas represent Fe-rich and Mg-rich compositional fields and arrow represents the major temporal trend. (From Mozley and Carothers, 1992)

The Ca, Mg, Mn and Fe composition of carbonates in the Cardium Formation were analyzed to see if there is any correlation between elemental composition and environment of formation.

6.2 Analytical Procedure

The Ca, Mg, Mn, Fe, and Sr concentrations of siderite and calcite were determined by the Sciex-Elan Inductively Coupled Plasma Mass Spectrometer (ICPMS) at McMaster University. Elemental analysis by ICPMS was performed using external standard calibration curves and an internal rhodium (Rh) standard. For ICPMS analysis, the isotope dilution method can yield better precision than the standard calibration curve method (Li, 1989). However, the latter method is more cost and time effective and can produce very reliable results if the samples are diluted to concentration levels of 0.1 to 1.0 ppm (Table 6.1).

The dissolved siderite samples (see Chapter 4.2.2) were diluted with distilled water and analyzed on the ICPMS. Samples which registered saturation or threshold warnings, or exhibited high errors were rerun at different dilution levels. Two standard solutions of 0.1 and 0.5 ppm were run after every 10 samples on an alternating basis. To minimize any interference with the argon plasma and any associated argon ionic complexes, the concentration of Ca and Fe was determined using mass ^{44}Ca and ^{54}Fe respectively.

Sample Concentration (ppm)

Percent Error	0.05	0.10	0.50	1.00
Mg	7.4	3.4	3.2	1.4
Al	1.4	3.4	3.8	1.0
Ca	9.9	5.1	0.2	1.8
Mn	8.6	6.0	5.4	0.2
Fe	71.7	2.6	4.9	3.0
Rb	6.7	3.8	3.8	0.5
Sr	9.2	7.1	6.6	0.5

Table 6.1 Percent error levels for Mg, Al, Ca, Mn, Fe, Rb and Sr of samples diluted to the range of 0.05 to 1.00 ppm. The samples were analysed by Inductively Coupled Plasma Mass Spectrometry (ICPMS) using the external standard calibration curve method and an internal rhodium standard. For Ca and Fe the concentrations were determined using mass ^{44}Ca and ^{54}Fe to overcome interference by the argon plasma and argon complexes.

6.3 Discussion

The Al concentration was used as a monitor for possible radiogenic Sr contamination from clays. Samples with high Al level are accompanied by higher Sr concentrations and suggests that during siderite dissolution (Chapter 4.2.2), radiogenic Sr from clays was mixed with sideritic Sr. All samples that registered high Al concentrations were rerun for $^{87}Sr/^{86}Sr$ ratios and elemental analysis. This was usually a problem with samples that have a low siderite to clay ratio. Such samples require 350 to 650 mg of 200 mesh powder to yield sufficient siderite for Sr analysis. Considerable cost and time can be saved if the samples are first analyzed for Al by ICPMS before they are analyzed for the Sr isotopic ratios.

The Sr concentration of various mineral phases in the Cardium Formation is presented in Table 6.2. The Sr concentration of the siderites ranges from 77 to 279 ppm. For calcites, the Sr concentration is considerably higher, ranging from 1,298 to 4774 ppm. Sr from clays, in the exchangeable sites, have concentrations ranging from 12 to 98 ppm. These exchangeable sites are the main source of radiogenic Sr contamination when dealing with siderite dissolution as discussed in Chapter 4.2. Heavy minerals, kaolinite and framework-locked Sr in alumino-silicates have low Sr concentrations (Table 6.2) that can be easily managed and therefore should not have an effect on the original Sr isotopic signature of the carbonates.

There appears to be a lack of correlation between the elemental data and environment of formation (Figs. 6.3 and 6.4). Fe and Mn rich siderites are characteristic of terrestrial environments while increased Mg and Ca substitution are characteristic of

Table 6.2 Rb and Sr concentration of various mineral phases in the Cardium Fm. Sample were analysed by ICPMS.

Sample Type	Concentration (ppm) Sr	Rb
Marine Siderite	198	4
	128	7
	279	4
	211	5
	248	6
	77	6
Transitional Siderite	145	7
	98	7
Calcite I	2,718	3
	2,902	3
	3,912	15
	2,691	3
Calcite II	2,652	5
	2,467	2
	4,715	5
	5,918	10
	1,576	1
	1,750	2
	2,023	2
	3,340	1
	4,774	1
	3,554	1
	3,593	1
	4,046	1
	4,713	5
	2,377	2
Fracture-Filling Calcite	2,020	2
	1,878	3
	1,983	14
	2,201	1
	4,063	1
	3,480	1
	2,072	2
	2,216	3
	1,298	2
Kaolinite	12	4
	14	5
	14	3
	15	5
Clays (Exchangable Sites)	60	14
	98	8
	31	9
	12	1
	19	3
	28	7
Alumino-silicates (Framework Locked)	11	34
	4	9
	7	12
	14	20
	17	33
Heavy Minerals	4	0

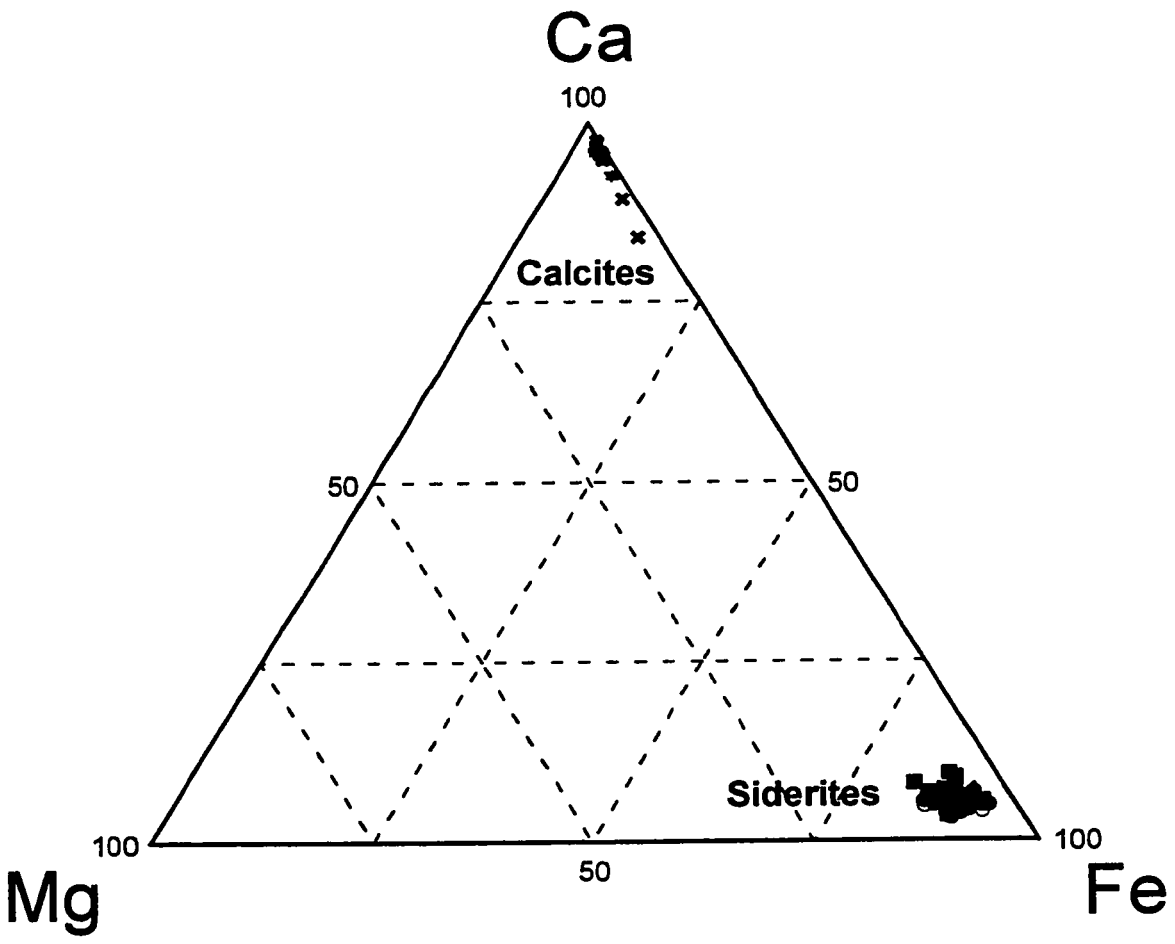

Figure 6.3 Ternary $CaCO_3$—$MgCO_3$—$FeCO_3$ diagram of calcites and siderites from the Cardium Formation. Analysed by ICPMS.

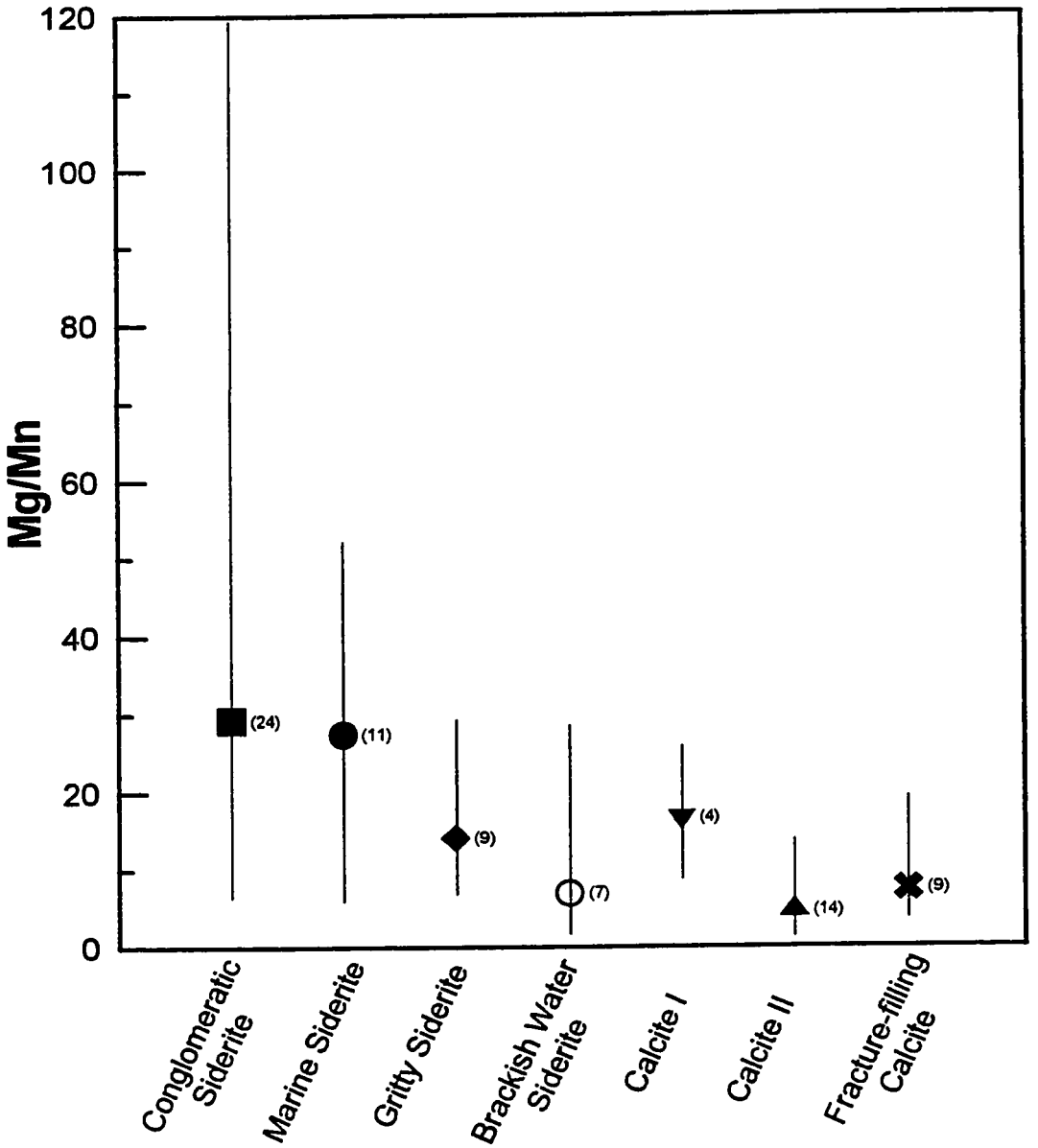

Figure 6.4 Mg/Mn ratios of calcites and siderites from the Cardium Formation. Symbols represent the mean, vertical bars the range, and bracketed values the number of samples. Analysed by ICPMS.

brackish to marine environments (Matsumoto and Iijima, 1981; Curtis et al., 1986; Mozley, 1989). A $CaCO_3$-$MgCO_3$-$FeCO_3$ ternary plot of the siderites fails to resolve the marine siderites from the brackish-terrestrial siderites (Fig. 6.3). Although there is some Mg and Ca substitution for the Fe, the marine siderites plot in the freshwater siderite field (see Fig. 6.1). It is unlikely that the analytical data is questionable, since these values agree with marine siderites from the Pembina field (Machemer and Hutcheon, 1988) and the northern Rocky Mountain Foothills (Hart et al., 1992). The brackish water siderites can be distinguished from their marine counterparts by their mean Mg/Mn ratios (Fig. 6.4). However, there is too much of an overlap in the data and its reliability as an environmental indicator in the Cardium Formation is therefore questionable.

The change in the Fe/Mg ratio of authigenic siderites has been attributed to:

1) migration and mixing of porewaters form freshwater and brackish-marine sediments during compaction (Matsumoto and Iijima, 1981);
2) depletion of iron as a result of precipitation of iron rich mineral such as pyrite and siderite (Curtis and Coleman, 1986);
3) increased Mg concentrations as a result of diagenetic modification of Mg-clays during later stages of sediment compaction (Pearson, 1974b; Curtis et al., 1986);
4) increased Mg concentration due to decay of Mg-enriched bacteria within the sediments (Mosley and Carothers, 1992).

The lack of any significant elemental diversity in the siderites may be due to early siderite precipitating over a relatively short time interval, and prior to any porewater mixing or significant Mg-rich clay mineral dissolution. Additionally, the domination of

Fe reducing microorganisms in the sediment sequence could have maintained a high Fe^{2+} concentration in the porewater. Finally, the marine elemental signature may have been masked due to the chemical nature of the terrestrial derived sediments hosting these siderites (ie. very little Mg- and Ca-rich marine precipitates were incorporated into the sediment). The petrographic evidence along with the oxygen and Sr isotopic compositions rule out the possibility that the siderites may have precipitated from meteoric waters during a regressional event.

CHAPTER 7

Interpretation and Conclusions

7.1 Introduction

Petrographic investigations of numerous core samples from the Cardium Formation revealed a sequence of events preserved in the textural relationship of the various diagenetic mineral precipitates within the sediments (Fig. 3.4). Pyrite precipitated very early, followed by siderite and then calcite. Later events precipitated quartz, kaolinite and finally fracture-filling calcite. Although these clastic sediments were deposited in a marine environment (Plint et al, 1986), the petrographic evidence alone cannot verify this. To solve this problem, we can investigate the carbon, oxygen and strontium isotopic composition of the earliest formed diagenetic minerals within the sediments. The oxygen and strontium isotopic ratios of the early carbonate precipitates will reveal the isotopic composition of the sediment porewaters. The carbon isotopic ratios will indicate the probable diagenetic environment under which these minerals precipitated.

There is no correlation between the observed mineral form of the siderites (Fig. 3.1) and isotopic composition. The siderite form appears to be related to available porespace during mineral growth and not water composition. Sparry and rhombic siderites precipitated in zones with open porespace, whereas micritic siderites formed in zones where the porspace was filled with mud. Granular and spherulitic siderites formed in regions where porespace was partly occluded.

7.2 Stable and Radiogenic Isotope Correlation

The Inoceramid shells found within the marine mudstones, precipitated directly from the coeval seawater. These carbonate shells have an $^{87}Sr/^{86}Sr$ ratio of 0.70434. This is well within the range of the strontium isotopic composition of Turonian age seawater (0.70723 - 0.70751). Brackish water oysters from lagoonal sediments, have a higher $^{87}Sr/^{86}Sr$ ratio of 0.70805.

The diagenetic siderites (gritty and concretionary) hosted within marine mudstones have an $^{87}Sr/^{86}Sr$ ratio ranging between those for the seawater and brackish water shells (Fig. 4.12). This indicates that the siderites precipitated from diagenetically altered marine waters. Siderite concretions within marine sediments can be distinguished from those hosted in brackish/continental sediments by their strontium isotopic ratios. In marine siderites the $^{87}Sr/^{86}Sr$ = 0.70788 - 0.70825 and the continental/brackish siderites have an $^{87}Sr/^{86}Sr$ = 0.70825 - 0.70918. Compared to the marine mudstone hosted siderites, the siderite cements within the conglomeratic unit have a strontium isotopic ratio broader in range and more radiogenic ($^{87}Sr/^{86}Sr$ = 0.70778 - 0.70863). This is due to the higher porosity and permeability of the conglomerates which could easily introduce more radiogenic Sr released from detrital clays and other alumino-silicates during diagenesis. Incorporation of radiogenic Sr is more evident in the later stage conglomeratic calcite cements ($^{87}Sr/^{86}Sr$ = 0.70823 - 0.70986) and the fracture filling calcite ($^{87}Sr/^{86}Sr$ = 0.70959 - 0.71146).

The oxygen isotopic composition of the carbonates (Fig. 5.5) indicates that the marine siderites ($\delta^{18}O$ = -4 to -10‰), brackish siderites ($\delta^{18}O$ = -9 to -14‰) and

calcite cements ($\delta^{18}O$ = -15 to -18‰) precipitated from different waters and/or under different temperature conditions. Figure 5.6 shows the calculated $\delta^{18}O$ composition of waters in the Cardium Formation from which the early diagenetic mineral phases precipitated. The calculations are based on a maximum temperature of 30°C for the Turonian Interior Seaway. The Inoceramid shells and the two marine siderite phases suggests that they were precipitated from seawater having an oxygen isotopic composition of -2.4 to -6.8‰. The oxygen isotopic composition of the earliest calcite cement and the lightest $\delta^{18}O$ of the brackish/continental siderites, suggests that the runoff water entering the seaway had a $\delta^{18}O \approx$ -13‰. The gritty siderite, precipitated within bioturbated silts and muds during a stillstand (Bergman, 1987). Calculated oxygen isotopic composition of the water that precipitated the gritty siderites ($\delta^{18}O_{SMOW}$ = -5.6 to -8.8‰), indicates that they formed in marine waters with a strong meteoric component.

It is unlikely that the temperature of the Turonian Seaway could have been much higher than 30°C, and it is therefore difficult to understand why the water would have such a light oxygen isotopic composition. Low $\delta^{18}O$ in marine carbonates is not unique to this study. Tourtelot and Rye (1969) and Kyser et al. (1993) also reported low $\delta^{18}O$ for Cretaceous carbonate shells, which would suggest precipitation from a seaway with a meteoric water component. A compilation of oxygen isotopic data on marine calcites and siderites concretions by Mozley and Burns (1993) showed similar anomalous depletion of ^{18}O. Kyser et al. (1993) noted that although the $\delta^{18}O$ values of the Late Cretaceous Seaway (Greenhorn sea) imply a substantial meteoric water component and subnormal saline conditions, the fauna in the sea suggests that the salinity could not have

been too low. The magnitude of the ^{18}O depletion in the Greenhorn sea is therefore an enigma. It is possible that these ^{18}O depleted carbonates could have precipitated within sediments under conditions where the surface waters had a reasonably low $\delta^{18}O$ of -4‰ and high temperatures (30°C) and below the sediment water interface $\delta^{18}O$ was approximately -6.5‰. The lower $\delta^{18}O$ in the sediment would have to be attributed to mineral-water interaction such as ultrafiltration by shales, precipitation of ^{18}O enriched authigenic minerals and alteration of organic matter (see Mozley and Burns, 1993 for a review).

The lightest oxygen isotopic values for planktonic forams during the past 120 Ma are in Turonian age open ocean sediments (Anderson and Arthur, 1983). The Turonian forams have an oxygen isotopic composition as light as -4‰ and precipitated from waters with an inferred temperature of approximately 28°C. The Interior Seaway shells ($\delta^{18}O$ = -6.1 to -9.5) have a significantly lighter oxygen isotopic composition which would infer that it is a result of a local phenomenon. Specific samples were not collected with this problem in mind, but the topic warrants future investigations.

Figure 7.1 shows a plot of the calcite and siderite phases in the Cardium Formation. The figure reveals prominent clustering between the $^{87}Sr/^{86}Sr$ and $\delta^{18}O$ values of the carbonate minerals. The Inoceramid shells have $^{87}Sr/^{86}Sr$ ratios characteristic of Turonian seawater. The $\delta^{18}O$ of the carbonate shells indicates precipitation from light $\delta^{18}O$ coeval sea.

The marine siderites represent the early diagenetic stage. These carbonates were precipitated under reducing conditions below the sediment-water interface. As with

Figure 7.1 Strontium and oxygen isotopic composition of various calcite and siderite phases in the Cardium Formation.

◇ - oyster shells, brackish water

◆ - Inoceramid shells, marine

◆ - gritty siderite

● - concretionary siderite nodules/bands, marine

○ - concretionary siderite nodules/bands, continental/brackish

■ - conglomeratic siderite cement

▼ - conglomeratic calicte I

▲ - conglomeratic calcite II

✖ - fracture filling calcite

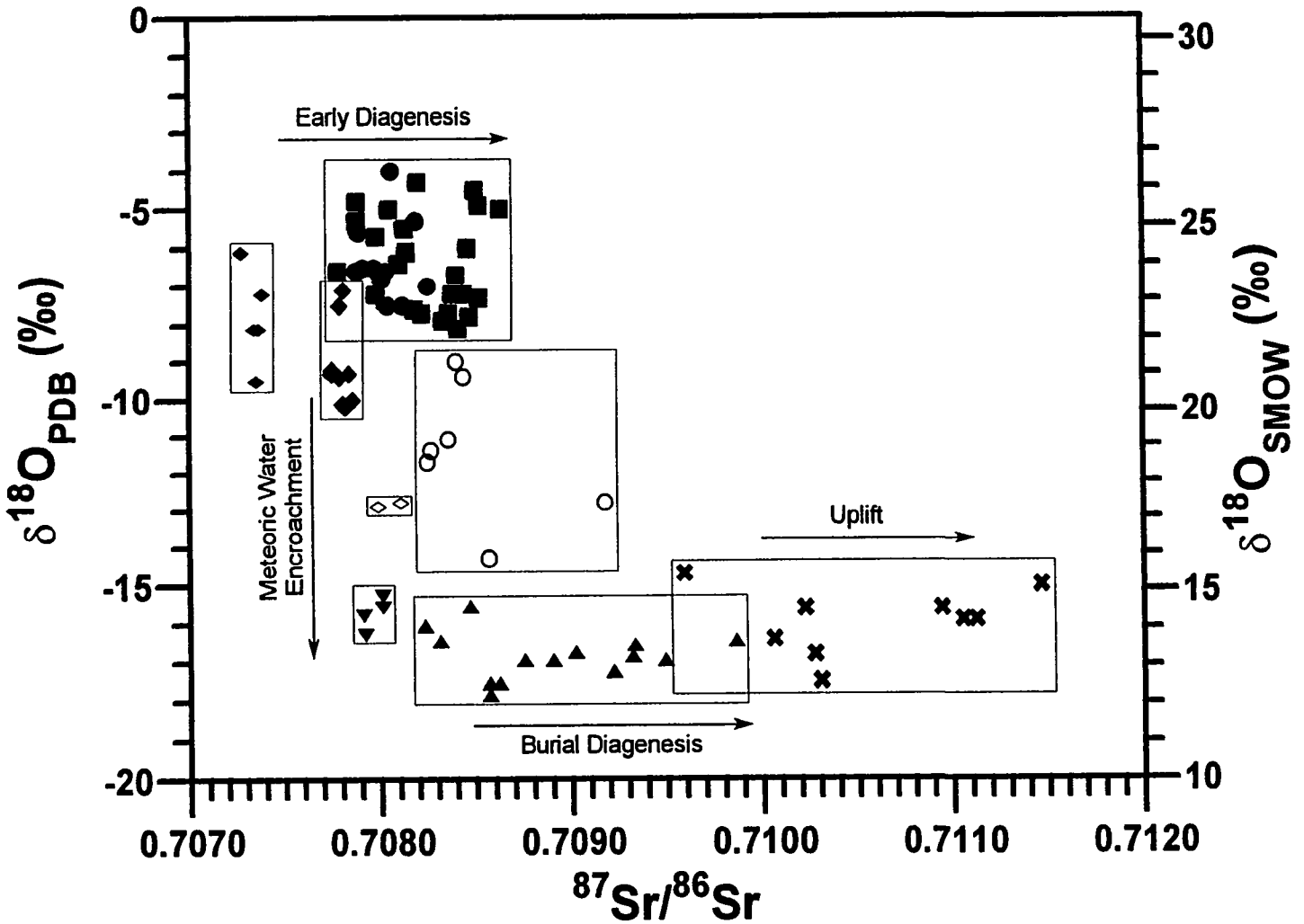
Early Diagenesis
Meteoric Water Encroachment
Uplift
Burial Diagenesis
0
-5
-10
-15
-20
30
25
20
15
10
0.7070
0.7080
0.7090
0.7100
0.7110
0.7120
$\delta^{18}O_{PDB}$ (‰)
$\delta^{18}O_{SMOW}$ (‰)
$^{87}Sr/^{86}Sr$

the Inoceramid shells, the siderites have $\delta^{18}O$ values characteristic of carbonates precipitated from ^{18}O depleted marine porewaters. The Sr isotopic ratio of these siderites has become more radiogenic due to diagenetic processes (ie. clay mineral dissolution) within the sediment. The marine siderite concretions can easily be distinguished from their brackish/continental counterparts by the differences in their Sr and oxygen isotopic ratios (Fig 7.1). The brackish water siderite concretions have lighter $\delta^{18}O$ and more radiogenic $^{87}Sr/^{86}Sr$ ratios.

The earliest calcite cements within the conglomerate units, have significantly lower $\delta^{18}O$ values but their $^{87}Sr/^{86}Sr$ ratio are similar to that of the marine siderites (Fig 7.1). These isotopic values signify the introduction of meteoric water (low $\delta^{18}O$ and low Sr concentration) into the basin. The low Sr concentration in the meteoric waters ($\approx$0.068 ppm) would have an insignificant effect on the $^{87}Sr/^{86}Sr$ ratio of the porewaters (Sr conc. $\approx$ 7.7 ppm).

The higher $^{87}Sr/^{86}Sr$ ratio in the diagenetically later conglomerate calcite cements can be attributed to the release of radiogenic Sr from detrital minerals via mineral dissolution and transformation processes during burial diagenesis.

During uplift, fractures and other pore spaces are filled with calcite. At this stage the porewaters have equilibrated with the detrital sediment, which is reflected in the $^{87}Sr/^{86}Sr$ ratio of the fracture-filling calcites (0.7100 to 0.7115).

The siderites precipitated below the sediment-seawater interface, in marine hosted sediments that have passed through at least three different diagenetic zones (bacterial oxidation, bacterial sulphate reduction and microbial methanogenesis). It can

be expected that during these diagenetic processes radiogenic Sr was released into the porewaters and thus incorporated into the precipitating siderites. It would therefore be unlikely that these siderites would have an original coeval seawater signature. During late burial diagenesis, more clays and other detrital alumino-silicates had undergone dissolution with additionally more radiogenic Sr entering the porewater. Eventually the Sr isotopic ratio of the original porewater will be lost and replaced with that of the surrounding sediments. Any carbonates precipitating at this stage will also acquire the $^{87}Sr/^{86}Sr$ ratio of the porewaters.

7.3 Conclusions

Siderite is a common diagenetic mineral in the Cardium Formation and occurs in sediments of both marine (Carrot Creek) and brackish/continental (Kakwa) water sediments. Interlocked with these sedimentary siderites are detrital clay minerals with high radiogenic Sr ratios. An analytical procedure was established to "clean" the siderite and achieve reliable $^{87}Sr/^{86}Sr$ ratios so that they could be used to interpret the origin of the porewaters from which they precipitated.

The siderite cleaning procedure involved the removal of the clay from siderite with a heavy liquid solution. Progressive leaching of the remaining siderite-clay powder with a 1M sodium acetate solution (buffered to pH = 5) for 2 hours, followed by a 0.5M HCl for 20 minutes removed any remaining contaminant Sr within the clays and $CaCO_3$. The treated samples can then be partially dissolved with 6M HCl for 20 minutes for Sr isotopic analysis.

Petrographic investigations of diagenetic mineral phases in the Cardium Formation defines the sequence of mineral precipitation to be:

pyrite→siderite→calcite(I)→calcite(II)→quartz→kaolinite→fracture-filling calcite

Siderite can precipitate from marine porewaters under reducing conditions where sulphate has been removed from the porewaters via sulphate reduction and pyrite precipitation. A rapid sedimentation rate will prevent further sulphate diffusion into the sedimentary pile. Bacterial reduction of organic rich matter within the sediments will increase the DIC required for siderite formation. The high Fe/Ca ratio is attained by reducing Fe^{3+} adsorbed on clays within the terrigenous sediments.

A plot of $^{87}Sr/^{86}Sr$ vs $\delta^{18}O$ (Fig. 7.1) reveals that contemporaneous marine (Carrot Creek) and continental/brackish (Kakwa) siderite precipitates are distinguishable by their oxygen and strontium isotopic composition. The continental/brackish water siderite concretions have a more radiogenic Sr isotopic composition and lighter $\delta^{18}O$ values. These siderites formed during early stages of diagenesis. This was followed by encroachment of meteoric water into the basin. With the onset of meteoric water encroachment, marine siderite precipitation ceased and calcite became the more stable phase. This is reflected by the considerably lower $\delta^{18}O$ of the calcite cements in the conglomeratic units. Alumino-silicate and clay mineral dissolution during burial diagenesis released radiogenic Sr into the porewaters and is reflected in the higher $^{87}Sr/^{86}Sr$ ratios in later stage calcites.

The oxygen isotopic composition of the marine siderites and Inoceramid shells suggests that the carbonates precipitated from waters having $\delta^{18}O$ = -2.4 to -6.8‰, at

temperatures no higher than 30°C. Light oxygen isotopic values for the Cretaceous Interior Seaway have also been reported by other authors. Although some of these values can been explained by the introduction of meteoric water into the seaway, at present it is uncertain as to what could account for the more negative $\delta^{18}O$ marine values.

REFERENCES

Albarède, F., Michard, A., Minster, J.F., and Michard, G., 1981. $^{87}Sr/^{86}Sr$ ratios in hydrothermal waters and deposits from the East Pacific Rise at 21°N. Earth and Planetary Science Letters, **55**, 229-236.

Almon, W.R., 1979. Petrophysical evidence of cementation differences in the Cardium sandstone. Canadian Well Logging Society, Seventh Formation Evaluation Symposium, Calgary, Alberta, K1-K15.

Anderson, T.F., and Arthur, M.A., 1983. Stable isotopes of oxygen and carbon and their implication to sedimentologic and paleoenvironmental problems. *In*, Stable Isotopes in Sedimentary Geology. SEPM Short Course No. 10, p.1-1 to 1-151.

Arthur, M.A., 1979. North Atlantic Cretaceous Black Shales: The record at Site 398 and a brief comparison with other occurrences. *In,* Initial Reports of the DSDP, **47B**, 719-751.

Barron, E.J., 1983. A warm, equable Cretaceous: The nature of the problem. Earth Science Reviews, **19**, 305-338.

Bartlett J.J. 1987. An analysis of sequence boundaries of the event stratigraphy of the Cardium Formation, Alberta. M.Sc. thesis, McMaster University, Hamilton, Ontario, Canada, 185p.

Basov, V.A., Lopatin, G.B., Gramberg, I.S., Danjushevskaya, A.I., Kaban'Kov, V.Ya, Lazurkin, V.M., and Patrunov, D.K., 1979. Lower Cretaceous Lithostratigraphy Near Galicia Bank (W. Spain). *In,* Initial Reports of the DSDP, **47B**, 683-717.

Beall, Jr., A.O. and Fischer, A.G., 1969. Chapter 24: Sedimentology. *In,* Initial Reports of the DSDP, **1**, 521-594.

Beall, Jr. A.O., Laury, R., Dickinson, K. and Pusey III, W.C., 1973. Chapter 27: Sedimentology. *In,* Initial Reports of the DSDP, **10**, 699-729.

Becker, R.H. and Clayton, R.N., 1976. Oxygen isotope study of Precambrian banded iron-formation, Hamersley Range, Western Australia. Geochimica et Cosmochimica Acta, **40**, 1153-1165.

Bell, P.E., Mills, A.L., and Herman, J.S., 1987. Biological conditions favoring magnetite formation during anaerobic iron reduction. Applied Environmental Microbiology, **53**, 2610-2616.

Bergman, K.M. 1987. Erosion surfaces and gravel shore face deposits: the influence of tectonics on the sedimentology of the Carrot Creek Member, Cardium Formation (Turonian, Upper Cretaceous), Alberta, Canada. Ph.D. thesis, McMaster University, Hamilton, Ontario, Canada, 404p.

Bergman, K.M. and Walker, R.G. 1988. Formation of Cardium erosion surface E5, and associated deposition of conglomerate; Carrot Creek Field, Cretaceous Western Interior Seaway, Alberta. *In* D.P. James, and D. A. Leckie, (*eds.*), Sequences, Stratigraphy, Sedimentology: Surface and Subsurface. Canadian Society of Petroleum Geologists, Memoir 15, 15-24.

Berner, R.A., 1964. Stability fields of iron minerals in anaerobic marine sediments. Geochimica et Cosmochimica Acta, **28**, 1497-1503.

Berner, R.A., 1971. Principles of Chemical Sedimentology. McGraw-Hill, New York, 240p.

Berner, R.A., 1980. Early Diagenesis: A Theoretical Approach. Princeton University Press, Princeton, New Jersey, 241p.

Berner, R.A., 1981. A new geochemical classification of sedimentary environments. Journal of Sedimentary Petrology, **51**, 359-365.

Blatt, H., Middleton, G., and Murray, R., 1980. Origin of Sedimentary Rocks. Prentice-Hall Inc., Englewood Cliffs, New Jersey, 782p.

Brookins D.G. 1988. Eh-pH Diagrams for Geochemistry. Springer-Verlag, Berlin, Germany, 176p.

Burke, W.H., Denison, R.E., Hetherington, E.A., Koepnick, R.B., Nelson, H.F., and Otto, J.B., 1982, Variation of seawater $^{87}Sr/^{86}Sr$ throughout Phanerozoic time. Geology **10**, 516-519.

Carothers, W.W., Adami, L.H., and Rosenbauer, R.J., 1988. Experimental oxygen isotope fractionation between siderite-water and phosphoric acid liberated CO_2-siderite. Geochimica et Cosmochimica Acta, **52**, 2445-2450.

Carroll, D., 1958. Role of clay minerals in the transportation of iron. Geochimica et Cosmochimica Acta, **14j**, 1-27.

Carroll, D. and Starkey, H.C., 1971. Reactivity of clay minerals with acids and alkalies. Clays and Clay Minerals, **19**, 321-333.

Chamley, and Shipboard Scientific Party, 1979. Chapter 11: Mineralogy and Geochemistry of Cretaceous and Cenozoic Atlantic Sediments off the Iberian Peninsula (Site 398, DSDP LEG 47B). *In,* Initial Reports of the DSDP, **47B**, 329-449.

Claypool, G.E., and Kaplan, I.R., 1974. The origin and distribution of methane in marine sediments. *In* I.R. Kaplan (*ed.*), Natural Gases in Marine Sediments. Plenum Press, New York, 99-139.

Cortecci, G. and Frizzo, P., 1993. Origin of siderite deposits from Lombardy Valleys, northern Italy: a carbon, oxygen and strontium isotope study. Chemical Geology, **105**, 293-303.

Craig. H., 1957. Isotopic standards for carbon and oxygen and correction factors for mass-spectrometric analysis of carbon dioxide. Geochimica et Cosmochimica Acta, **12**, 133-149.

Craig, H., 1969. Chemistry and origin of the Red Sea brines. *In* E.T. Degens and D.A. Ross (*eds.*), Hot Brines and Recent Heavy Metal Deposits in the Red Sea. Springer-Verlag, New York, 208-243.

Curtis, C.D., and Coleman, M.L., 1986. Controls on the precipitation of early diagenetic calcite, dolomite and siderite concretions in complex depositional sequences. *In* D. Gautier (*ed.*), Roles of Organic Matter in Sediment Diagenesis. SEPM Special Publication **38**, 23-33.

Curtis, C.D., Coleman, M.L., and Love, L.G., 1986. Porewater evolution during sediment burial from isotopic and mineral chemistry of calcite, dolomite and siderite concretions. Geochimica et Cosmochimica Acta, **50**, 2321-2334.

Deer, W.A., Howie, R.A. and Zussman, J., 1966. An Introduction To The Rock Forming Minerals. Longman Group Limited, London, 528p.

Deines, P., 1970. Mass spectrometer correction factors for the determination of small isotopic composition variations of carbon and oxygen. International Journal of Mass Spectrometry and Ion Physics, **4**, 283-295.

Dickin, A.P, 1995. Radiogenic Isotope Geology. Cambridge University Press, Cambridge, England, 452p.

Douglas, R.G. and Savin, S.M., 1975. Oxygen and carbon isotope analyses of Tertiary and Cretaceous microfossils from Shatsky Rise and other sites in the North Pacific Oceans. *In*, Initial Reports of the DSDP, **32**, 509-520.

Einsele, G. and von Rad, U., 1979. Facies and Paleoenvironment of Lower Cretaceous Sediments at DSDP Site 397. and in the Aaiun Basin (Northwest Africa). *In,* Initial Reports of the DSDP **47A**, 559-577.

Elderfield, H. and Gieskes, J.M., 1982. Sr isootopes in interstitial waters of marine sediments from Deep-Sea Drilling Project cores. Nature, **300**, 493-497.

Elderfield, H. and Grieves, M.J., 1981. Strontium isotope geochemistry of Icelandic geothermal systems and implications for seawater chemistry. Geochimica et Cosmochimica Acta, **45**, 2201-2212.

Ellwood, B.B., Chrzanowski, T.H., Hrouda, F., Long, G.J., Buhl, M.L., 1988. Siderite formation in anoxic deep-sea sediments: A synergetic bacterially controlled process with important implications in paleomagnetism. Geology, **16**, 980-982.

Eyles, C.H. and Walker, R.G., 1988. "Geometry" and facies characteristics of stacked shallow marine sandier-upward sequences in the Cardium Formation at Willesden Green, Alberta. *In* D.P. James, and D.A. Leckie, (*eds.*), Sequences, Stratigraphy, Sedimentology: Surface and Subsurface. Canadian Society of Petroleum Geologists, Memoir 15, 85-96.

Farrah, H., Hatton, D., and Pickering, W.F., 1980. The afinity of metal ions for clay surfaces. Chemical Geology, **28**, 55-68.

Faure, G., 1986. Principles of Isotope Geology. John Wiley & Sons, New York, 589p.

Faure, G., and Jones, L.M., 1969. Anomalous strontium in the Red Sea Brines. *In* E.T. Degens and D.A Ross (*eds.*), Hot Brines and Recent Heavy Metal Deposits in the Red Sea. Springer-Verlag New York Inc., 243-250.

Friedman, I. and O'Neil, J.R., 1977. Composition of stable isotope fractionation factors of geochemical interest. *In* M. Fleischer *(ed.)*, Data of Geochemistry, 6th Edition. U.S.G.S. Prof. Paper 440-KK, 12p.

Frimmel, H., 1988. Strontium isotopic evidence for the origin of siderite, ankerite and magnesite mineralizations in the Eastern Alps. Mineralium Deposita, **23**, 268-275.

Fritz, P., Binda, P.L., Folinsbee, F.E., and Krouse, H.R., 1971. Isotopic composition of diagenetic siderites from Cretaceous sediments in Western Canada. Journal of Sedimentary Petrology, **41**, 282-288.

Froelich, P.N., Klinkhammer, G.P., Bender, M.L., Luedtke, N.A., Heath, G.R., Cullen, D., Dauphin, P., Hammond, D., Hartman, B., and Maynard, V., 1979. Early oxidation of organic matter in pelagic sediments of the eastern equatorial Atlantic: suboxic diagenesis. Geochimica et Cosmochimica Acta, **43**, 1075-1090.

Garrels, R.M. and Christ, C.L., 1965. Solutions, Minerals and Equilibria. Harper & Row, New York, 450p.

Gautier, D.L. and Claypool, G.E., 1984. Interpretation of methanic diagenesis in ancient sediments by analogy with processes in modern diagenetic environments. *In* D.A. McDonald and R.C. Surdam, (*eds.*), Clastic Diagenesis. AAPG Mem. **37**, 111-123.

Glancy, Jr. T.J., Arthur, M.A., Barron, E.J. and Kauffman, E.G., 1993. A paleoclimate model for the North American Cretaceous (Cenomanian-Turonian) epicontinental sea. *In*, Caldwell, W.G.E. and Kauffman, E.G. (*eds.*), Evolution of the Western Interior Basin. Geological Assiciation of Canada, Special Paper 39, 219-241.

Goldhaber, M.B., and Kaplan, I.R., 1974. The sulfur cycle. *In* E.D. Goldberg (*ed.*), The Sea, Volume 5 - Marine Chemistry. Wiley Interscience Publishers, New York, 569-655.

Goldstein, J.S. and Jacobsen, S.B., 1987. The Nd and Sr isotopic systematic of river-water dissolved material; implications for the source of Nd and Sr in seawater. Chemical Geology, **66**, 245-272.

Golyshev, S.I., Padalko, N.L., and Pechenkin, S.A., 1981. Fractionation of stable oxygen and carbon isotopes in carbonate systems. Geochemistry International, **18**, 85-99.

Gould, K.W., and Smith, J.W., 1979, The genesis and isotopic composition of carbonates associated with some Permian Australian coals. Chemical Geology, **24**, 137-150.

Griffith, L.A., 1981. Depositional Environment and Conglomerate Diagenesis of the Cardium Formation, Ferrier Field, Alberta. M.Sc. thesis, University of Calgary, Calgary, Alberta, Canada, 131p.

Hart, B.S., Longstaffe, F.J., and Plint, A.G., 1992. Evidence for the relative sea level change from isotopic and elemental composition of siderite in the Cardium Formation, Rocky Mountain Foothills. Bulletin of Canadian Petroleum Geology, **40**, 52-59.

Hayes, B.J.R. and Smith, D.G. 1987. Discussion: Cardium Formation 6. Stratigraphic framework of the Cardium in subsurface. Bulletin of Canadian Petroleum Geology, **35**, 363-365.

Hennessy, J., and Knauth, L.P., 1985. Isotope variations in dolomite concretions from the Monterey Formation, California. Journal of Sedimentary Petrology, **55**, 120-130.

Hollister, C.D., et al, 1972a. Chapter 4: Site 101 - Blake-Bahama Outer Ridge (South End). *In,* Initial Reports of the DSDP, **11**, 105-134.

Hollister, C.D., et al, 1972b. Chapter 6: Site 105 - Lower Continental Rise Hills. *In,* Initial Reports of the DSDP, **11**, 219-312.

Hollister, C.D., et al, 1972c. Chapter 7: Site 106 - Lower Continental Rise. *In,* Initial Reports of the DSDP, **11**, 313-349.

Irwin, H., 1980. Early diagenetic carbonate precipitation and pore fluid migration in the Kimmeridge Clay of Dorset , England. Sedimentology, **27**, 577-591.

Irwin, H., Curtis, C. D., and Coleman, M., 1977. Isotopic evidence for source of diagenetic carbonates formed during burial of organic-rich sediments. Nature, **269**, 209-213.

Jackson, M.L., 1969. Soil Chemical Analysis—Advanced Course. University of Wisconsin Press, Madison, Wisconsin, 895p.

Keith, M.L. and Weber, J.N., 1964. Carbon and oxygen isotopic composition of selected limestones and fossils. Geochimica et Cosmochimica Acta, **28**, 1787-1816.

Koepnick, R.B., Burke, W.H., Denison, R.E.,Hetherington, E.A., Nelson, H.F., Otto, J.B., and Waite, L.E., 1985, Construction of the seawater $^{87}Sr/^{86}Sr$ curve for the Cenozoic and Cretaceous: Supporting Data. Chemical Geology, **58**, 55-81.

Kralik, M., 1984. Effects of cation-exchange treatment and acid leaching on the Rb-Sr system of illite from Fithian, Illinois. Geochimica et Cosmochimica Acta, **48**, 527-533.

Kyser, T.K., Caldwell, W.G.E., Whittaker, S.G. and Cadrin, A.J., 1993. Paleoenvironment and geochemistry of the Northern Portion of the Western Interior Seaway during Late Cretaceous Time. *In*, Caldwell, W.G.E. and Kauffman, E.G. (*eds.*), Evolution of the Western Interior Basin. Geological Assiciation of Canada, Special Paper 39, 355-378.

Lancelot, Y. and Ewing, J.I., 1972. Chapter 27: Correlation of Natural Gas Zones and Carbonate Diagenesis in Tertiary Sediments From The North-West Atlantic. *In,* Initial Reports of the DSDP, **11**, 791-779.

Lancelot, Y., Hathaway, C.J., and Hollister, C.D., 1972. Chapter 31: Lithology of Sediments from the Western North Atlantic Leg 11 Deep Sea Drilling Project. *In,* Initial Reports of the DSDP, **11**, 901-949.

Land, L.S., 1980. The isotopic and trace element geochemistry of dolomite: The state of the art. SEPM Special Publication, **28**, 87-110.

Laughton, A.S., et al., 1972. Chapter 3: Site 111. *In,* Initial Reports of the DSDP, **12**, 33-159.

Leggitt, S.M. 1987. Facies geometry and erosion surfaces in the Cardium Formation, Pembina Field, Alberta. M.Sc. thesis, McMaster University, Hamilton, Ontario, Canada, 140p.

Li, Wangxing, 1989. Isotopic Studies Of The Groundwaters And Their Host Rocks And Minerals From The Underground Research Laboratory (URL), Pinawa, Manitoba, Canada. M.Sc. thesis, McMaster University, Hamilton, Ontario, Canada, 202p.

Longstaffe, F.J., 1989. Stable isotopes as tracers in clastic diagenesis. *In*, I.A. Hutcheon (*ed.*) Burial Diagenesis. Mineralogical Association of Canada, Short Course Handbook, **15**, 201-277.

Lovely, D.R. and Phillips, J.P., 1987. Competitive mechanisms for inhibition of sulphate reduction and methane produciton in the zone of ferric iron reduction in sediments. Applied and Environmental Microbiology, **35**, 2636-2641.

Loveley, D.R., Stolz, J.F., Nord Jr., G.L., and Phillips, J.P., 1987. Anaerobic production of magnetite by a dissimilatory iron-reducing microorganism. Nature, **330**, 252-254.

Machemer, S.D., and Hutcheon, I., 1988. Geochemistry of early carbonate cements in the Cardium Formation, Central Alberta. Journal of Sedimentary Petrology, **58**, 136-147.

Matsumoto, R., 1983. Mineralogy an Geochemistry of Carbonate Diagenesis of Pliocene and Pleistocene Hemipelagic Mud on the Blake Outer Ridge, Site 533, Leg 76. *In,* Initial Reports of the DSDP, **76**, 411-427.

Matsumoto, R., and Iijima, A., 1981. Origin and diagenetic evolution of Ca-Mg-Fe carbonates in some coalfields of Japan. Sedimentology, **28**, 239-259.

McCrea, J.M., 1950. On the isotopic chemistry of carbonates and paleotemperture scale. Journal of Chemical Physics, **18**, 849-857.

Morton, J.P., 1985. Rb-Sr dating of diagenesis and source age of clays in Upper Devonian black shales of Texas. Geological Society of America bulletin, **96**, 1043-1049.

Mozley, P.S., 1989. Relationship between depositional environment and the elemental composition of early diagenetic siderite. Geology, **17**, 704-706.

Mozley , P.S. and Burns, S.J., 1993. Oxygen and carbon isotopic composition of marine carbonate concretions: An overview. Journal of Sedimentary Petrology, **63**, 73-83.

Mozley, P.S. and Carothers, W.W., 1992. Elemental and isotopic composition of siderite in the Kuparuk Formation, Alaska: Effect of microbial activity and water/sediment interaction on early pore-water chemistry. Journal of Sedimentary Petrology, **62**, 681-692.

Mozley, P.S. and Wersin, P., 1992. Isotopic composition of siderite as an indicator of depositional environment. Geology, **20**, 817-820.

O'Neil, J.R., Clayton, R.N., and Mayeda, T.K., 1969. Oxygen isotope fractionation in divalent metal carbonates. Journal of Chemical Physics, **51**, 5547-5558.

Ostrom, M.E., 1961. Separation of clay minerls from carbonate rocks by using acid. Journal of Sedimentary Petrology, **31**, 123-129.

Palmer, M.R. and Elderfield, H., 1985. Sr isotopic composition of sea water over the past 75 Myr. Nature, **314**, 526-528.

Pattison, S.A.J. 1988. Transgressive, incised shoreface deposits of the Burnstick Member (Cardium "B" Sandstone) at Caroline, Crossfield, Garrington and Lochend; Cretaceous Western Interior Seaway, Alberta, Canada. *In* D.P. James, and D.A. Leckie, (*eds.*), Sequences, Stratigraphy, Sedimentology: Surface and Subsurface. Canadian Society of Petroleum Geologists, Memoir 15, 155-166.

Pearson, M.J., 1974a, Siderite concretions from Westphalian of Yorkshire: a chemical investigation of the carbonate phase. Mineralogical Magazine, **39**, 696-699.

Pearson, M.J., 1974b, Magnesian siderite in carbonate concretions from argillaceous sediments in the Westphalian of Yorkshire. Mineralogical Magazine, **39**, 700-704.

Peterman, Z.E., Hedge, C.E., and Tourtelot, H.A., 1970, Isotopic composition of strontium in sea water throughout Phanerozoic time. Geochimica et Cosmochimica Acta, **34**, 105-120.

Peterson, M.N.A., Edgar, N.T., von der Borch, C.C., and Rex, R.W., 1970. Chapter 20: Cruise Leg Summary and Discussion. *In,* Initial Reports of the DSDP, **2**, 413-427.

Piepgras, D.J. and Wasserburg, G.J., 1985. Strontium and Neodymium isotopes in hot springs on the East Pacific Rise and Guayamas Basin. Earth and Planetary Science Letters, **72**, 341-356.

Plint, A.G. and Walker, R.G. 1987. Cardium Formation 8. Facies and environments of the Cardium shoreline and coastal plain in the Kakwa Field and adjacent areas, Northwestern Alberta. Bulletin of Canadian Petroleum Geology, **35**, 48-64.

Plint, A.G., Walker, R.G. and Bergman, K.M. 1986. Cardium Formation 6. Stratigraphic framework of the Cardium in subsurface. Bulletin of Canadian Petroleum Geology, **34**, 213-225.

Plint, A.G., Walker, R.G. and Bergman, K.M. 1987. Discussion: Cardium Formation 6. Stratigraphic framework of the Cardium in subsurface. Bulletin of Canadian Petroleum Geology, **35**, 365-374.

Postma, D., 1981. Formation of siderite and vivianite and the pore-water composition of a Recent bog sediment in Denmark. Chemical Geology, **31**, 225-244.

Potts, P.J., 1987. A Handbook of Silicate Rock Analysis. Blackie and Son Ltd., London, England, 622p.

Pratt, L.M., Arthur, M.A., Dean, W.E. and Scholle, P.A., 1993. Paleo-oceanographic cycles and events during the Late Cretaceous in the Western Interior Seaway of North America. *In*, Caldwell, W.G.E. and Kauffman, E.G. (*eds.*), Evolution of the Western Interior Basin. Geological Assiciation of Canada, Special Paper 39, 333-353.

Pye, K., 1981. Marshrock formed by iron sulphide and siderite cementation in saltmarsh sediments. Nature, **294**, 650-652.

Rine, M.R., Helmold, K.P. and Bartlett, G.A. 1987. Discussion: Cardium Formation 6. Stratigraphic framework of the Cardium in subsurface. Bulletin of Canadian Petroleum Geology, **35**, 362-363.

Rosenbaum, J. and Sheppard, S.M.F., 1986. An isotopic study of siderites, dolomites and ankerites at high temperatures. Geochimica et Cosmochimica Acta, **50**, 1147-1150.

Savin, S.M. and Yeh, H., 1981. Stable isotopes in ocean sediments. *In*, C. Emiliani (*ed.*), The Sea, Vol. 7, The Oceanic Lithosphere. John Wiley and Sons, New York, 1521-1554.

Shackleton, N.J., 1967. Oxygen isotope analyses and Pleistocene temperature reassessed. Nature, **215**, 15-17.

Staley, G.H.S., 1987. Diagenetic alteration in the Cardium and Viking formations, western Canada. Ph.D. thesis, University of Sheffield, England, 205p.

Stueber, A.M., Pushkar, P., and Hetherington, E.A., 1984, A strontium isotopic study of Smackover brines and associated solids, southern Arkansas. Geochimica et Cosmochimica Acta, **48**, 1637-1649.

Surdam, R.C., Boese, S.W., and Crossey, L.J., 1984. The chemistry of secondary porosity. *In* D.A. McDonald and R.C. Surdam (*eds.*), Clastic Diagenesis. The American Association of Petroleum Geologists, Tulsa, 127-149.

Sweeney, D.E., 1983. Petrography of the Cardium Sandstones; Ricinus, Caroline and Garrington Fields, Alberta. B.Sc. thesis, McMaster University, Hamilton, Ontario, Canada, 197p.

Tessier, A., Campbell, P.G.C., and Bisson, M., 1979. Sequential extraction procedure for the speciation of particulate trace metals. Analytical Chemistry, **51**, 844-851.

Thompson, G.R. and Hower, J., 1973. An explanation for low radiogenic ages from glauconite. Geochimica et Cosmochimica Acta, **37**, 1473-1491.

Timofeyeva, Z.V., Kuznetsova, L.D., and Dontsova, Ye.I., 1976. Oxygen isotopes and siderite formation. Geochemistry International, **13**, 101-112.

Tourtelot, H.O. and Rye, R.O., 1969. Distribution of oxygen and carbon isotopes in fossils of Late Cretaceous age, Western Interior region of North America. **80**, 1903-1922.

Walker, R.G. 1983a. Cardium Formation 2. Sand-body geometry and stratigraphy in the Garrington-Caroline-Ricinus area, Alberta - the "Ragged Blanket" model. Bulletin of Canadian Petroleum Geology, **31**, 14-26.

Walker, R.G. 1983b. Cardium Formation 3. Sedimentology and stratigraphy in the Garrington-Caroline area, Alberta. Bulletin of Canadian Petroleum Geology, **31**, 213-230.

Walker, R.G. 1985. Cardium Formation at Ricinus Field, Alberta: A channel cut and filled by turbidity currents in Cretaceous Western Interior Seaway. The American Association of Petroleum Geologists Bulletin, **69**, 1963-1981.

Walker, R.G. 1986. Cardium Formation 7. Progress report compiling data from outcrop and subsurface in Southern Alberta. Tech. Memo 86-3, McMaster University, Hamilton, Ontario, 97p.

Walker, R.G. and Eyles, C.H. 1988. Geometry and facies of stacked shallow-marine sandier upward sequences dissected by erosion surface, Cardium Formation, Willesden Green, Alberta. The American Association of Petroleum Geologists Bulletin, **72**, 1469-1494.

Weber, J.N., Williams, E.G., and Keith, M.L., 1964. Paleoenvironmental significance of carbon isotopic composition of siderite nodules in some shales of Pennsylvanian age. Journal of Sedimentary Petrology, **34**, 818-818.

Whittaker, S.G, and Kyser, T.K., 1993. Variations in the neodymium and strontium isotopic composition and REE content of molluscan shells from the Cretaceous Western Interior seaway. Geochimica et Cosmochimica Acta, **57**, 4003-4014.

Woodland, B.G., and Stenstrom, R.C., 1979. The occurrence and origin of siderite concretions in the Francis Creek Shale (Pennsylvanian) of northeastern Illinois. *In* M.H. Nitechi (*ed.*), Mazon Creek Fossils. Academic Press, New York, 69-103.

Yariv, S., and Cross, H., 1979. Geochemistry of Colloid Systems. Springer.

Yertsever, Y., 1975. Word-wide survey of stable isotopes in precipitation. International Atomic Energy Association, Vienna, Report of Section on Isotope Hydrology, 152p.

Appendix

Initial Reports of the Deep Sea Drilling Project

National Science Foundation, Washington, U.S. Government Printing Office

There are over 240 references to siderite in 96 volumes of the Initial Reports of the Deep Sea Drilling Project. The following is a summary of some of the references where siderite was more than just a brief observation. Four Legs (13, 48, 65 and 66) mention the presence of siderite in a keyword search of a CDROM index for the DSDP, but these were not reviewed due to the volumes being unavailable.

BEALL, JR., A.O. AND FISCHER, A.G., 1969. Chapter 24: Sedimentology. *In,* IR of the DSDP, v.1, p.521-594. (010563)

They observed coarse terrigenous sediments containing siderite of terrigenous origin and pelagic siderite of a diagenetic origin.

PETERSON, M.N.A., EDGAR, N.T., VON DER BORCH, C.C., AND REX, R.W., 1970. Chapter 20: Cruise Leg Summary and Discussion. *In,* IR of the DSDP, v.2, p. 413-427. (020419)

Siderite is a locally significant carbonate in sediments at Site 9 (northeastern flank of the Bermuda Rise) where it occurs in association with rhodochrosite in amounts as high as 23%. Siderite also occurs in minor quantities at Site 10 (western flank of Mid-

Atlantic Ridge) in the Miocene zeolite clay zone and in calcareous oozes at depth. The presence of siderite, frequently in association with rhodochrosite and cristobalite, suggests some form of hydrothermal alteration of pre-existing tuffs. Rate of sediment accumulation at Site 9 is extremely high throughout post-Miocene times (4.3 cm/1000 yrs). Carbonate such as rhodochrosite, siderite and dolomite are the products of recrystallization.

BEALL, JR. A.O., LAURY, R., DICKINSON, K. AND PUSEY III, W.C., 1973. Chapter 27: Sedimentology. *In,* IR of the DSDP, v.10, p.699-729. (100708)

Lower Pleistocene sediments at Site 92 (continental shelf of the Texas-Louisiana Gulf Coast) contains abundant siderite (?) occurring as well-sorted, silt-sized spherulites. The spherulites consist of a single crystal which have syntaxially overgrown a rhombic nucleus. Although similar spherulites have been found in trace amounts in almost all holes drilled in Leg 10, and a detrital origin might be preferred, the large amount of siderite (?) present at Site 92 suggests an authigenic or diagenetic origin.

HOLLISTER, C.D., ET AL, 1972. Chapter 4: Site 101 - Blake-Bahama Outer Ridge (South End). *In,* IR of the DSDP, v.11, p.105-134. (110109)

Early Cretaceous black clays, intermediate between hemipelagic muds and carbonaceous clays is found at Site 101. The main components of these clays are clay minerals (with some quartz and heavy minerals), organic matter and siderite. Siderite is sometimes concentrated in lenses, hard nodules and layers. Some siderite spherules seem

to have a nucleus of organic matter. One dolomite rhomb was found enclosed within a twinned overgrowth of siderite.

HOLLISTER, C.D., ET AL, 1972. Chapter 6: Site 105 - Lower Continental Rise Hills. *In,* IR of the DSDP, v.11, p.219-312. (110225)

At Site 105 there are Early Cretaceous black clays, highly carbonaceous with thin silty beds. Some silt beds in the black layers consist entirely of pyrite cubes. Scattered zones of pyrite are also common. One zone contains 95% siderite.

HOLLISTER, C.D., ET AL, 1972. Chapter 7: Site 106 - Lower Continental Rise. *In,* IR of the DSDP, v.11, p.313-349. (110318)

At Site 106 there is a negative correlation between the amounts of siderite and calcareous microfossils. This strongly suggests that the microfossils were the source for the siderite.

LANCELOT, Y. AND EWING, J.I., 1972. Chapter 27: Correlation of Natural Gas Zones and Carbonate Diagenesis in Tertiary Sediments From The North-West Atlantic. *In,* IR of the DSDP, v.11, p.791-779. (110795)

Siderite appears first as isolated well-crystallized rhombs scattered in sediments, and deeper in the hole it tends to be concentrated in lenses and nodules. At Site 106 (Lower Continental Rise), in well-indurated sediments, siderite is frequently concentrated along vertical fractures and occurs as a filling of burrow-like structures (gas migration

structures). Alkalinity decreases with depth to very low values and where pH decreases to <7.8, dolomite and calcite disappear and the abundance of siderite increases. At Site 101 micro fossils were replaced by siderite, and in one sample a twinned overgrowth of siderite was observed on a dolomite rhomb. Occurrence of gas, pyrite, siderite and organic matter is indicative of reducing conditions in the sediments, and the Eh can be considered to be negative in most of the section. The very high rates of sedimentation, up to 20 cm/1000 yrs. were probably instrumental in maintaining anaerobic conditions very close to the sediment water interface.

LANCELOT, Y., HATHAWAY, C.J., AND HOLLISTER, C.D., 1972. Chapter 31: Lithology of Sediments from the Western North Atlantic Leg 11 Deep Sea Drilling Project. *In,* IR of the DSDP, v.11, p.901-949. (110924)

At Site 101 (Blake-Bahama Outer Ridge, South End), siderite is common throughout the interval. The mineral was found either in small grey nodules and silty lenses and layers or as isolated rhombs scattered in the sediment. The primary sedimentary structures noted in the hemipelagic sediments are horizontal laminations, lenses and spots of very fine silt, lenses and nodules of siderite, and near the top of the section occasional layers of foraminifera.

LAUGHTON, A.S., ET AL., 1972. Chapter 3: Site 111. *In,* IR of the DSDP, v.12, p.33-159. (120049)

Siderite occurs in the sandstone of Orphan Knoll at site 111. The interstices between grainy components are largely infilled with muddy matrix (15%). The mud is crowded with minute spherulites of siderite which measures about 0.005 to 0.010 mm in size and in places constitute the principal component, forming a loose, finely granular coating around the sand grains. In addition, small specks of carbonaceous matter are present. Most of the remaining pore space is infilled with patches of calcite cement (4%). Both calcite and siderite are considered to be of diagenetic origin. They may have been derived from admixed ferugenous and micritic matter present in the mud itself, or possibly, the carbonate was introduced by circulating waters from skeletal limestone beds that are known to occur a few feet higher up in the section.

COOK, A.C., 1974. Chapter 22: Report on Petrography of a Paleocene Brown Coal Sample From the Ninetyeast Ridge, Indian Ocean. *In,* IR of the DSDP, v.22, p.485-488. (220485)

Siderite does coexist in coal with minor pyrite, but is generally confined to coals which show little or no evidence of marine influence in the immediately overlying strata.

EINSELE, G. AND VON RAD, U., 1979. Facies and Paleoenvironment of Lower Cretaceous Sediments at DSDP Site 397. and in the Aaiun Basin (Northwest Africa). *In,* IR of the DSDP v.47A, p.559-577. (47A0566)

Siderite crystallites form a microsparitic cement in a compositionally graded terrigenous silt layer. Diagenesis of Lower Cretaceous deposits at Site 397 proceeded as 1) Formation of pyrite - precipitation of micritic calcite in nodules and thin irregular layers - full or partial replacement of calcite by siderite, or
2) Formation of pyrite - local precipitation of siderite in thin layers during early diagenesis without a calcite precursor.

CHAMLEY, AND SHIPBOARD SCIENTIFIC PARTY, 1979. Chapter 11: Mineralogy and Geochemistry of Cretaceous and Cenozoic Atlantic Sediments off the Iberian Peninsula (Site 398, DSDP LEG 47B). *In,* IR of the DSDP, v.47B, p.329-449. (47B0435)

Pyrite, siderite, rhodochrosite and gypsum were formed in the sediment during their deposition or shortly thereafter. They correspond to reducing or locally oxidizing conditions, and can determine important increases of Mn and/or Fe.

Basov, V.A., Lopatin, G.B., Gramberg, I.S., Danjushevskaya, A.I., Kaban'Kov, V.Ya, Lazurkin, V.M., and Patrunov, D.K., 1979. Lower Cretaceous Lithostratigraphy Near Galicia Bank (W. Spain). *In,* IR of the DSDP, v.47B, p.683-717. (47B0686)

The sediments contain numerous bands and lenses of siderite, up to 2 cm thick. Crystals of siderite are up to 0.1 mm in size. Concentrations, size and crystal perfection

change from layers to layers. The siderite distribution shows a direct correlation with the concentration of organic matter in predominantly clayey pelites. Siderite is known to be a characteristic diagenetic mineral produced in sediments under highly reducing conditions, high CO_2 partial pressure and low calcium (carbonate) content. The iron supply necessary to produce siderite is apparently absorbed on pelite particles.

ARTHUR, M.A., 1979. North Atlantic Cretaceous Black Shales: The record at Site 398 and a brief comparison with other occurrences. *In,* IR of the DSDP, v.47B, p.719-751 (47B0733)

Sediments of the Vigo Seamount, southern end of Galicia Bank, consist of Lower to Middle Cretaceous black shales. The sedimentation rate for these sediments is approximately 75 m/my. The high sedimentation rates and input of terrigenous organic matter can be suggested as the cause for establishment of anoxic conditions within the sediment after burial. Metabolizable matter in the sediments is consumed during bacterial sulphate reduction. The abundance of siderite in these sediments is evidence of complete reduction of sulphate. Some structures suggest obvious dissolution, migration and redeposition of carbonate in concentrations as siderite. Other sedimentary structures within hard, dense siderite layers (such as laminations and burrow mottling) imply replacement of original carbonate-rich layers. Most layers or lenses are <2 cm, but some may be as thick as 6 cm. Most of the siderite layers are fairly pure and probably represent dissolution of calcium carbonate and growth of siderite during early diagenesis. Oxygen and carbon isotope values of siderite may have been in response to equilibration

with anaerobic interstitial water of rapidly deposited carbonate-poor terrigenous sediments above and below. The reduced Fe/Ca ratio was probably high in the terrigenous sediment (which is favourable for siderite formation). Pyrite is a common constituent of the reducing sediments at Site 398.

MATSUMOTO, R., 1983. Mineralogy an Geochemistry of Carbonate Diagenesis of Pliocene and Pleistocene Hemipelagic Mud on the Blake Outer Ridge, Site 533, Leg 76. *In,* IR of the DSDP, v.76, p.411-427. (760422)

Investigation of Pleistocene-Pliocene core sediments reveals that siderite is more abundant and common at depth. Where it is abundant, it comprises 8%, with a maximum occurrence of 18%. The siderite is comprised of fine grained rhombohedral crystals 0.005mm in diameter. Local biogenic calcite has a Sr concentration of 1700 ppm. The Sr/Ca ratio of calcite-siderite mixtures plots near the biogenic calcite regression line (but with lower Sr concentrations, <480 ppm, roughly between 200-500 ppm). The estimated composition of siderite is $(Fe_{0.60}Mg_{0.32}Ca_{0.07}Mn_{0.01})CO_3$. This composition is similar to that of the deep sea siderite from site 439 off northeastern Japan (Matsumoto and Iijima, 1980) and falls within the range of shallow marine siderite from the Paleogene strata of Japan (Matsumoto and Iijima, 1981). Magnesian siderite precipitates early on. The estimated temperature for first appearance of siderite is approximately 6°C. Reworking of slowly accumulated pelagic clays with high Fe and Mn and redeposition on the Blake Outer Ridge may explain the high Fe and Mn contents in these rapidly accumulated sediments. The additional iron and manganese in zone III (at shallow depth, below zones

I and II) was probably derived from sediments beneath the zone by upward migrating pore waters. The shallow appearance of siderite at site 533 is caused by the originally high contents of leachable iron, abundant organic substrate, and rapid rate of sedimentation. These factors all favour the increase of the concentration of Fe^{2+} and carbonate species during burial.

MATSUMOTO, K., AND MATSUHISA, Y., 1986. Chemistry, Carbon and Oxygen Isotope Ratios, and Origin of Deep-Sea Carbonates at Sites 438, 439 and 584: Inner Slope of the Japan Trench. *In,* IR of the DSDP, v.87, p.669-678. (870673)

The $\delta^{18}O_{water}$ = +0.07‰ at shallow depths above 24.5 m. Below it decreases gradually at a rate of approximately -0.26‰/100 m to -0.9‰ at 590.1 m. Fluctuation of $\delta^{18}O$ of interstitial water commonly tends to correlate with the lithology of sediments (Lawrence et al., 1975). Based on the carbonate-water fractionation factors and temperature-depth relationships, the following was observed:

at 594m $\delta^{18}O$ of calcite expected = -1‰, actual = +4.43‰

at 720m $\delta^{18}O$ of siderite expected = -3‰, actual = -1.9‰

This disparity suggests that authigenic carbonates are not in equilibrium with coexisting interstitial water and probably did not and are not now precipitating at the present depths of burial. Based on $\delta^{18}O$ of carbonates, the different carbonate minerals were formed successively in the sediments with increasing depth. From shallow to deep, they are calcian dolomite, calcite, ferrous dolomite and siderite. Organic matter in marine sediments decomposed through three main processes: 1) oxidation; 2) sulphate reduction;

3) methane fermentation. Process 1 and 2 yields isotopically light carbon and occurs at shallow depths and process 3 generates heavy carbon at lower depths. An increase in $\delta^{13}C$ from -37 to -4.3‰ at approximately 100m, probably means that fermentation-derived $\delta^{13}C$ CO_2 dominates over the CO_2 generated through oxidation and/or sulphate reduction.

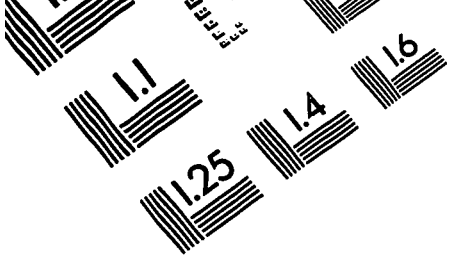

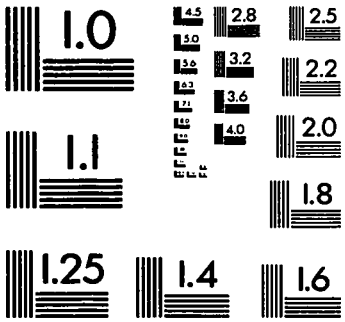

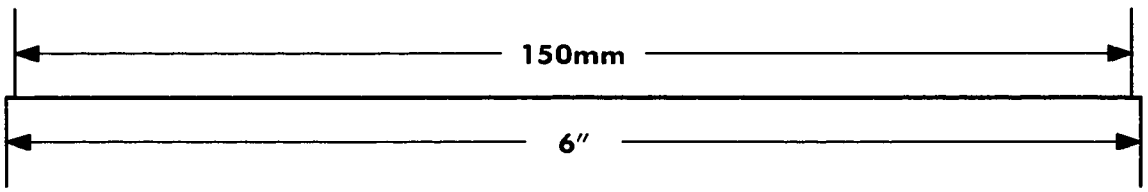

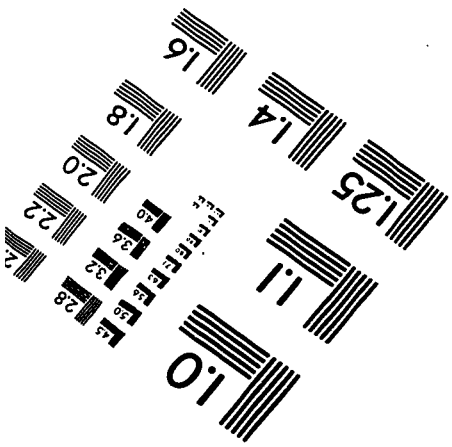

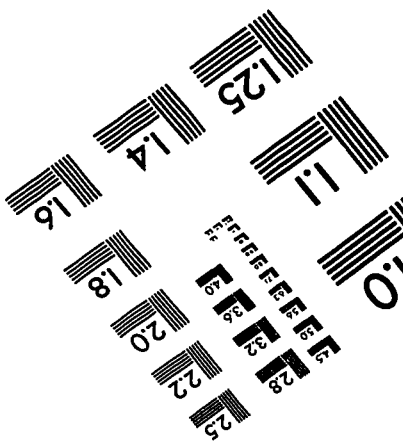

APPLIED IMAGE, Inc
1653 East Main Street
Rochester, NY 14609 USA
Phone: 716/482-0300
Fax: 716/288-5989